NISTIR 8357

Evaluation of Experimental and Predicted Vapor-Liquid Equilibrium Data for Systems Relevant to Biomass Fast Pyrolysis and Catalytic Upgrading

Eugene Paulechka
Vladimir Diky
Abhijit Dutta

This publication is available free of charge from:
https://doi.org/10.6028/NIST.IR.8357

National Institute of
Standards and Technology
U.S. Department of Commerce

NISTIR 8357

Evaluation of Experimental and Predicted Vapor-Liquid Equilibrium Data for Systems Relevant to Biomass Fast Pyrolysis and Catalytic Upgrading

Eugene Paulechka
Vladimir Diky
Applied Chemicals and Materials Division
Material Measurement Laboratory

Abhijit Dutta
Catalytic Carbon Transformation and Scale-up Center
National Renewable Energy Laboratory

This publication is available free of charge from:
https://doi.org/10.6028/NIST.IR.8357

March 2021

U.S. Department of Commerce
Gina M. Raimondo, Secretary

National Institute of Standards and Technology
James K. Olthoff, Performing the Non-Exclusive Functions and Duties of the Under Secretary of Commerce
for Standards and Technology & Director, National Institute of Standards and Technology

Certain commercial entities, equipment, or materials may be identified in this document in order to describe an experimental procedure or concept adequately. Such identification is not intended to imply recommendation or endorsement by the National Institute of Standards and Technology, nor is it intended to imply that the entities, materials, or equipment are necessarily the best available for the purpose.

National Institute of Standards and Technology Interagency or Internal Report 8357
Natl. Inst. Stand. Technol. Interag. Intern. Rep. 8357, 75 pages (March 2021)

This publication is available free of charge from:
https://doi.org/10.6028/NIST.IR.8357

This publication is available free of charge from: https://doi.org/10.6028/NIST.IR.8357

Abstract

The experimental vapor-liquid equilibrium (VLE) data for the binaries relevant to the catalytic fast pyrolysis of biomass have been collected and analyzed using the NIST-COSMO-SAC and NIST-modified UNIFAC models. The existing inconsistencies in the experimental data and the predicted values are discussed. For VLE with furan derivatives, *PTxy* data are normally reported, and the predicted values are in good agreement with them. For phenolic compounds, the gas phase compositions are available for only 36 % of the points, most results originate from a few laboratories, and each system has been typically studied in a single laboratory. The binaries are identified where more experimental VLE data are required to evaluate quality of the existing experimental and predicted results.

Key words

Catalytic fast pyrolysis; predictive models; vapor-liquid equilibria.

This publication is available free of charge from: https://doi.org/10.6028/NIST.IR.8357

Table of Contents

List of Tables

List of Figures

This publication is available free of charge from: https://doi.org/10.6028/NIST.IR.8357

This publication is available free of charge from: https://doi.org/10.6028/NIST.IR.8357

This publication is available free of charge from: https://doi.org/10.6028/NIST.IR.8357

1. Introduction

Biomass constituents include oxygenated polymeric material such as cellulose, hemicellulose, and polyaromatic lignin with hydroxy and methoxy groups [1, 2]. Fast pyrolysis is a process of thermal deconstruction of these materials at nearly 500°C with rapid heat transfer in a non-oxidative atmosphere, which produces solid char, non-condensable gases such as CO, CO_2, CH_4, and vapors including H_2O and numerous organic species [3]. Biomass reactions under these conditions are non-selective and the organic vapors include material of different molecular weights from the depolymerization process; additional reactions including the fragmentation of the monomeric constituents result in the formation of thousands of chemical species during fast pyrolysis. Condensation of fast pyrolysis vapors results in a liquid product known as bio-oil or pyrolysis-oil, which is unstable with regard to further chemical transformations because of its various oxygenated species including sugars, acids, and aldehydes [4]. Catalytic upgrading of the vapors prior to condensation, either within the fast pyrolysis reactor (*in situ*) or in a separate reactor following the fast pyrolysis reactor (*ex situ*) can help to improve the quality of the vapors by reducing the oxygen content and related reactivity [5]. Catalytic upgrading can also help funnel the numerous species from fast pyrolysis into a smaller subset of compounds suitable for production of valuable products, for example, Benzene-Toluene-Xylene (BTX) using zeolite catalysts [6, 7]. However, even after the catalytic upgrading of vapors, hundreds of chemical species can still be present in the pyrolysis oil. The species and types of molecules and functional groups is a strong function of the type of catalyst used [8]. While zeolite catalysts produce aromatic compounds even from carbohydrates, other catalysts result in different chemistry. An efficient catalytic fast pyrolysis (CFP) should significantly eliminate the most reactive entities such as sugars and acids relative to its non-catalytic counterpart.

There is strong interest in the production of oxygenated compounds from biomass which allows the preservation and utilization of the high proportion of oxygen in biomass [9], instead of complete deoxygenation when the desired final products are only hydrocarbon fuels [10, 11, 12]. For the CFP process, increasing the selectivity towards specific oxygenated compounds via catalytic upgrading and effective separations are two prerequisites for the production of oxygenated chemicals. Separation of individual chemical compounds is challenging because of the often-small content of each of the species in a soup of numerous compounds [12, 13]. Phase behavior and related operations need to be strategically employed for the efficient separation of desired species. The significant quantity of water from CFP results in two or three liquid phases upon condensation, as discussed in the previous publication [14]. In addition to post-condensation liquid-liquid separation, vapor-liquid equilibrium (VLE) is also important for any distillation or fractional condensation for separating chemical species. It should be noted that although oxygen content and reactivity is reduced via catalytic upgrading of pyrolysis vapors, higher molecular weight species and remaining reactive functional groups can keep the pyrolysis-oil prone to repolymerization upon reheating. Thus, in addition to distillation, fractional condensation is another separation method considered in conceptual designs and experimental setups [10]. The available literature on multiphase equilibria for the fast pyrolysis bio-oils was partially considered recently [15]. The main idea of that paper was to extend the group-contribution associating equation of state to lignin derivatives.

This publication is available free of charge from: https://doi.org/10.6028/NIST.IR.8357

Various versions of the UNIFAC model [16] are widely used for VLE prediction. To calculate the liquid-phase activity coefficients with this model, a solution is presented as a mixture of functional groups. The group characteristics and binary interaction parameters are determined from the experimental data. This model is fast, performs well for multiple mixtures, but is limited to the systems for which the empirical parameters are available. A dielectric continuum model COSMO [17] or similar models [18] are used in quantum-chemical calculations to determine polarization charge density on the molecular surface. These results are coupled with statistical thermodynamic equations in the thermodynamic models like COSMO-RS [19] or COSMO-SAC [20]. The models of this type have a relatively small number of empirical parameters and wider applicability domain. Also, they are less sensitive to the training set quality than fully empirical models. The UNIFAC and COSMO-type thermodynamic models are based on different physical principles and are essentially uncorrelated. Therefore, it is reasonable to use these models as two independent sources of information for analysis of the available experimental data.

The models considered above are primarily used to predict liquid-phase activity coefficients. If VLE involves a supercritical component and/or high temperatures and pressures, it is reasonable to combine an equation of state with an activity-coefficient model. Examples of this approach include the group-contribution equations of state PSRK [21] and CGA-EOS [22]. The VLE pressures below 0.2 MPa are considered in this paper and none of the components is supercritical. Therefore, the group-contribution equations of state are excessive for this work.

In this report, we explore the literature for VLE information on some of the known species from CFP and similar compounds towards the purpose of using the information for process modeling of the separation of oxygenated compounds, as well as segregation of potential fuel precursors into more optimal cuts. We analyze the effectiveness of two predictive methods, NIST-Modified-UNIFAC and NIST-COSMO-SAC, in predicting VLE behavior using the available experimental data for binary mixtures and specify the mixtures for which additional experimental data are needed.

2. Calculation

2.1. Compound selection

The compounds relevant to CFP and other industrial processes as well as their isomers and homologs were considered. They were divided into principal and secondary components. The principal ones included furan derivatives and phenolic compounds because of the greater availability of experimental data for those groups. All possible binary mixtures were generated assuming that at least one principal component was present in a mixture, and the literature search was performed. The compounds listed in Table 1 have at least one binary VLE data point available in the literature. A list of the binary mixtures is presented in Table 2.

This publication is available free of charge from: https://doi.org/10.6028/NIST.IR.8357

Table 1. Principal and secondary components considered in this work.

Chemical Name	CASRN	Formula	Chemical Name	CASRN	Formula
Principal components			Secondary components		
Furan derivatives			water	7732-18-5	H_2O
furan	110-00-9	C_4H_4O	methanol	67-56-1	CH_4O
2-furaldehyde	98-01-1	$C_5H_4O_2$	acetic acid	64-19-7	$C_2H_4O_2$
2-methylfuran	534-22-5	C_5H_6O	ethanol	64-17-5	C_2H_6O
furfuryl alcohol	98-00-0	$C_5H_6O_2$	1,2-ethanediol	107-21-1	$C_2H_6O_2$
γ-valerolactone	108-29-2	$C_5H_8O_2$	acetone	67-64-1	C_3H_6O
2-acetylfuran	1192-62-7	$C_6H_6O_2$	1-propanol	71-23-8	C_3H_8O
2,5-dimethylfuran	625-86-5	C_6H_8O	2-propanol	67-63-0	C_3H_8O
Phenolic compounds			butanone	78-93-3	C_4H_8O
phenol	108-95-2	C_6H_6O	1-butanol	71-36-3	$C_4H_{10}O$
1,2-benzenediol	120-80-9	$C_6H_6O_2$	2-butanol	78-92-2	$C_4H_{10}O$
1,3-benzenediol	108-46-3	$C_6H_6O_2$	2-methyl-1-propanol	78-83-1	$C_4H_{10}O$
1,4-benzenediol	123-31-9	$C_6H_6O_2$	benzene	71-43-2	C_6H_6
2-methylphenol	95-48-7	C_7H_8O	4-methylpentan-2-one	108-10-1	$C_6H_{12}O$
3-methylphenol	108-39-4	C_7H_8O	toluene	108-88-3	C_7H_8
4-methylphenol	106-44-5	C_7H_8O	methoxybenzene	100-66-3	C_7H_8O
2-methoxyphenol	90-05-1	$C_7H_8O_2$	1,2-dimethylbenzene	95-47-6	C_8H_{10}
4-methoxyphenol	150-76-5	$C_7H_8O_2$	1,3-dimethylbenzene	108-38-3	C_8H_{10}
2,4-dimethylphenol	105-67-9	$C_8H_{10}O$	1,4-dimethylbenzene	106-42-3	C_8H_{10}
2,5-dimethylphenol	95-87-4	$C_8H_{10}O$	ethylbenzene	100-41-4	C_8H_{10}
2,6-dimethylphenol	576-26-1	$C_8H_{10}O$	acetophenone	98-86-2	C_8H_8O
3,4-dimethylphenol	95-65-8	$C_8H_{10}O$	2-octanone	111-13-7	$C_8H_{16}O$

This publication is available free of charge from: https://doi.org/10.6028/NIST.IR.8357

Chemical Name	CASRN	Formula	Chemical Name	CASRN	Formula
3,5-dimethylphenol	108-68-9	$C_8H_{10}O$	1-octanol	111-87-5	$C_8H_{18}O$
2,4,6-trimethylphenol	527-60-6	$C_9H_{12}O$	isopropylbenzene	98-82-8	C_9H_{12}
			2-methylnaphthalene	91-57-6	$C_{11}H_{10}$

This publication is available free of charge from: https://doi.org/10.6028/NIST.IR.8357

Table 2. Binary mixtures with VLE data evaluated in this work.

Mixture	GPM[a]	Reference	Status[b]	*T* range / K	*P* range / kPa	Data type
Furan derivative + aromatic hydrocarbon						
furan + toluene	IG	Nala *et al.* [30]		305 to 382	101[d]	*PTxy*
		Thévaneau *et al.* [31]		313 to 353	13 to 173[c]	*PTxy*
2-furaldehyde + benzene	IG	Thornton and Garner [33]		356 to 428	101	*PTxy*
		Kenny [34]		298	0.21 to 13	*PTx*
		Stephenson and Van Winkle [35]		373 to 386	53	*PTxy*
		Garner and Ellis [36]	N	357, 365	101[d]	*PTx*
2-furaldehyde + toluene	IG	Garner and Ellis [36]		390 to 402	101	*PTx*
		Thornton and Garner [37]	N	384 to 426	101	*PTxy*
		Garner and Hall [38]		386 to 419	101	*PTxy*
		Rivenq [39]		343 to 435	27 to 101	*PTxy*
2-furaldehyde + 1,4-dimethylbenzene	IG	Puri and Raju [40]		407 to 429	96	*PTxy*
2-furaldehyde + ethylbenzene	IG	Puri and Raju [40]		405 to 428	96	*PTxy*
2-methylfuran + benzene	IG	Krevor and Prausnitz [32]		324, 339	37 to 109	*PTxy*
Two furan derivatives						
furan + 2-furaldehyde	IG	Tai *et al.* [41]	A	353 to 408	45 to 195[c]	*PTxy*
		Auger *et al.* [42]	A	305 to 434	101[d]	*PTx*
		Chen *et al.* [43]	A	304 to 435	101	*PTxy*
2-methylfuran + 2-furaldehyde	IG	Holdren and Hixon [44]		293 to 403	0.4 to 98	*PTxy*, *PTx*

This publication is available free of charge from: https://doi.org/10.6028/NIST.IR.8357

Mixture	**GPM**[a]	**Reference**	**Status**[b]	***T* range / K**	***P* range / kPa**	**Data type**
2-furaldehyde + furfuryl alcohol	V	Myles and Wingard [46]		342 to 358	3.3	*PTxy*
		Tsirlin and Vasil'eva [47]	N	348 to 370	6.7	*PTxy*
2-furaldehyde + *γ*-valerolactone	IG	Pokki *et al.* [48]		395 to 434	30	*PTxy*
2-furaldehyde + 2-acetylfuran	IG	Zheng *et al.* [49]		342 to 361	3.6, 5.2	*PTxy*
2-furaldehyde + 5-methylfurfural	IG	Fele and Grilic [50]		343 to 371	3.5, 5.0	*PTxy*
		Zheng *et al.* [49]		342 to 373	3.6, 5.2	*PTxy*
2-methylfuran + furfuryl alcohol	V	Tai *et al.* [41]		353 to 408	19 to 198[c]	*PTxy*
2-acetylfuran + 5-methylfurfural	IG	Zheng *et al.* [49]		353 to 373	3.6, 5.2	*PTxy*
2,5-dimethylfuran + furfuryl alcohol	V	Negadi *et al.* [45]			0.24 to 213	*PTx*
		Furan derivative + acid or ketone				
2-furaldehyde + acetic acid	HOC	Fele and Grilic [50]		368 to 430	49, 89	*PTxy*
2-furaldehyde + acetone	IG	Myles and Wingard [46]		329 to 435	101	*PTxy*
		Ma *et al.* [51]	A	330 to 435	101	*PTxy*
2-furaldehyde + 4-methylpentan-2-one	IG	Hauschild *et al.* [52]		368, 383	11 to 85	*PTxy*
		Zaitseva *et al.* [53]		333 to 369	4.2 to 32	*PTxy*, *Txy*
2-methylfuran + butanone	IG	Smith and Labonte [54]		338 to 351	101	*PTxy*, *Pxy*[e]
furfuryl alcohol + acetone	V	Dudutkina and Lutugina [55]		329 to 370	101	*PTx*
furfuryl alcohol + butanone	V	Dudutkina and Lutugina [55]		353 to 388	101	*PTx*
2,5-dimethylfuran + 4-methylpentan-2-one	IG	Negadi *et al.* [45]		313 to 393	6 to 213	*PTx*

This publication is available free of charge from: https://doi.org/10.6028/NIST.IR.8357

Mixture	**GPM^{a}**	**Reference**	**Status^{b}**	***T* range / K**	***P* range / kPa**	**Data type**
		Furan derivative + alcohol				
furan + ethanol	V	Auger *et al.* [42]		305 to 351	101^{d}	*PTxy*
2-furaldehyde + methanol	V	Ni and Wang [58]		338 to 435	101	*PTxy*
		Staroske and Figurski [59]		298	0.2 to 17	*PTxy*
2-furaldehyde + ethanol	V	Kharin *et al.* [60]	N	298 to 435	3.9 to 107	*PTxy*
2-methylfuran + methanol	HOC	Hickman and Hall [56]		324 to 336	99^{g}	*PTxy*
furfuryl alcohol + ethanol	V	Dudutkina and Lutugina [55]		351 to 380	101	*PTx*
γ-valerolactone + methanol	HOC	Havasi *et al.* [61]		338 to 375	101	*PTxy*
γ-valerolactone + ethanol	HOC	Havasi *et al.* [61]		352 to 390	101	*PTxy*
2,5-dimethylfuran + ethanol	HOC	Mejía *et al.* [57]		329 to 364	50 to 94	*PTxy*
furan + 1-octanol	V	Auger *et al.* [42]		305 to 382	101^{d}	*PTxy*
2-furaldehyde + 1-butanol	V	Hauschild *et al.* [52]		368, 383	11 to 77	*PTxy*
2-furaldehyde + 2-butanol	V	Zaitseva *et al.* [53]		333 to 353	4.2 to 47	*PTxy*, *Txy*
2-furaldehyde + 1-octanol	V	Rigamonti and Spaccamela Marchetti [62]	N	341 to 362	3.3	*PTxy*
furfuryl alcohol + 2-propanol	V	Tai *et al.* [41]		353 to 408	9.5 to 180^{c}	*PTxy*
γ-valerolactone + 2-propanol	HOC	Havasi *et al.* [61]		355 to 388	101	*PTxy*
		Furan derivative + water				
2-furaldehyde + water	V	Mains [63]	N	371 to 434	101	*PTxy*, *Pxy*^{f}

This publication is available free of charge from: https://doi.org/10.6028/NIST.IR.8357

Mixture	GPM[a]	Reference	Status[b]	*T* range / K	*P* range / kPa	Data type
		Pearce and Gerster [64]	A	311 to 366	2.0 to 85	*PTx*
		Tsirlin [65]	A	313 to 426	7.3 to 101	*PTxy*
		Kharin *et al.* [60]	N	323 to 408	3.7 to 101	*PTxy*
		Ni and Wang [58]	A	371 to 435	101	*PTxy*
		Staroske and Schuberth [66]	A	298	0.21 to 3.3	*PTxy*
		Sunder and Prasad [67]	N	369 to 432	95	*PTx*
furfuryl alcohol + water	V	Boldyrev *et al.* [68]	A	313 to 366	7.3	*PTxy*
		Dudutkina *et al.* [69]	N	304 to 352	4.0	*PTx*, *Pxy*[e]
γ-valerolactone + water	HOC	Havasi *et al.* [70]		320 to 480	10 to 101	*PTxy*
		Zaitseva *et al.* [71]		350	1.2 to 42	*PTxy*
		Two phenolic compounds				
phenol + 2-methylphenol	V	Fox and Barker [72]		455 to 464	101	*PTx*
		Schneider and Oberkobusch [73]		455 to 464	101	*PTxy*
		Vostrikova *et al.* [74]		359 to 362	2.7	*PTxy*
		Clausse *et al.* [75]		399 to 405	16	*PTxy*
		Selvam *et al.* [76]		412 to 462	27, 96	*PTx*
phenol + 3-methylphenol	V	Fox and Barker [72]		456 to 476	101	*PTx*
		Schneider and Oberkobusch [73]		455 to 475	101	*PTxy*
		Vostrikova *et al.* [77]		394 to 411	13	*PTxy*
		Cepeda *et al.* [78]		395 to 409	13	*PTxy*

This publication is available free of charge from: https://doi.org/10.6028/NIST.IR.8357

Mixture	GPM[a]	Reference	Status[b]	*T* range / K	*P* range / kPa	Data type
phenol + 4-methylphenol	V	Fox and Barker [72]		455 to 475	101	*PTx*
		Selvam *et al.* [76]		412 to 473	27, 96	*PTx*
1,2-benzenediol + 4-methylphenol	V	Hwang *et al.* [79]		423 to 453	4.3 to 56	*PTx*
1,2-benzenediol + 1,4-benzenediol	V	Shi *et al.* [80]	N	469 to 497	20	*PTxy*
1,2-benzenediol + 4-methoxyphenol	V	Hwang *et al.* [79]		438, 453	7.4 to 16	*PTxy*
2-methylphenol + 3-methylphenol	V	Fox and Barker [72]		464 to 476	101	*PTx*
		Wang *et al.* [81]		411 to 422	20	*PTxy*
2-methylphenol + 4-methylphenol	V	Vostrikova *et al.* [82]		401 to 409	13	*PTxy*
		Selvam *et al.* [76]		420 to 473	27, 96	*PTx*
2-methylphenol + 2,6-dimethylphenol	V	Ye *et al.* [83]		392 to 425	10, 25	*PTxy*
		Wang *et al.* [81]		411 to 418	20	*PTxy*
2-methylphenol + 2,4,6-trimethylphenol	V	Ye *et al.* [83]		392 to 444	10, 25	*PTxy*
3-methylphenol + 2,6-dimethylphenol	V	Wang *et al.* [81]		418 to 422	20	*PTxy*
4-methylphenol + 2,4-dimethylphenol	V	Selvam *et al.* [76]		430 to 482	27, 96	*PTx*
4-methylphenol + 4-methoxyphenol	V	Hwang *et al.* [79]		423 to 453	4.3 to 56	*PTxy*
2,5-dimethylphenol + 3,5-dimethylphenol	V	Schneider and Oberkobusch [73]		486 to 494	101	*PTxy*
3,4-dimethylphenol + 3,5-dimethylphenol	V	Schneider and Oberkobusch [73]		398 to 444	10, 25	*PTxy*
2,6-dimethylphenol + 2,4,6-trimethylphenol	V	Ye *et al.* [83]		495 to 500	101	*PTxy*
Phenolic compound + alkylbenzene						
phenol + benzene	V	Weissenberger *et al.* [84]	A	288	5.7 to 7.3	*PTx*

Mixture	GPM[a]	Reference	Status[b]	*T* range / K	*P* range / kPa	Data type
		Martin and George [85]		343	1.1to 71	*PTxy*
		Garner and Ellis [36]		366	101	*PTx*
		Gmehling [86]		353	2.1 to 101	*PTxy*
		Nienhaus *et al.* [87]		414	30 to 192[c]	*PTx*
phenol + toluene	V	Weissenberger *et al.* [84]	A	288	1.6 to 2.1	*PTx*
		Drickamer *et al.* [88]		384 to 446	101	*PTx*
		Garner and Ellis [36]		394 to 409	101	*PTx*
		Nienhaus *et al.* [87]		414	29 to 196[c]	*PTx*
		Klauck *et al.* [89]		333, 363	6.9 to 51	*PTxy*
phenol + ethylbenzene	V	Anderko [90]		393, 403	13 to 85	*PTx*
phenol + isopropylbenzene	V	Byk and Stroiteleva [91]		424 to 451	101	*PTxy*
		Anderko [90]		393, 403	13 to 55	*PTx*
		Cepeda *et al.* [92]		361 to 455	13 to 101	*PTxy*
2-methylphenol + benzene	V	Weissenberger and Piatti [93]	A	291	1.6 to 8.6	*PTx*
2-methylphenol + toluene	V	Weissenberger *et al.* [94]		288	1.2 to 2.0	*PTx*
		Klauck *et al.* [89]		333, 363	4.2 to 48	*PTxy*
2-methylphenol + 1,2-dimethylbenzene	V	Prasad *et al.* [95]	N	416 to 462	96	*PTx*
2-methylphenol + 1,3-dimethylbenzene	V	Prasad *et al.* [95]	N	410 to 462	96	*PTx*
2-methylphenol + 1,4-dimethylbenzene	V	Prasad *et al.* [95]	N	409 to 462	96	*PTx*
2-methylphenol + ethylbenzene	V	Prasad *et al.* [96]	N	407 to 462	95	*PTx*

This publication is available free of charge from: https://doi.org/10.6028/NIST.IR.8357

This publication is available free of charge from: https://doi.org/10.6028/NIST.IR.8357

Mixture	**GPM**[a]	**Reference**	**Status**[b]	***T* range / K**	***P* range / kPa**	**Data type**
3-methylphenol + benzene	V	Weissenberger and Piatti [93]	A	291	1.9 to 11	*PTx*
		Savitt and Othmer [97]	N	353 to 476	101	*PTxy*
3-methylphenol + toluene	V	Weissenberger *et al.* [94]		288	1.0 to 2.0	*PTx*
		Sartakova *et al.* [98]		391 to 455	101	*PTx*
		Klauck *et al.* [89]		333, 363	4.8 to 53	*PTxy*
3-methylphenol + 1,2-dimethylbenzene	V	Prasad *et al.* [99]	N	415 to 474	96	*PTx*
3-methylphenol + 1,3-dimethylbenzene	V	Prasad *et al.* [99]	N	429 to 474	96	*PTx*
3-methylphenol + 1,4-dimethylbenzene	V	Prasad *et al.* [99]	N	409 to 474	96	*PTx*
3-methylphenol + isopropylbenzene	V	Cepeda *et al.* [78]		362 to 398	13	*PTxy*
3-methylphenol + 2-methylnaphthalene	V	Othmer *et al.* [100]	A	476 to 514	101	*PTxy*
		Schmelzer *et al.* [101]		393 to 453	2.6 to 55	*PTxy*
4-methylphenol + benzene	V	Weissenberger and Piatti [93]	A	291	2.0 to 9.1	*PTx*
4-methylphenol + toluene	V	Weissenberger *et al.* [94]		288	1.1 to 2.0	*PTx*
		Marks and Wingard [102]		384 to 475	101	*PTxy*
		Klauck *et al.* [89]		333, 363	8.7 to 50	*PTxy*
4-methylphenol + 1,2-dimethylbenzene	V	Prasad *et al.* [103]	N	415 to 473	95	*PTx*
4-methylphenol + 1,3-dimethylbenzene	V	Prasad *et al.* [103]	N	410 to 473	95	*PTx*
4-methylphenol + 1,4-dimethylbenzene	V	Prasad *et al.* [103]	N	409 to 473	95	*PTx*
4-methylphenol + ethylbenzene	V	Prasad *et al.* [96]	N	407 to 473	95	*PTx*
4-methylphenol + 2-methylnaphthalene	V	Othmer *et al.* [100]	A	475 to 514	101	*PTxy*

This publication is available free of charge from: https://doi.org/10.6028/NIST.IR.8357

Mixture	GPM[a]	Reference	Status[b]	*T* range / K	*P* range / kPa	Data type
2-methoxyphenol + benzene	V	Weissenberger *et al.* [104]		290	3.8 to 7.2	*PTx*
		Phenolic compound + methoxybenzene				
phenol + methoxybenzene	V	Lebedeva *et al.* [105]	N	370 to 398	13	*PTxy*
2-methylphenol + methoxybenzene	V	Lebedeva *et al.* [105]	N	370 to 397	13	*PTxy*
2-methoxyphenol + methoxybenzene	V	Li *et al.* [106]		429 to 469	101	*PTxy*
		Phenolic compound + water				
phenol + water	V	Schreinemakers [107]		32 to 363	14 to 71	*PTxy*
		Schükarew [108]		342	23 to 30	*PTx*
		Rhodes *et al.* [109]		313		*Txy*
		Ferguson [110]		348	39	*PTx*
		Campbell and Campbell [111]	N	275 to 308	0.47 to 1.4	*PTxy,* *PTx,* *Txy*
		Brusset and Gaynès [112]	N	373 to 455	101	*PTxy*
		Markuzin [113]		288	0.02 to 1.7	*PTxy*
		Weller *et al.* [114]		318	0.23 to 9.4	*PTxy*
		Kliment *et al.* [115]		340 to 400	27	*PTxy*
		Kiva *et al.* [116]	N	328 to 397	15	*PTx*
		Kolyuchkina *et al.* [117]		361 to 440	67	*PTx*
		Hakuta [118] [e]		354 to 394	48 to 203	*PTxy*
		Karavaeva *et al.* [119]		332 to 381	20	*PTxy*

This publication is available free of charge from: https://doi.org/10.6028/NIST.IR.8357

Mixture	**GPM**[a]	**Reference**	**Status**[b]	***T* range / K**	***P* range / kPa**	**Data type**
		Lyzlova and Susarev [120]		298	1.6	*PTxy*
		Chou *et al.* [121]		373 to 455	101	*PTxy*
		Tabai *et al.* [122]		313 to 363	7.4 to 71	*PTx*
		Shi *et al.* [80]	N	334 to 396	20	*PTxy*
		Klauck *et al.* [89]		333 to 363	11 to 69	*PTx*
1,3-benzenediol + water	V	Shakhparonov and Martynova [123]		273 to 298	0.57 to 3.2	*PTx*
2-methylphenol + water	V	Brusset and Gaynès [112]	N	372 to 464	101	*PTxy*
3-methylphenol + water	V	Klauck *et al.* [89]		333 to 363	11 to 70	*PTxy*
	Phenolic compound + ketone					
phenol + acetone	V	Weissenberger *et al.* [84]	A	288	1.1 to 11	*PTx*
		Weissenberger *et al.* [124]	N	293	0.81 to 14	*PTx*
		Chalov *et al.* [125]	A	329 to 454	101	*PTxy*
		Gölles [126]	A	323 to 348	0.40 to 97	*PTx*
		Motina *et al.* [127]	N	330 to 425	101[d]	*PTxy*
		Vasil’eva *et al.* [128]	A	323 to 420	9.5 to 101	*PTxy*
phenol + butanone	V	Byk and Shcherbak [129]	N	325 to 450	27 to 101	*PTxy*
		Oscarson *et al.* [130]		393 to 453	19 to 182[c]	*PTxy*
phenol + acetophenone	V	Fried and Pick [131]		394 to 442	13, 40	*PTxy*
		Aarna and Kaps [132]		455 to 476	101	*PTxy*
		Giles and Wilson [133]		373, 433	3.1 to 53	*PTx*

This publication is available free of charge from: https://doi.org/10.6028/NIST.IR.8357

Mixture	**GPM**[a]	**Reference**	**Status**[b]	***T* range / K**	***P* range / kPa**	**Data type**
2-methylphenol + acetone	V	Weissenberger and Schuster [134]		291	0.32 to 16	*PTx*
		Weissenberger and Piatti [135]		291	0.20 to 15	*PTx*
		Piatti [136]		329 to 464	101	*PTx*
		Chalov *et al.* [125]	A	329 to 455	101	*PTxy*
2-methylphenol + 2-octanone	V	Aarna and Kaps [132]		446 to 465	101	*PTxy*
2-methylphenol + acetophenone	V	Aarna and Kaps [132]		464 to 478	101	*PTxy*
3-methylphenol + acetone	V	Weissenberger and Schuster [134]		291	0.39 to 15	*PTx*
		Weissenberger and Piatti [135]		291	0.35 to 16	*PTx*
		Piatti [136]		329 to 475	101	*PTx*
4-methylphenol + acetone	V	Weissenberger and Schuster [134]		291	0.24 to 16	*PTx*
		Weissenberger and Piatti [135]		291	0.33 to 17	*PTx*
		Piatti [136]		329 to 475	101	*PTx*
1,3-benzenediol + acetone	V	Weissenberger *et al.* [104]		293	2.6 to 16	
		Shakhparonov and Martynova [123]		273, 278	5.5 to 11	
2-methoxyphenol + acetone	V	Weissenberger *et al.* [104]		290	1.9 to 13	*PTx*
		Chalov *et al.* [125]		329 to 468	101	*PTxy*
		Phenolic compound + alcohol				
phenol + methanol	V	Weissenberger *et al.* [84]		288	1.1 to 6.5	*PTx*

This publication is available free of charge from: https://doi.org/10.6028/NIST.IR.8357

Mixture	**GPM**[a]	**Reference**	**Status**[b]	***T* range / K**	***P* range / kPa**	**Data type**
		Weissenberger *et al.* [124]		293	1.5 to 8.5	*PTx*
		Chalov *et al.* [125]	A	338 to 455	101	*PTxy*
		Hu *et al.* [138]	A	338 to 455	101	*PTxy*
phenol + ethanol	V	Weissenberger *et al.* [84]		288	0.81 to 3.2	*PTx*
		Weissenberger *et al.* [124]		293	0.59 to 4.0	*PTx*
		Garner and Ellis [36]		374	101	*PTx*
		Chou *et al.* [121]		352 to 451	101	*PTxy*
		Cesari *et al.* [139]		303 to 390	9 to 99	*PTx*
phenol + 1-propanol	V	Ravikumar *et al.* [140]		341 to 439	27, 95	*PTx*
phenol + 2-propanol	V	Weissenberger *et al.* [124]		293	0.24 to 3.5	*PTx*
		Veeranna *et al.* [141]		327 to 435	28 to 95	*PTx*
phenol + 1,2-ethanediol	V	Brusset *et al.* [142]		455 to 468	100	*PTxy*
2-methylphenol + methanol	V	Weissenberger and Schuster [134]		288	2.0 to 7.6	*PTx*
		Chalov *et al.* [125]	A	338 to 464	101	*PTxy*
		Prasad *et al.* [143]	N	336 to 462	96	*PTx*
2-methylphenol + ethanol	V	Weissenberger and Piatti [135]		291	0.37 to 4.1	*PTx*
		Prasad *et al.* [143]	N	350 to 462	96	*PTx*
		Cesari *et al.* [139]		302 to 394	9.0 to 100	*PTx*
2-methylphenol + 1-propanol	V	Prasad *et al.* [143]	N	369 to 62	96	*PTx*
2-methylphenol + 2-propanol	V	Prasad *et al.* [143]	N	354 to 462	96	*PTx*

This publication is available free of charge from: https://doi.org/10.6028/NIST.IR.8357

Mixture	**GPM**^{a}	**Reference**	**Status**^{b}	***T* range / K**	***P* range / kPa**	**Data type**
2-methylphenol + 1-butanol	V	Prasad *et al.* [143]	N	389 to 462	96	*PTx*
2-methylphenol + 2-butanol	V	Prasad *et al.* [143]	N	371 to 462	96	*PTx*
2-methylphenol + 2-methyl-1-propanol	V	Prasad *et al.* [143]	N	380 to 462	96	*PTx*
2-methylphenol + 1,2-ethanediol	V	Kurtyka [144]		463	101	*PTx*
3-methylphenol + methanol	V	Weissenberger *et al.* [94]		288	2.1 to 7.6	*PTx*
		Prasad *et al.* [145]	N	336 to 474	96	*PTx*
3-methylphenol + ethanol	V	Weissenberger and Piatti [135]		291	0.80 to 3.9	*PTx*
		Piatti [146]		351 to 475	101	*PTx*
		Prasad *et al.* [145]	N	350 to 474	96	*PTx*
3-methylphenol + 1-propanol	V	Prasad *et al.* [145]	N	369 to 474	96	*PTx*
3-methylphenol + 2-propanol	V	Prasad *et al.* [145]	N	355 to 474	96	*PTx*
3-methylphenol + 1-butanol	V	Prasad *et al.* [145]	N	389 to 474	96	*PTx*
3-methylphenol + 2-butanol	V	Prasad *et al.* [145]	N	371 to 474	96	*PTx*
3-methylphenol + 2-methyl-1-propanol	V	Prasad *et al.* [145]	N	380 to 474	96	*PTx*
3-methylphenol + 1,2-ethanediol	V	Othmer *et al.* [100]		468 to 476	101	*PTxy*
		Brusset *et al.* [142]		468 to 473	100	*PTxy*
4-methylphenol + methanol	V	Weissenberger *et al.* [94]		288	2.2 to 7.5	*PTx*
		Prasad *et al.* [143]	N	336 to 473	95	*PTx*
4-methylphenol + ethanol	V	Weissenberger and Piatti [135]		291	0.53 to 4.0	*PTx*
		Prasad *et al.* [143]	N	350 to 473	95	*PTx*

This publication is available free of charge from: https://doi.org/10.6028/NIST.IR.8357

Mixture	GPM[a]	Reference	Status[b]	*T* range / K	*P* range / kPa	Data type
4-methylphenol + 1-propanol	V	Prasad *et al.* [143]	N	369 to 473	95	*PTx*
4-methylphenol + 2-propanol	V	Prasad *et al.* [143]	N	354 to 473	95	*PTx*
4-methylphenol + 1-butanol	V	Prasad *et al.* [143]	N	392 to 473	95	*PTx*
4-methylphenol + 2-butanol	V	Prasad *et al.* [143]	N	372 to 473	95	*PTx*
4-methylphenol + 2-methyl-1-propanol	V	Prasad *et al.* [143]	N	380 to 473	95	*PTx*
4-methylphenol + 1,2-ethanediol	V	Othmer *et al.* [100]		468 to 475	101	*PTxy*
		Brusset *et al.* [142]		464 to 473	100	*PTxy*
1,3-benzenediol + methanol	V	Shakhparonov and Martynova [123]		273 to 298	2.5 to 17	*PTx*
1,3-benzenediol + ethanol	V	Weissenberger *et al.* [104]		290	1.7 to 3.9	*PTx*
		Shakhparonov and Martynova [123]		273 to 298	0.67 to 7.9	*PTx*
1,3-benzenediol + 1-butanol	V	Shakhparonov and Martynova [123]		293, 298	0.38 to 0.93	*PTx*
1,4-benzenediol + methanol	V	Kodama *et al.* [137] [e]		337	98 to 100	*PTxy*
1,4-benzenediol + ethanol	V	Kodama *et al.* [137] [e]		351	99	*PTxy*
2-methoxyphenol + methanol	V	Chalov *et al.* [125]		338 to 478	101	*PTxy*
2-methoxyphenol + ethanol	V	Weissenberger *et al.* [104]		290	1.0 to 3.6	*PTx*
		Cesari *et al.* [139]		300 to 409	9.0 to 100	*PTx*

[a]Gas-phase model: IG, ideal gas; V, virial; HOC, Hayden-O'Connell. [b]A, new experimental data are required to identify the reason of inconsistency either between the available experimental data or between the experimental and predicted values; N, not recommended. More details about each case are provided in the text. [c]The results at $P > 200$ kPa available in the paper were not used in this work. [d]Reported as "atmospheric pressure". [e]Data at very low mole fractions of the first component; [f]*Pxy* data are not considered; [g]estimated experimental pressure based on the reported boiling temperatures of pure liquids.

This publication is available free of charge from: https://doi.org/10.6028/NIST.IR.8357

2.2. Models

pTx or *pTxy* experimental data were considered for this analysis. For a given (x, T) pair, the pressure over the solution and the gas-phase composition were calculated using the component activity coefficients predicted with the NIST-COSMO-SAC [23] and NIST-modified UNIFAC [24] models. The σ profiles were generated at the B3LYP/6-311G(d,p) theory level using Gaussian 09 [25].[1] The detailed procedure has been described earlier [23]. All thermodynamic calculations were carried out with the NIST ThermoData Engine (TDE) v. 10.4 [26]. The vapor pressures of pure compounds critically evaluated by TDE were used. The evaluation procedures [27,28] did not involve either of the models. The real-gas model was automatically selected by the software and specified in Table 2. Predictions were not reported if (a) the pure-compound vapor pressure could not be evaluated; (b) a model predicted the liquid-liquid equilibrium for an experimental point; or (c) the UNIFAC parameters were missing.

The NIST-COSMO-SAC parameters were determined using the experimental data in the temperature range T = (15 to 457) K [23]. NIST-modified UNIFAC [24] uses the temperature-dependent formulation similar to that in the modified UNIFAC [29]. For this model, the upper temperature of experimental data in the training set for different parameters varied from (293 to 644) K, and the average value was close to T = 400 K. 67 % of the VLE points considered in this work were reported at T < 404 K and 95 % of the data were at T < 468 K. NIST-COSMO-SAC was parameterized using the experimental VLE data at $P \leq 127$ K assuming the ideal-gas behavior for the vapor phase [23]. In this work, the considered pressure range was extended to P < 200 kPa and the gas-phase non-ideality was taken into account. Thus, we do not *a priori* expect problems caused by the use of the model parameters beyond their applicability domain.

2.3. Uncertainties

Uncertainties and differences between the calculated and experimental values will further be considered in terms of the relative values of pressures and absolute values of mole fractions in the gas phase. The uncertainties are converted to combined uncertainties accounting for the contribution propagated from the uncertainties in the state variables. The combined uncertainties of pressures are partially caused by uncertainty of the pressure measurements. The latter can be the major contribution, however, the contributions due to uncertainties for the temperature and liquid-phase composition are often also significant.

If the gas phase is ideal, the pressure P over a binary solution equals

$$P = P_{01}x_1\gamma_1 + P_{02}(1 - x_1)\gamma_2 \quad (1)$$

where x_1 is the mole fraction of the first component in the liquid phase; p_{0i} and γ_i are the vapor pressure and liquid-phase activity coefficient of the ith component, respectively. In an ideal solution, $\gamma_i = 1$ and the uncertainty in temperature propagates to VLE pressure as

---

[1] Trade names are provided only to specify procedures adequately and do not imply endorsement by the National Institute of Standards and Technology or the National Renewable Energy Laboratory. Similar products by other manufacturers may be found to work as well or better.

This publication is available free of charge from: https://doi.org/10.6028/NIST.IR.8357

$$\frac{u_{\mathrm{r}}(P)}{u(T)} \approx \frac{d\log P}{dT} = \frac{1}{P}\left(P_{01}x_1\frac{\Delta_{\mathrm{vap}}H_1}{RT^2} + P_{02}(1-x_1)\frac{\Delta_{\mathrm{vap}}H_2}{RT^2}\right) \tag{2}$$

here $\Delta_{\mathrm{vap}}H_i$ is the enthalpy of vaporization of the ith component; R is the molar gas constant; T is the experimental temperature; $u(T)$ is the standard uncertainty of temperature; and $u_{\mathrm{r}}(P)$ is the relative standard uncertainty of pressure. Typically, a temperature change of 1 K corresponds to a pressure change of several per cent. For example, if the partial pressure of the first component dominates in the total VLE pressure and its enthalpy of vaporization is $\Delta_{\mathrm{vap}}H_1 = 50\ \mathrm{kJ\cdot mol^{-1}}$ at $T = 350$ K, $u_{\mathrm{r}}(P) \approx 0.049u(T)$. Eq. (2) can also be used to estimate deviations between the predicted and experimental VLE temperatures, if the pressure deviations are known and *vice versa.*

Uncertainties for the pressure and mole fraction for the ideal solution are related by the equation

$$\frac{u_{\mathrm{r}}(P)}{u(x)} \approx \frac{d|\ln P|}{dx} = \frac{|P_{01}-P_{02}|}{P} \tag{3}$$

The effect will be minimal at $P_{01} \approx P_{02}$. If $P_{01} >> P_{02}$ or $P_{01} << P_{02}$, $u_{\mathrm{r}}(P) \approx u(x_1)$. For non-ideal solutions, the dependence of the activity coefficients on the liquid-phase composition should be considered.

An effect of the sample purity on the uncertainty should also be considered. To quantify this contribution, the nature of the impurity must be known. This information is typically not available in the literature.

2.4. Criteria for analysis of the experimental and predicted data

A universal rigorous criterion to evaluate the quality of VLE data does not exist. All methods evaluate the mutual consistency with other data or models. Previously, we demonstrated that the relative standard uncertainty close to $u_{\mathrm{r}}(P) = 0.15$ can be expected for both NIST-COSMO-SAC and NIST-modified-UNIFAC models [23]. Thus, any difference between the predicted and experimental pressure significantly exceeding this value would require special attention. A similar limit for the gas-phase mole fractions has been estimated to be close to 0.05 [14] and is supported by the statistical analysis below.

Two scenarios are possible. First, all available experimental data for a mixture are mutually consistent and are also consistent with the predicted values. This includes the cases where a single dataset is available. In this case, no action is required. Second, inconsistency of some kind is detected. This may include inconsistent experimental data sets, predicted and experimental values, or results from two models. In this scenario, the inconsistencies are further analyzed using the following criteria: (i) consistency of results for the same mixture obtained in different laboratories; (ii) consistency of the data for chemically similar systems (for example, those with isomers or homologs); (iii) model performance for chemically similar systems; (iv) overall data quality originating from a laboratory. If a model is found to give unsatisfactory results for a mixture, it is specified in the text. The experimental data found to be problematic are marked with the N letter in the last column of Table 2. If the

This publication is available free of charge from: https://doi.org/10.6028/NIST.IR.8357

available information is not conclusive, the data are marked with the letter A meaning new VLE measurements are suggested for this mixture. The flags for the experimental data are independent of evaluation of the predicted values. For example, new experimental data can be needed, and the predictions can be not satisfactory for the same mixture.

3. Results

3.1. VLE for furan derivatives

We considered 1630 data points for 39 binaries with furan derivatives. For 1295 points, the gas-phase composition was reported. The results are presented in Figs. 1–8.

3.1.1. VLE with aromatic compounds

These results include the data for (furan + toluene), (2-methylfuran + benzene), and four binaries with 2-furaldehyde (Fig. 1). The predicted values are generally in good agreement with the experimental data. Krevor and Prausnitz [32] reported that the component activity coefficients for (2-methylfuran + benzene) are within (1 to 1.06). This behavior is very well reproduced by both considered models. A similar behavior with γ within (1.0 to 1.12) is predicted for (furan + toluene) by NIST-COSMO-SAC, the only model available for this mixture. The reported experimental pressures [30,31] are generally lower than corresponding pressures over an ideal solution. However, consistency of the predicted and experimental values is still acceptable.

The experimental data for the 2-furaldehyde mixtures with benzene and toluene have been reported in multiple works, primarily by Garner *et al.* (Table 2). The gas-phase compositions for (2-furaldehyde + toluene) reported in Ref. [37] deviate by up to 0.1 mole fraction from the other data for this mixture, including those from the same laboratory. The same problem exists for the pressures of (2-furaldehyde + benzene) reported by Garner and Ellis [36]. These results will not be further used.

The vapor pressure of 2-furaldehyde in Ref. [34] is inconsistent with multiple data available in the literature. However, its partial pressure is relatively small at most compositions. Thus, this problem should not affect most of the VLE data. This is a typical problem also found in the results by Staroske *et al.* for (2-furaldehyde + methanol) [59] and (2-furaldehyde + water) [66] and by Holdren and Hixon for (2-methylfuran + 2-furaldehyde) [44].

This publication is available free of charge from: https://doi.org/10.6028/NIST.IR.8357

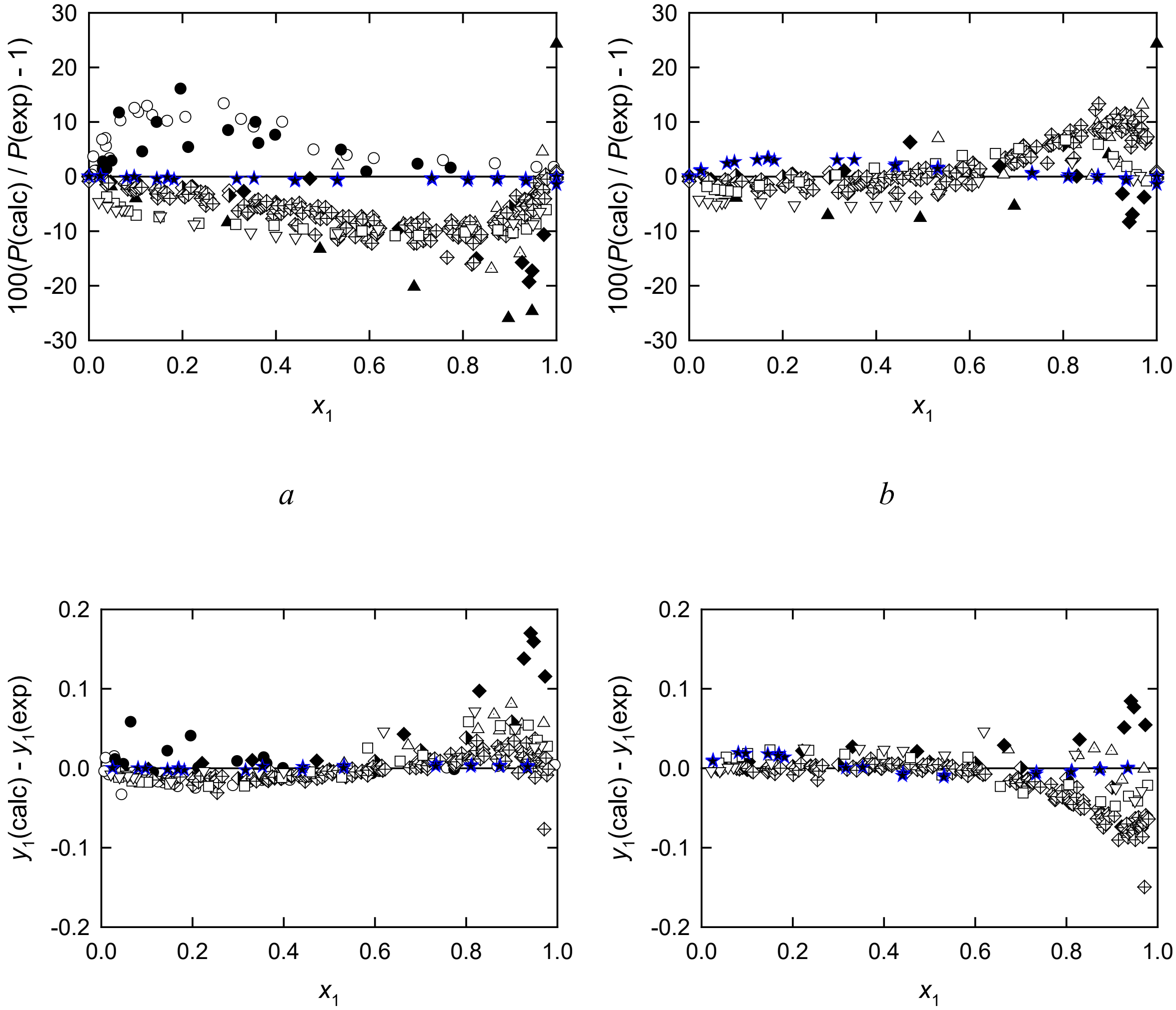

a *b*

c *d*

Fig. 1. Comparison of the predicted and experimental pressures P and first-component mole fractions y_1 in the gas phase at different first-component mole fractions in the liquid phase x_1 for the binaries of furan derivatives with aromatic compounds: a, c, NIST-COSMO-SAC; b, d: NIST-Modified UNIFAC.

Circles are for furan + toluene: ○, Nala *et al.* [30]; ●, Thévaneau *et al.* [31].
Stars (★) are for 2-methylfuran + benzene, Krevor and Prausnitz [32].
Triangles are for 2-furaldehyde + benzene: △, Thornton and Garner [33]; ▲, Kenny [34]; ◬, Stephenson and Van Winkle [35]. The results of Garner and Ellis [36] obtained in the same laboratory as Ref. [33] are not shown because of a large deviation.
Diamonds are for 2-furaldehyde + toluene: ◇, Garner and Ellis [36]; ◆, Thornton and Garner [37]; ⬖, Garner and Hall [38]; ◈, Rivenq [39].
Squares (□) are for 2-furaldehyde + 1,4-dimethylbenzene, Puri and Raju [40].
Triangles down (▽) are for 2-furaldehyde + ethylbenzene, Puri and Raju [40].

This publication is available free of charge from: https://doi.org/10.6028/NIST.IR.8357

3.1.2. VLE of two furan derivatives

The experimental data are available for the mixtures with furan, 2-methyl-, and 2,5-dimethylfurans (Fig. 2) and five mixtures containing two furan derivatives with polar substituents (Fig. 3). For the first group, significant inconsistencies exist for both the experimental and computed results. VLE for (furan + 2-furaldehyde) have been reported in three publications [41, 42, 43]. Despite the pressures predicted with the two models differ significantly (Fig. 2), it is seen that these experimental results are inconsistent. The gas-phase compositions from both models agree with ones reported by Tai *et al.* [41] and disagree by up to 0.2 mole fraction with the data of Chen *et al.* [43]. The pressure deviations [42] are supported by those for (2-methylfuran + 2-furaldehyde) [44] and (2,5-dimethylfuran + furfuryl alcohol) [45] and those of Ref. [43] are consistent with the data for (2-methylfuran + furfuryl alcohol) [41]. While the analysis above gives a certain preference to the *PTx* data by Auger *et al.* [42], the results are inconclusive. New experimental data are required for (furan + 2-furaldehyde). Also, efforts should be made to resolve the existing inconsistencies between the VLE pressures predicted with NIST-COSMO-CAS and NIST-modified UNIFAC.

The pressures and gas-phase compositions predicted with NIST-COSMO-SAC for the polar binaries are generally in good agreement with the experimental data (Figs. 3a and 3c). The (2-furaldehyde + furfuryl alcohol) VLE data at low pressures have been published in two papers [46, 47]. Only NIST-COSMO-SAC predictions are available for this system due to lack of the UNIFAC parameters. The predicted pressures are about 30 % lower than those in Ref. [47] for all but three points, and this problem does not exist for the results from Ref. [46]. Both works reported isobars at reduced pressure (6.7 and 3.3 kPa, respectively). Thus, a similar correlation between the predicted and experimental values is expected. Considering good performance of the NIST-COSMO-SAC model for this group of mixtures, the data of Myles and Wingard [46] should be preferred. A reasonable explanation could be that the real pressure in most experiments from Ref. [47] was 4.7 kPa instead of 6.7 kPa stated by the authors.

The (2-furaldehyde + 5-methylfurfural) binary was studied in two works [49, 50]. These results are mutually consistent though the values predicted with NIST-modified UNIFAC deviate from them (Figs. 3b and 3d). We believe the predictions are inadequate for this binary. This problem does not occur in the NIST-COSMO-SAC predictions (Figs. 3a and 3c).

This publication is available free of charge from: https://doi.org/10.6028/NIST.IR.8357

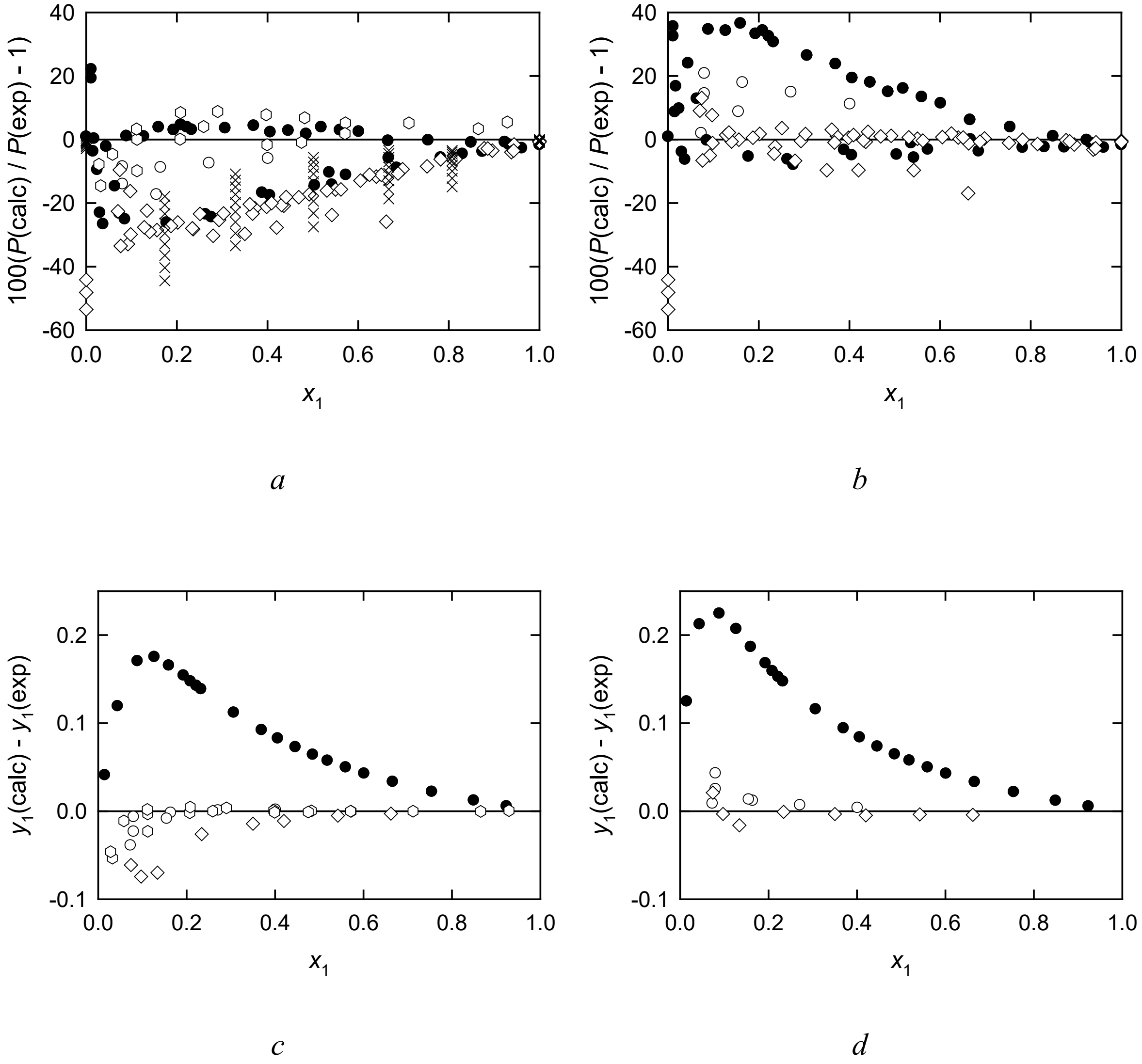

Fig. 2. Comparison of the predicted and experimental pressures *P* and first-component mole fractions y_1 in the gas phase at different first-component mole fractions in the liquid phase x_1 for the binaries of furan derivatives one of which is furan or methylfuranes: a, c, NIST-COSMO-SAC; b, d: NIST-Modified UNIFAC.

Circles are for furan + 2-furaldehyde: ○, Tai *et al.* [41]; ●, Auger *et al.* [42]; ◑, Chen *et al.* [43].
Diamonds (◇) are for 2-methylfuran + 2-furaldehyde, Holdren and Hixon [44].
Hexagons (⬡) are for 2-methylfuran + furfuryl alcohol, Tai *et al.* [41].
Crosses (×) are for 2,5-dimethylfuran + furfuryl alcohol, Negadi *et al.* [45].

This publication is available free of charge from: https://doi.org/10.6028/NIST.IR.8357

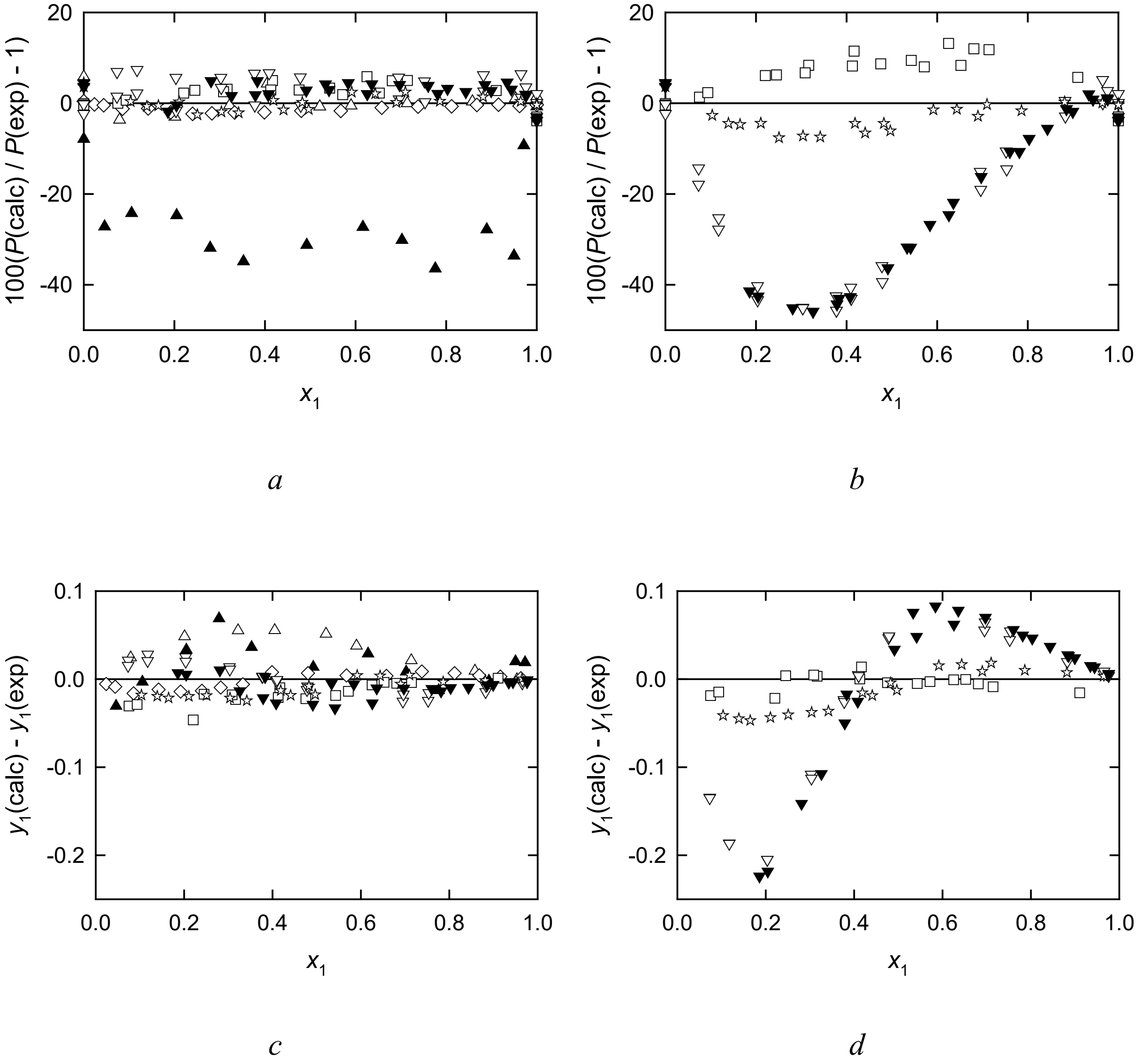

a *b*

c *d*

Fig. 3. Comparison of the predicted and experimental pressures *P* and first-component mole fractions y_1 in the gas phase at different first-component mole fractions in the liquid phase x_1 for the binaries of furan derivatives: a, c, NIST-COSMO-SAC; b, d: NIST-Modified UNIFAC.

Triangles are for 2-furaldehyde + furfuryl alcohol: △, Myles and Wingard [46]; ▲, Tsirlin and Vasil'eva [47].
Diamonds (◇) are for 2-furaldehyde + *γ*-valerolactone, Pokki *et al.* [48].
Squares (□) are for 2-furaldehyde + 2-acetylfuran, Zheng *et al.* [49].
Triangles down are for 2-furaldehyde + 5-methylfurfural: ▽, Fele and Grilic [50]; ▼, Zheng *et al.* [49]. The data obtained with NIST-modified UNIFAC seem to be incorrect.
Stars (☆) are for 2-acetylfuran + 5-methylfurfural, Zheng *et al.* [49].

This publication is available free of charge from: https://doi.org/10.6028/NIST.IR.8357

3.1.3. VLE with ketones and acetic acid

For this group (Fig. 4), the experimental and predicted results are generally in good agreement. NIST-COSMO-SAC describes the experimental data somewhat better at $x_1 > 0.8$ than NIST-modified UNIFAC though the consistency trends are similar. The predicted pressures and gas-phase compositions are in good agreement with the experimental data for (2-methylfuran + butanone) [54]. The deviations close to -20 % are observed for (2,5-dimethylfuran + 4-methylpentan-2-one) [45] at the pressures close to 10 kPa. At the higher pressures, the deviations decrease becoming comparable to those for other mixtures for NIST-COSMO-SAC (Fig. 4a).

A few points at high mole fractions of 2-furaldehyde in its mixtures with acetone reported by Ma et al. [51] have anomalous deviations of the predicted P and y for both considered models. This behavior is not observed for any other mixture of this group. Additional experimental data are required to support these experimental results.

The gas-phase compositions of (2-furaldehyde + 4-methylpentan-2-one) predicted with NIST-modified UNIFAC significantly deviate from the values reported by Hauschild *et al.* [52] and Zaitseva *et al.* [53]. This deviation is specific to this model is probably not related to the quality of the experimental data.

3.1.4. VLE with alcohols

For most furan and alkylfuran mixtures with alcohols, NIST-COSMO-SAC is the only available model (Fig. 5) due to the lack of NIST-modified UNIFAC parameters. The predicted pressures are typically (10 to 25) % lower than the experimental ones. For these mixtures, the model incorrectly predicts gas-phase mole fractions unless one of the components is predominant in the gas phase ($y > 0.95$). The deviations are consistent, which indicates that the experimental data do not have significant problems.

The predicted pressures and gas-phase compositions for the other binaries with alcohols agree with the experimental data (Figs. 6 and 7) except two datasets. The pressures and gas-phase compositions of (2-furaldehyde + ethanol) at $x_1 > 0.9$ [60] notable deviate from the values predicted with both models (Fig. 6). Since this problem does not occur for 2-furaldehyde binaries with other alcohols, these data should be discarded. The gas-phase compositions for (2-furaldehyde + 1-octanol) [62] are inconsistent with both models. 1-octanol used in Ref. [62] is actually a mixture of alcohols with 0.85 mass fraction of 1-octanol. Therefore, the results obtained in this work should not be used.

This publication is available free of charge from: https://doi.org/10.6028/NIST.IR.8357

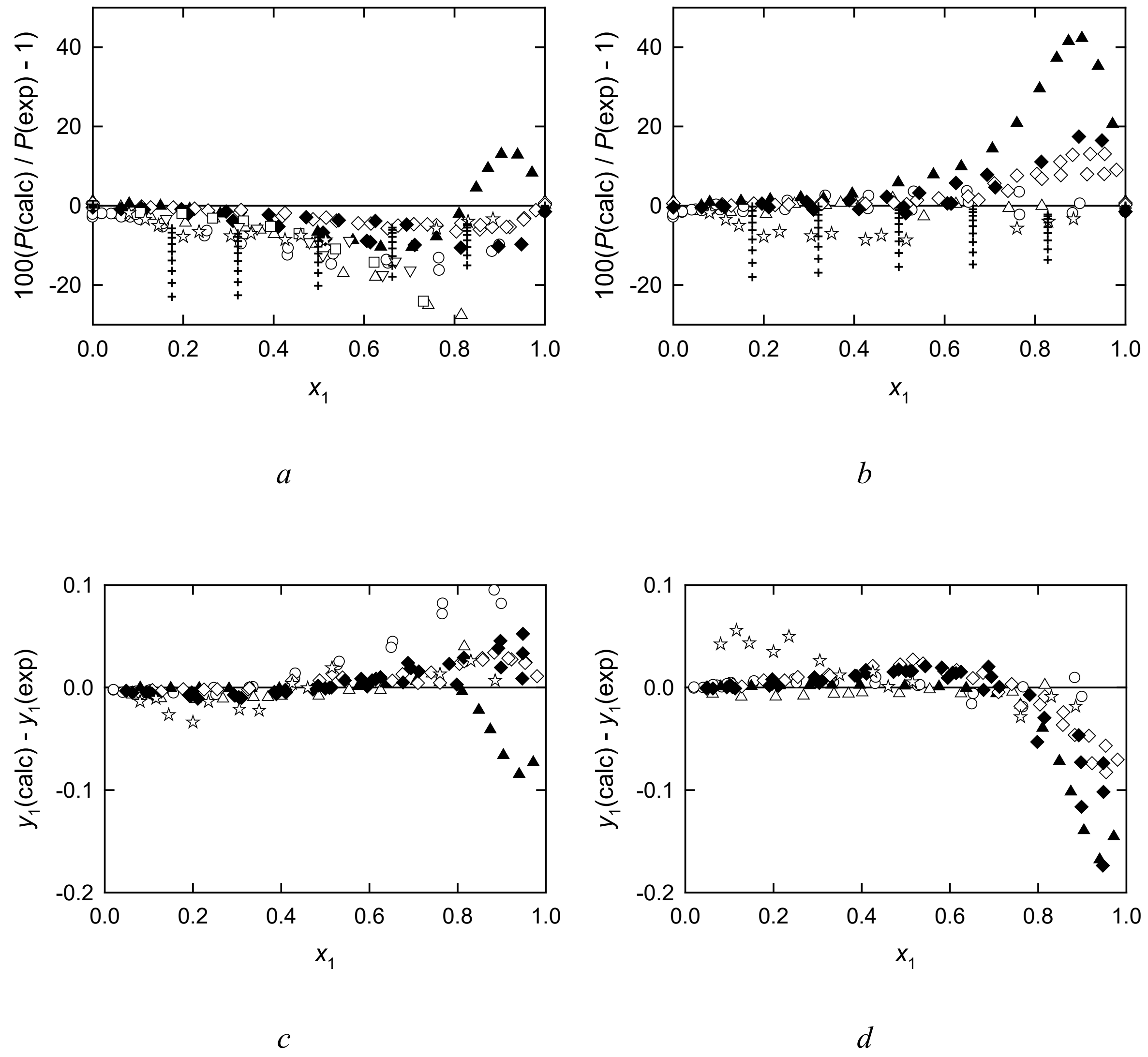

Fig. 4. Comparison of the predicted and experimental pressures P and first-component mole fractions y_1 in the gas phase at different first-component mole fractions in the liquid phase x_1 for the binaries of furan derivatives with ketones and acetic acid: a, c, NIST-COSMO-SAC; b, d: NIST-Modified UNIFAC.

Circles (○) are for 2-furaldehyde + acetic acid, Fele and Grilic [50].
Triangles are for 2-furaldehyde + acetone: △, Myles and Wingard [46]; ▲, Ma *et al.* [51].
Diamonds are for 2-furaldehyde + 4-methylpentan-2-one: ◇, Hauschild *et al.* [52]; ◆, Zaitseva et al. [53].
Stars (☆) are for 2-methylfuran + butanone, Smith and Labonte [54].
Pluses (+) are for 2,5-dimethylfuran + 4-methylpentan-2-one, Negadi *et al.* [45].
Squares (□) are for furfuryl alcohol + acetone, Dudutkina and Lutugina [55].
Triangles down (▽) are for furfuryl alcohol + butanone, Dudutkina and Lutugina [55].

This publication is available free of charge from: https://doi.org/10.6028/NIST.IR.8357

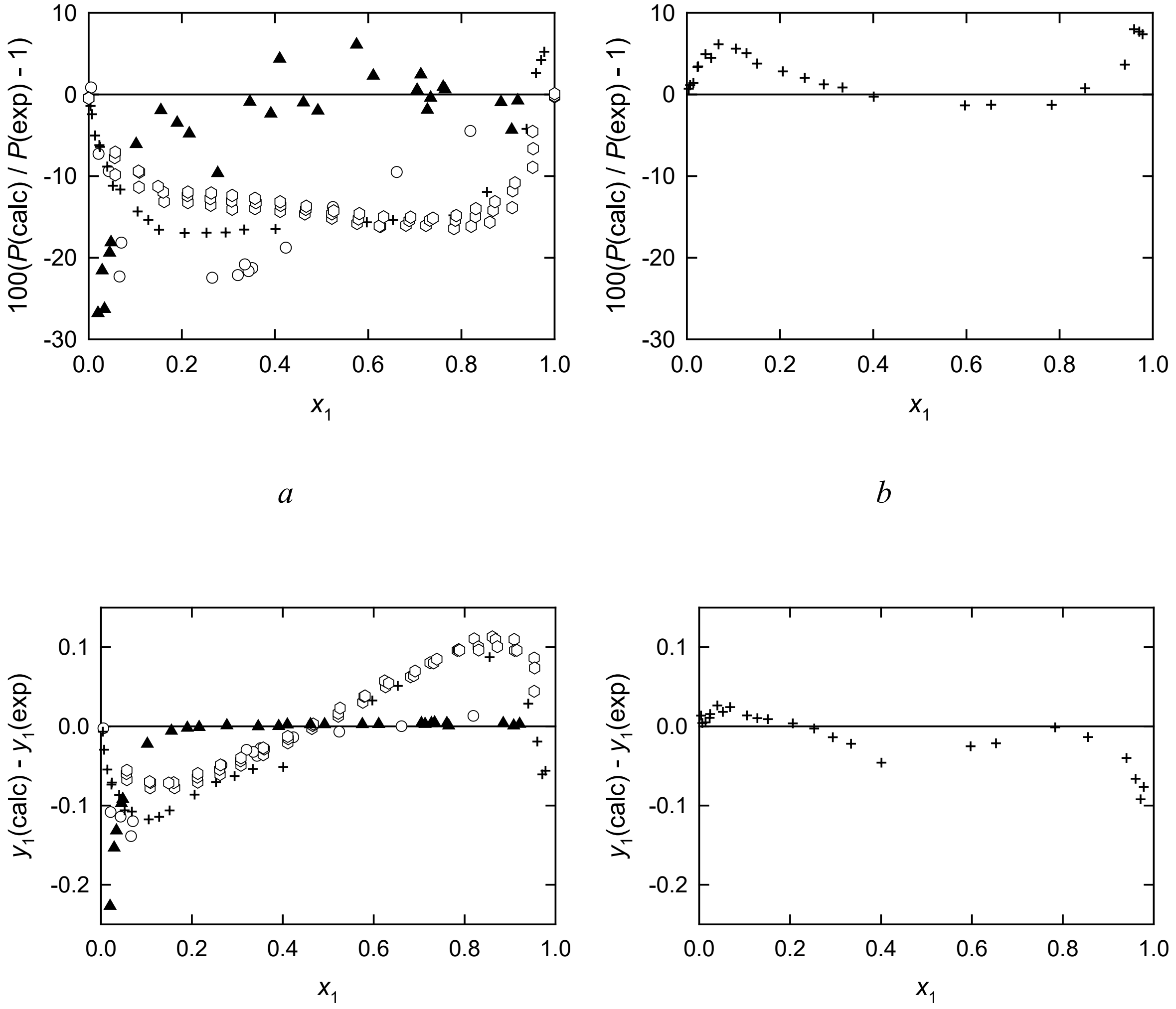

a

b

c

d

Fig. 5. Comparison of the predicted and experimental pressures *P* and first-component mole fractions y_1 in the gas phase at different first-component mole fractions in the liquid phase x_1 for the binaries of furan and methylfuranes with methanol and ethanol: a, c, NIST-COSMO-SAC; b, d: NIST-Modified UNIFAC.

Circles (○) are for furan + ethanol, Auger *et al.* [42].
Triangles (▲) are for furan + 1-octanol, Auger *et al.* [42].
Pluses (+) are for 2-methylfuran + methanol, Hickman and Hall [56].
Hexagons (⬡) are for 2,5-dimethylfuran + ethanol, Mejía *et al.* [57].

This publication is available free of charge from: https://doi.org/10.6028/NIST.IR.8357

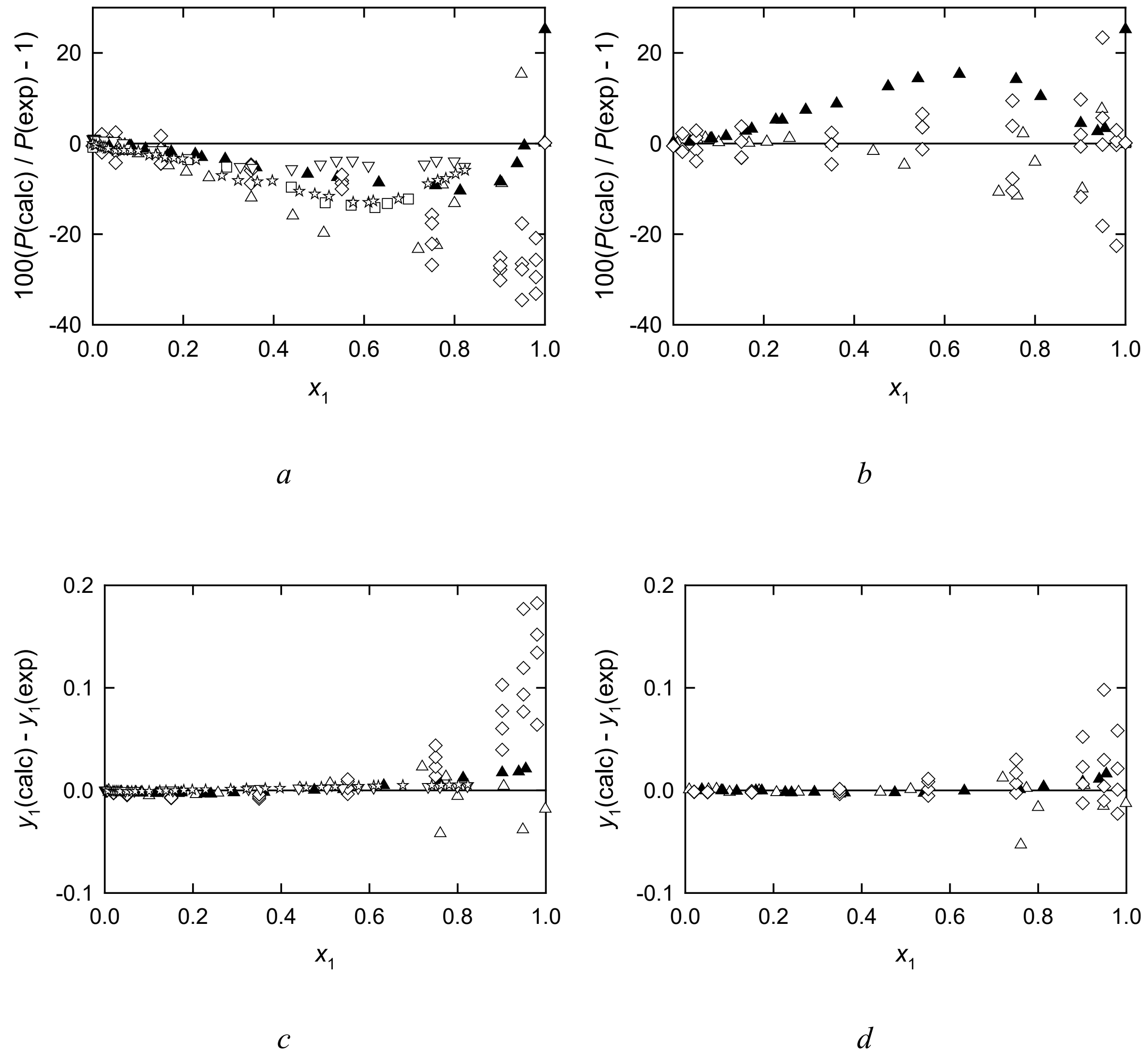

Fig. 6. Comparison of the predicted and experimental pressures *P* and first-component mole fractions y_1 in the gas phase at different first-component mole fractions in the liquid phase x_1 for the binaries of furan derivatives with methanol and ethanol: a, c, NIST-COSMO-SAC; b, d: NIST-Modified UNIFAC.

Triangles are for 2-furaldehyde + methanol: △, Ni and Wang [58]; ▲, Staroske and Figurski [59].
Diamonds (◇) are for 2-furaldehyde + ethanol, Kharin *et al.* [60].
Squares (□) are for furfuryl alcohol + ethanol, Dudutkina and Lutugina [55].
Triangles down (▽) are for γ-valerolactone + methanol, Havasi *et al.* [61].
Stars (☆) are for γ-valerolactone + ethanol, Havasi *et al.* [61].

This publication is available free of charge from: https://doi.org/10.6028/NIST.IR.8357

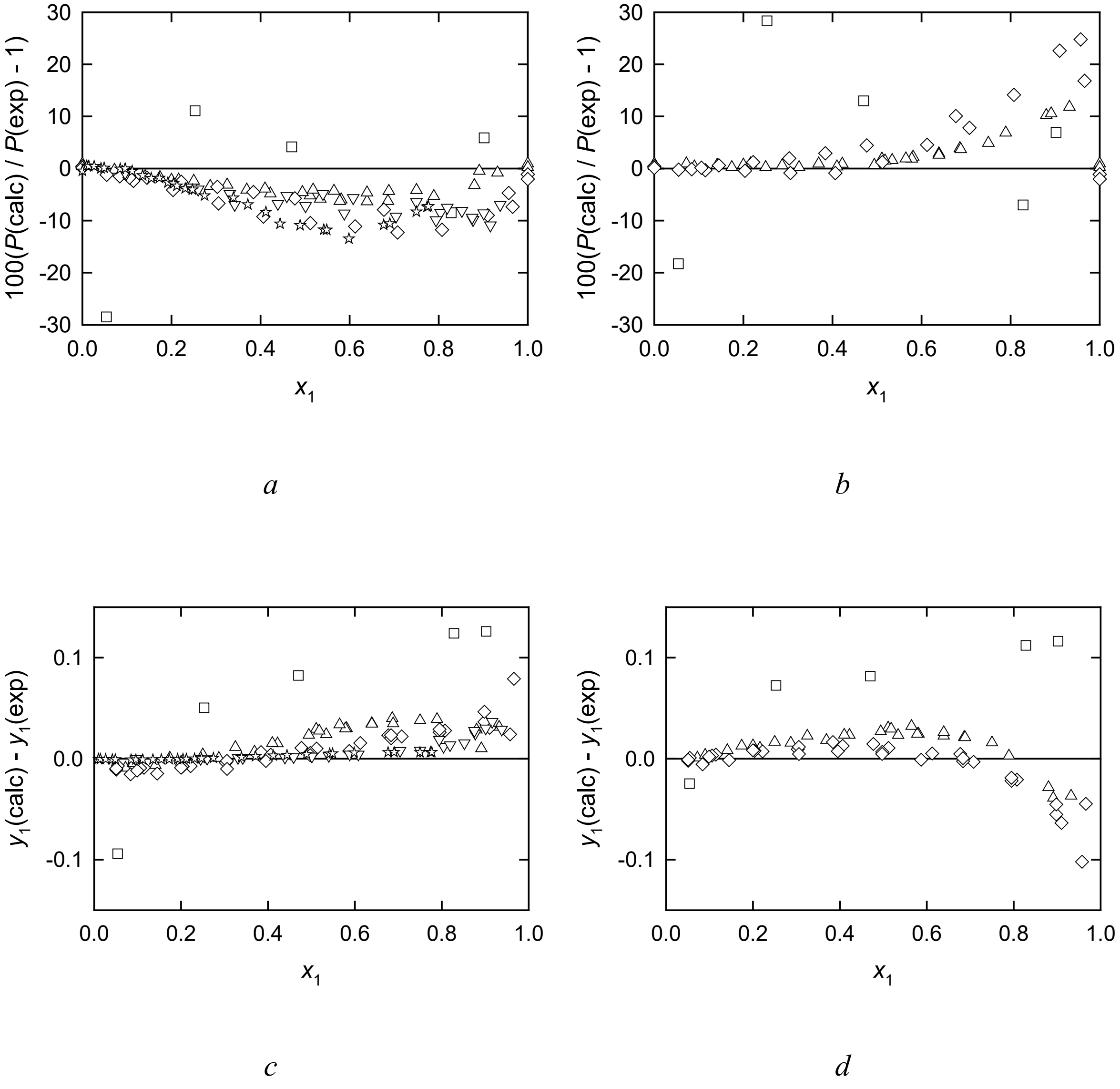

a

b

c

d

Fig. 7. Comparison of the predicted and experimental pressures *P* and first-component mole fractions y_1 in the gas phase at different first-component mole fractions in the liquid phase x_1 for the binaries of furan derivatives with longer-chain alcohols: a, c, NIST-COSMO-SAC; b, d: NIST-Modified UNIFAC.

Triangles (△) are for 2-furaldehyde + 1-butanol, Hauschild *et al.* [52].
Diamonds (◇) are for 2-furaldehyde + 2-butanol, Zaitseva *et al.* [53].
Squares (□) are for 2-furaldehyde + 1-octanol, Rigamonti and Spaccamela Marchetti [62].
Triangles down (▽) are for furfuryl alcohol + 2-propanol, Tai *et al.* [41].
Stars (☆) are for γ-valerolactone + 2-propanol, Havasi *et al.* [61].

This publication is available free of charge from: https://doi.org/10.6028/NIST.IR.8357

3.1.5. VLE with water

(2-furaldehyde + water) is the most studied mixture in this group (Fig. 8). The results for the binaries with furfuryl alcohol and γ-valerolactone are also available. The vapor pressure of water significantly exceeds that of the organic components. At low water content, the consistency between the experimental and predicted pressures and gas-phase compositions will be sensitive to the correctness of the experimental liquid-phase compositions. At x(water) > 0.2 ($x_1 < 0.8$), a good agreement is observed in Fig. 8. However, at x(water) < 0.2, the deviations and agreement between the experimental data are not satisfactory. As demonstrated below, this problem is caused by both systematic errors in determination of the liquid compositions and limitations of the models. A similar problem for (phenol + water) discussed later exists in a significantly shorter mole fraction range (x(water) < 0.05). In Figs. 8b and 8d, there are no data points from x_1 = (0.05 to 0.45). This happens because of the predicted (2-furaldehyde + water) LLE and the lack of the NIST-modified UNIFAC parameters for the other two binaries.

The differences between the computed and experimental pressures of (2-furaldehyde + water) at $x_1 > 0.8$ vary from (-18 to 138) % for NIST-COSMO-SAC and (-18 to 58) % for NIST-modified UNIFAC. Similar deviations in the gas-phase mole fractions are (0.04 to -0.47) and (0.06 to -0.27), respectively. Generally, the deviation increases with pressure/temperature. A scatter of the experimental data is large and additional efforts are required to identify all problematic datasets. Several comments can be made though.

The results of Mains [63] have the largest deviation at x_1 close to unity. The author claimed that the uncertainty of the temperature measurements at $x_1 > 0.78$ was at least 1 K. Also, the gas-phase composition had a significant uncertainty due to fractionation in a flask. Therefore, the *PTxy* dataset from Ref. [63] should not be used. Also, the author provided an improved *Pxy* dataset for water-rich compositions, which does not cover the questionable range.

At T = 338.1 K and x_1 = 0.949, the NIST-COSMO-SAC prediction is 104 % higher than the experimental pressure P = 6.8 kPa reported by Kharin *et al.* [60]. Such a large deviation is not supported by other experimental data [64, 65] at similar pressures and compositions. An identical problem with the results (2-furaldehyde + ethanol) reported in Ref. [60] was discussed in Sec. 3.1.4. Therefore, this dataset should also be excluded.

Sunder and Prasad [67] reported VLE for the entire composition range including the LLE region. The liquid-liquid phase separation was not discussed in that paper. A large uncertainty is expected for these results, as discussed below.

Two isobars at reduced pressure have been reported [68,69] for (furfuryl alcohol + water). The *PTxy* results of Boldyrev *et al.* [68] at P = 7.3 kPa are within the expected deviations from the predicted values. The NIST-COSMO-SAC pressures are systematically higher than the data of Dudutkina *et al.* [55] (P = 4.0 kPa) over the entire composition range, even for very low water content. This is the only dataset demonstrating this behavior. For most points, the predicted pressures are close to P = 4.4 kPa, and the difference may be caused by the incorrect pressure determination. Two experimental points at $x_1 > 0.8$ have very large (> 100 %) differences with the predicted values. This is inconsistent with the deviation trend for the other work [68]. The latter results seem to be preferable, however, new measurements are required to clarify the behavior of this system at $x_1 > 0.8$.

For (γ-valerolactone + water), two consistent datasets are available [70,71]. At $x_1 > 0.8$, the predicted pressures are up to 56 % higher than the experimental counterparts (Fig. 8a), which seems to be caused by the model limitations. The predicted and experimental gas-phase compositions are still in good agreement (Fig. 8b).

Overall, the models demonstrated similar deviations from the experimental VLE pressures and gas-phase compositions (Table 3). The relative standard deviations for the pressures were comparable to those reported previously [23]. For the considered dataset with furan derivatives, the reported vapor pressures of pure liquids have a relative standard deviation of about 2 % from the TDE recommendations, which indicates that the temperature and pressure measurements have a relatively small contribution to the inconsistencies between the predicted and experimental pressures. The NIST-COSMO-SAC model demonstrated significantly lower standard deviations for the binaries with organic components only. Consistency with experimental data was further improved when the problematic data considered above (code N in Table 2) were excluded. Surprisingly, the performance of the NIST-modified UNIFAC model remained virtually the same upon removal of the doubtful data. This limitation seems to be caused by the quality of the training set used to derive the empirical parameters of this model.

This publication is available free of charge from: https://doi.org/10.6028/NIST.IR.8357

This publication is available free of charge from: https://doi.org/10.6028/NIST.IR.8357

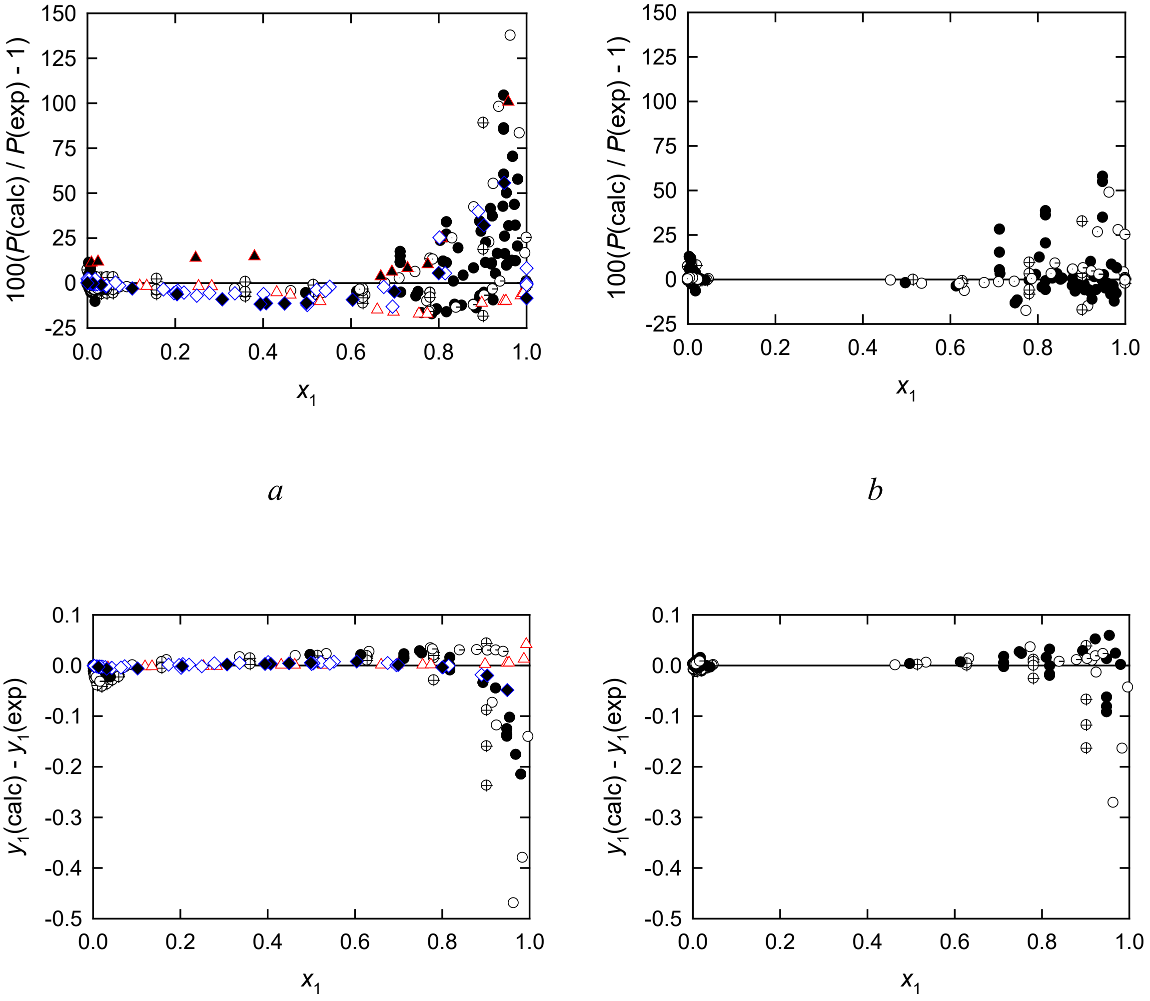

a

b

c

d

Fig. 8. Comparison of the predicted and experimental pressures *P* and first-component mole fractions y_1 in the gas phase at different first-component mole fractions in the liquid phase x_1 for the binaries of furan derivatives with water: a, c, NIST-COSMO-SAC; b, d: NIST-Modified UNIFAC.

Circles are for 2-furaldehyde + water: ○, Mains [63]; ●, Pearce and Gerster [64]; ⊕, Tsirlin [65]; ◑, Kharin *et al.* [60]; ◕, Ni and Wang [58]; ◐, Staroske and Schuberth [66]; ⊙, Sunder and Prasad [67].
Red triangles are for furfuryl alcohol + water: △, Boldyrev *et al.* [68]; ▲, Dudutkina *et al.* [69].
Blue diamonds are for γ-valerolactone + water: ◇, Havasi *et al.* [70]; ◆, Zaitseva *et al.* [71].

This publication is available free of charge from: https://doi.org/10.6028/NIST.IR.8357

Table 3. Statistical analysis of the reported data.

Subset	NIST-COSMO-SAC		NIST-mod. UNIFAC	
	(Rel. std. dev. for p)·100	Std. dev. for y	(Rel. std. dev. for p)·100	Std. dev. for y
Furan derivatives				
All data	12.8	0.042	10.6	0.045
Organics only	8.8	0.038	10.7	0.045
Cleaned dataset w/o water [a]	8.2	0.034	10.6	0.045
Phenolic compounds				
All data	20.5	0.055	19.5	0.069
Organics only	20.9	0.053	19.7	0.068
Cleaned dataset w/o water [a]	12.3	0.052	15.2	0.067

[a] without the data marked with N in Table 2.

This publication is available free of charge from: https://doi.org/10.6028/NIST.IR.8357

3.2. VLE for phenolic compounds

The considered main components are listed in Table 1. Out of 2838 points, 1238 were reported for the phenol binaries; 1511 points are available for monomethylphenols. The points for (phenol + methylphenol) are included in both scores. The high availability of the methylphenol data is explained by the activity of Prasad *et al.* who reported the results for 32 binaries of phenols with alcohols, dimethylbenzenes, and ethylbenzene [95,96,99,103,143,145]. A significant contribution to the VLE studies for phenolic compounds was also made by Weissenberger *et al.* [84,93,94,104,124,134,135,136,146]. The gas-phase compositions were only reported for 36 % of the data points. In many cases, the component volatilities differed significantly, and the more volatile component predominated in the gas phase.

3.2.1. VLE with two phenolic compounds

The phenol mixtures with methylphenols are close to the ideal ones. The pressures predicted with both models are in very good agreement with the experimental results (Fig. 9). The predictions for (1,2-benzenediol + 4-methylphenol) and (1,2-benzenediol + 4-methoxyphenol) (Fig. 10) are also consistent with the experimental data [79]. The only exception is the pressure over pure 1,2-benzenediol at $T = 423.15$ K, which is inconsistent with multiple data available in the literature, per the data analysis performed with NIST ThermoData Engine. For (1,2-benzenediol + 1,4-benzenediol), however, both models consistently predict the experimental pressure of about 25 kPa instead of 20 kPa reported in the original publication [80] despite this mixture is expected to behave as an ideal solution. We believe the results from that work may be incorrect and should not be used. For methylphenols, the agreement between the experimental and predicted values is generally very good (Figs. 11 and 12).

The experimental and predicted gas-phase compositions typically agree within ±0.04 mole fraction. However, differences up to 0.1 mole fraction are observed for some systems (Figs. 10c, 10d, 12d).

This publication is available free of charge from: https://doi.org/10.6028/NIST.IR.8357

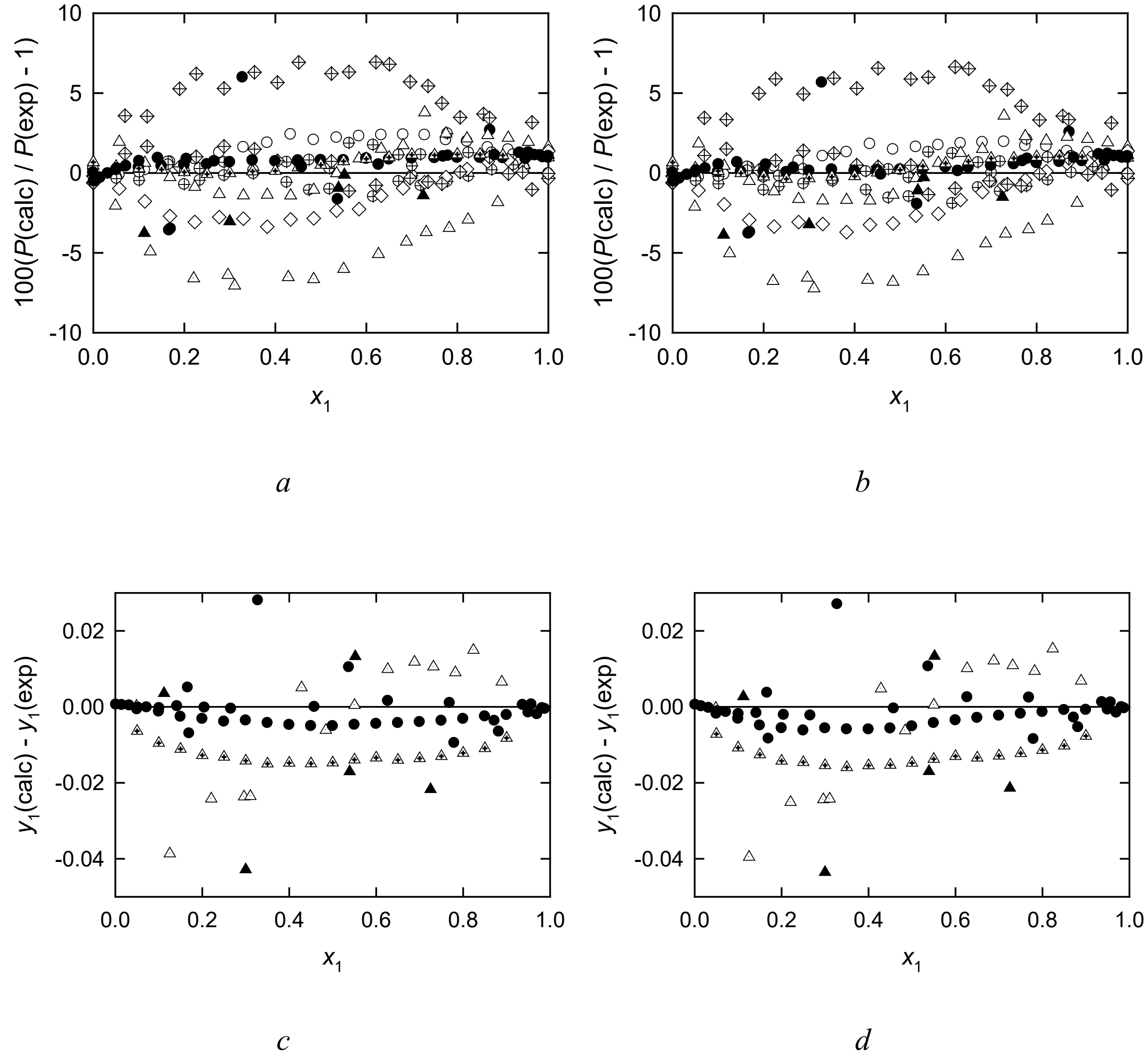

Fig. 9. Comparison of the predicted and experimental pressures *P* and first-component mole fractions y_1 in the gas phase at different first-component mole fractions in the liquid phase x_1 for the binaries of phenol with methylphenols: a, c, NIST-COSMO-SAC; b, d: NIST-Modified UNIFAC.

Circles are for phenol + 2-methylphenol: ○, Fox and Barker [72]; ◑, Schneider and Oberkobusch [73]; ●, Vostrikova *et al.* [74]; ⊗, Clausse *et al.* [75]; ⊕, Selvam *et al.* [76].

Triangles are for phenol + 3-methylphenol: △, Fox and Barker [72]; ◬, Schneider and Oberkobusch [73]; ▲, Vostrikova *et al.* [77]; ⟁, Cepeda *et al.* [78].

Diamonds are for phenol + 4-methylphenol: ◇, Fox and Barker [72]; ⟐, Selvam *et al.* [76].

This publication is available free of charge from: https://doi.org/10.6028/NIST.IR.8357

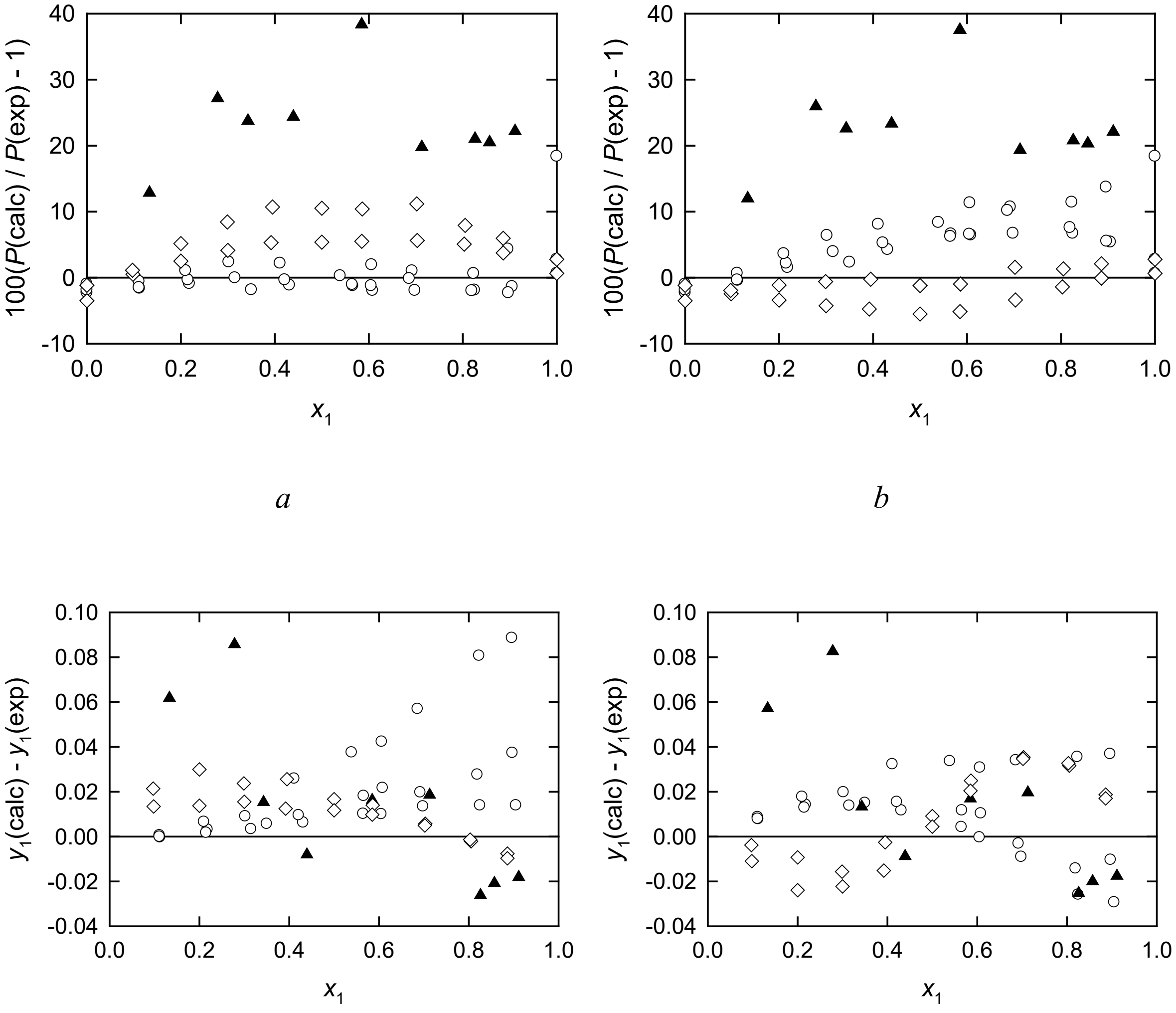

a *b*

c *d*

Fig. 10. Comparison of the predicted and experimental pressures P and first-component mole fractions y_1 in the gas phase at different first-component mole fractions in the liquid phase x_1 for the 1,2-benzenediol binaries: a, c, NIST-COSMO-SAC; b, d: NIST-Modified UNIFAC.

Circles (○) are for 1,2-benzenediol + 4-methylphenol, Hwang *et al.* [79].
Triangles (▲) are for 1,2-benzenediol + 1,4-benzenediol, Shi *et al.* [80].
Diamonds (◇) are for 1,2-benzenediol + 4-methoxyphenol, Hwang *et al.* [79].

This publication is available free of charge from: https://doi.org/10.6028/NIST.IR.8357

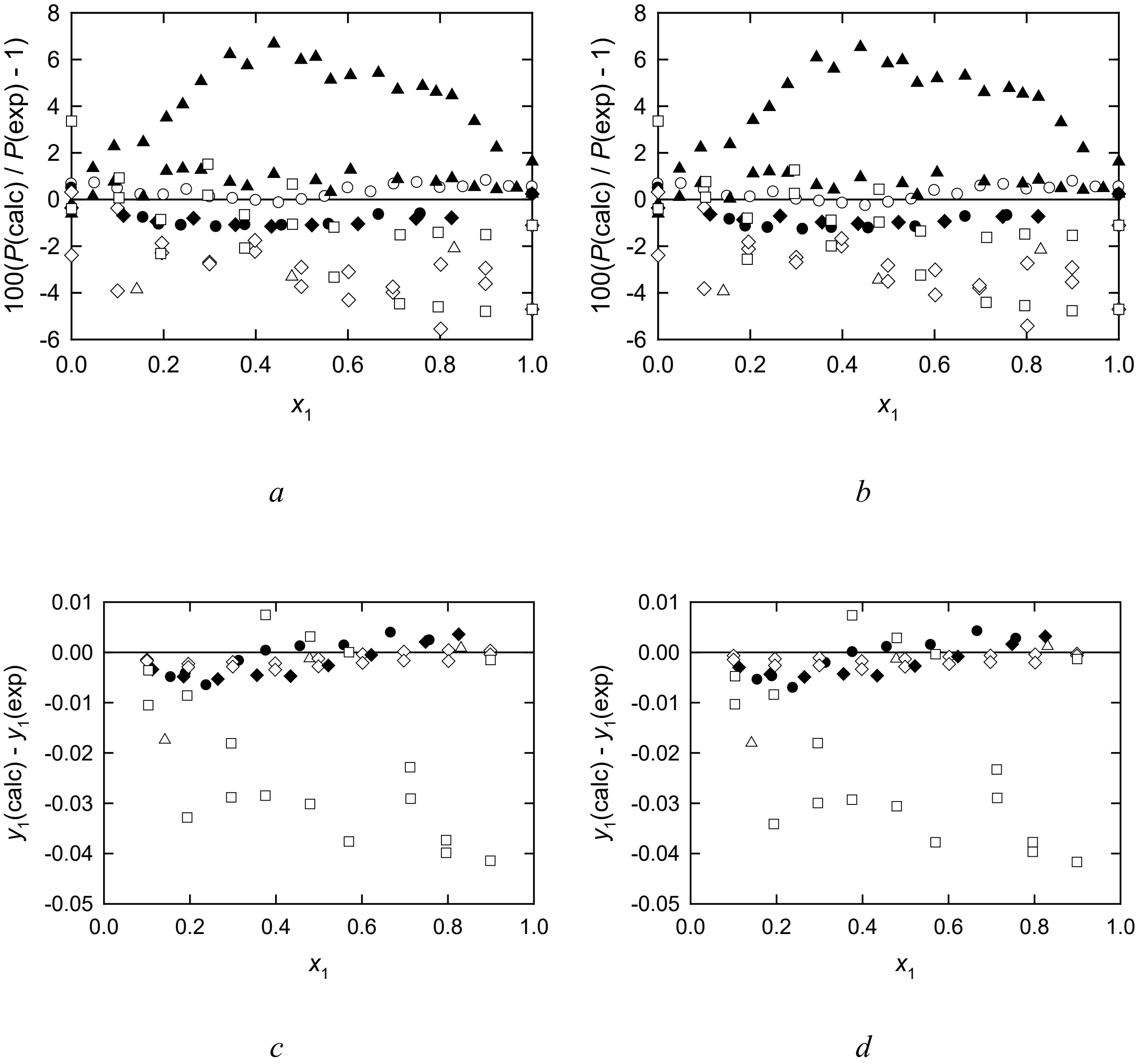

a *b*

c *d*

Fig. 11. Comparison of the predicted and experimental pressures *P* and first-component mole fractions y_1 in the gas phase at different first-component mole fractions in the liquid phase x_1 for the 2-methylphenol binaries: a, c, NIST-COSMO-SAC; b, d: NIST-Modified UNIFAC.

Circles are for 2-methylphenol + 3-methylphenol: ○, Fox and Barker [72]; ●, Wang *et al.* [81].
Triangles are for 2-methylphenol + 4-methylphenol: △, Vostrikova *et al.* [82]; ▲, Selvam *et al.* [76].
Diamonds are for 2-methylphenol + 2,6-dimethylphenol: ◇, Ye *et al.* [83]; ◆, Wang *et al.* [81].
Squares (□) are for 2-methylphenol + 2,4,6-trimethylphenol, Ye *et al.* [83].

This publication is available free of charge from: https://doi.org/10.6028/NIST.IR.8357

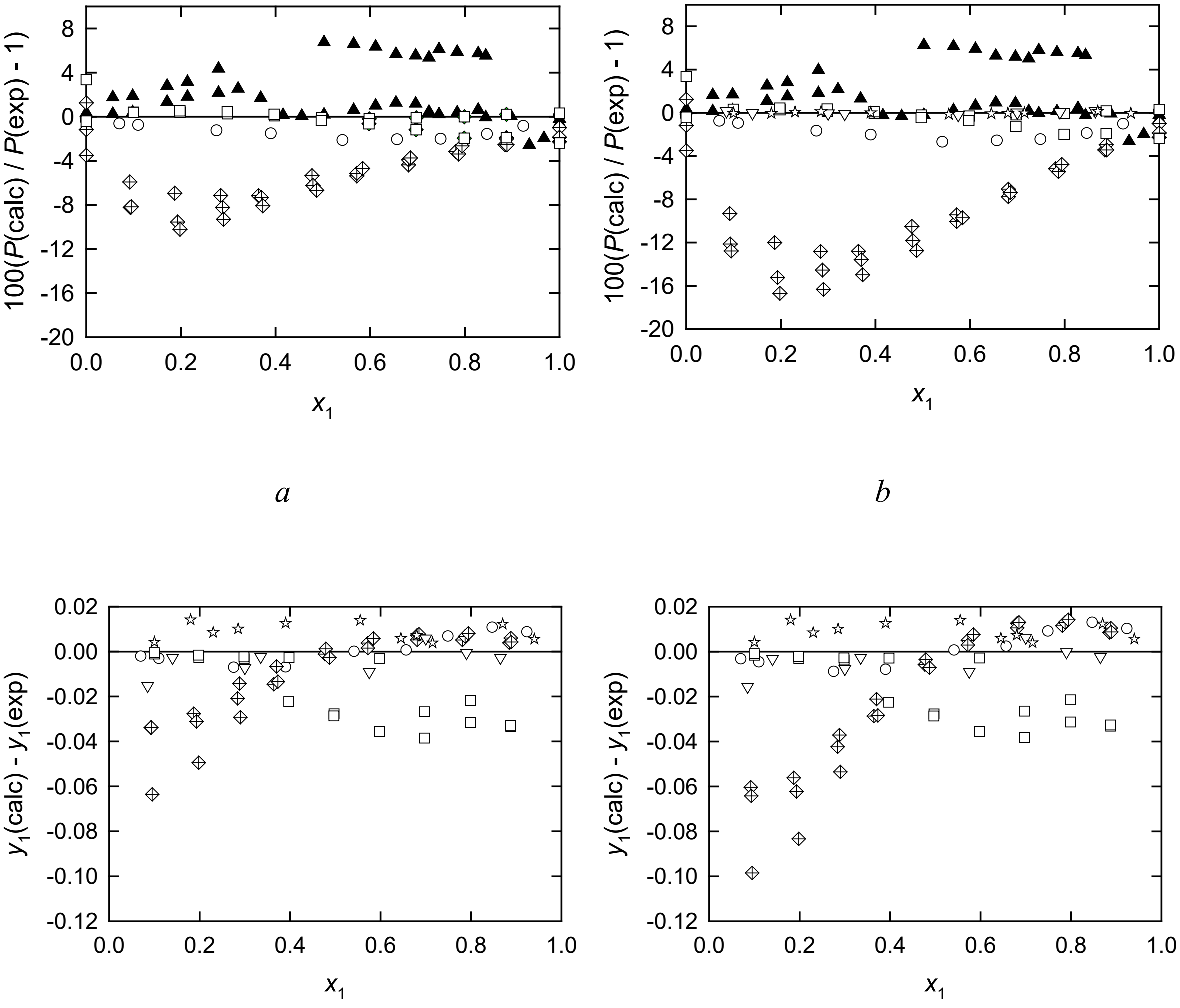

a

b

c

d

Fig. 12. Comparison of the predicted and experimental pressures P and first-component mole fractions y_1 in the gas phase at different first-component mole fractions in the liquid phase x_1 for the binaries with methylphenols: a, c, NIST-COSMO-SAC; b, d: NIST-Modified UNIFAC.

Circles (○) are for 3-methylphenol + 2,6-dimethylphenol, Wang *et al.* [81].
Triangles (▲) are for 4-methylphenol + 2,4-dimethylphenol, Selvam *et al.* [76].
Diamonds (◈) are for 4-methylphenol + 4-methoxyphenol, Hwang *et al.* [79].
Triangles down (▽) are for 2,5-dimethylphenol + 3,5-dimethylphenol, Schneider and Oberkobusch [73]. The equilibrium temperature for the point at $x_1 = 0.200$ is inconsistent with the other results and not shown here.
Stars (☆) are for 3,4-dimethylphenol + 3,5-dimethylphenol, Schneider and Oberkobusch [73].
Squares (□) are for 2,6-dimethylphenol + 2,4,6-trimethylphenol, Ye *et al.* [83].

This publication is available free of charge from: https://doi.org/10.6028/NIST.IR.8357

3.2.2. VLE with benzene and alkylbenzenes

Agreement between the experimental and predicted values for the binaries with phenol is very good at the low content of phenol and satisfactory when its mole fraction is high (Fig. 13). For the other phenols, the results of Prasad *et al.* [95,96,99,103] predominate. Significant data scatter and the non-systematic nature of the deviations (empty symbols in Figs. 14–16) for chemically similar systems indicate that these results have a large uncertainty. For example, the maximum deviation of the vapor pressures predicted with NIST-COSMO-SAC from the experimental values are 40 %, 30 %, 19 %, and 7 % for the 2-methylphenol binaries with 1,3-dimethyl-, 1,2-dimethyl-, ethyl-, and 1,4-dimethylbenzene, respectively. The trend remains for the predictions with NIST-modified UNIFAC though the magnitude of deviations change. Even larger (>150 %) non-systematic deviations can be found in the data for alkylphenols with alcohols discussed below. For many binaries, the results by Prasad *et al.* are the only available data. However, one should avoid using them because of their low reliability.

The NIST-COSMO-SAC predicted pressures for the isomeric methylphenol binaries with benzene and the phenol binaries with benzene and toluene systematically deviate from the values reported by Weissenberger *et al.* [84,93]. The deviation is lower for the predictions with the NIST-modified UNIFAC. All results from these works seem to have a large uncertainty though poor model performance cannot be fully excluded. More experimental data are necessary to resolve this inconsistency.

The (3-methylphenol + benzene) pressures reported by Savitt and Othmer [97] and the gas-phase compositions of 2-methylnaphthalene binaries from the same laboratory [100] have anomalously high deviations from the values predicted by both models (Figs. 15 and 16). The pressures [97] have the largest deviations among all similar systems and seem to have a large uncertainty of the reported VLE temperatures. The gas-phase composition problem is not that obvious. These results are the only data for 2-methylnaphthalene mixtures at P = 101 kPa and the equilibrium temperatures are high (close to 500 K). Therefore, the available information is not conclusive and more experimental efforts are required to resolve this inconsistency.

The pressures of (2-methoxyphenol + benzene) [104] significantly deviate from the ones predicted with NIST-modified UNIFAC (Fig. 16b). This inconsistency is not observed for the NIST-COSMO-SAC predictions and is probably due to parameterization of the former model.

This publication is available free of charge from: https://doi.org/10.6028/NIST.IR.8357

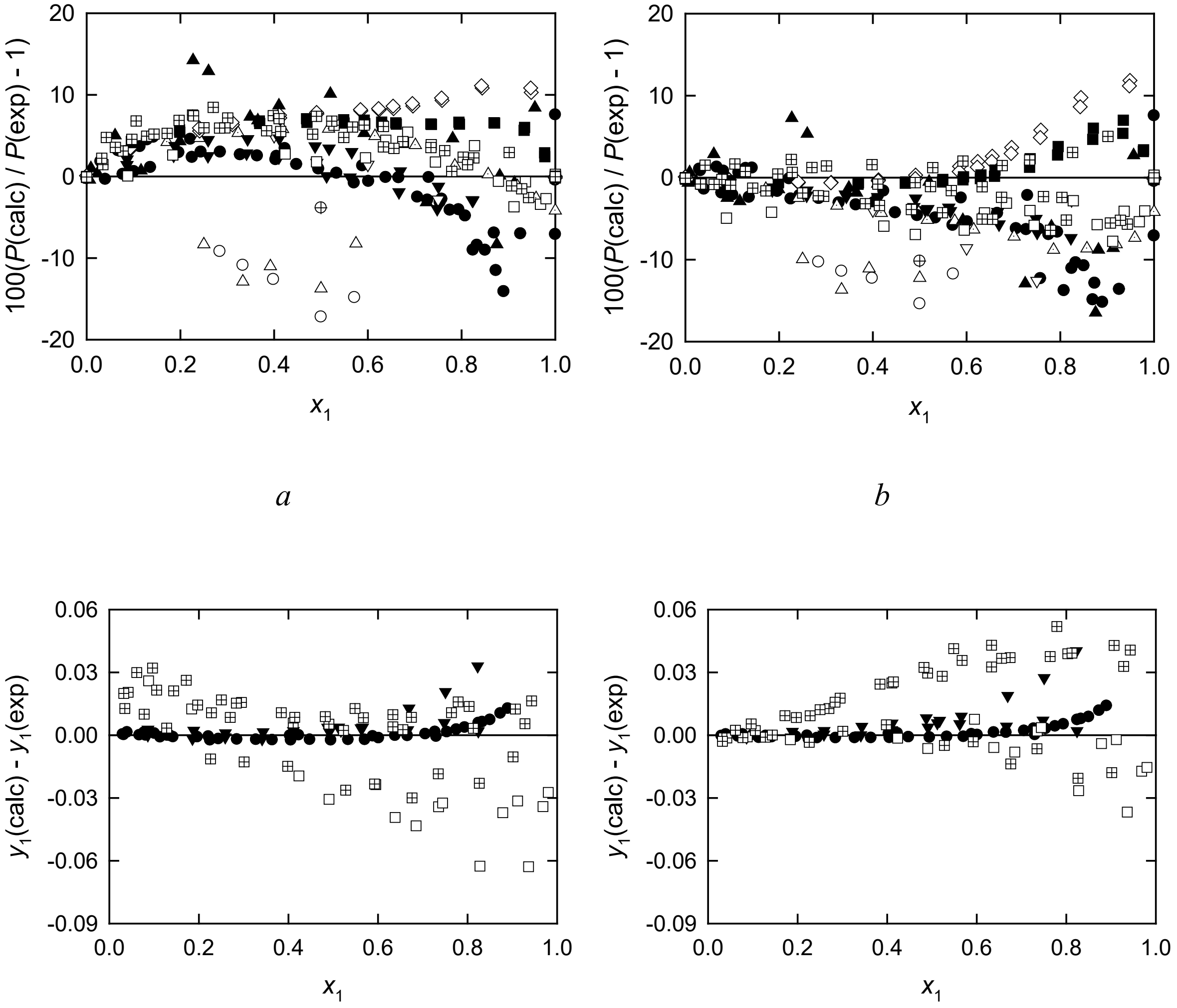

a *b*

c *d*

Fig. 13. Comparison of the predicted and experimental pressures *P* and first-component mole fractions y_1 in the gas phase at different first-component mole fractions in the liquid phase x_1 for the binaries of phenol with alkylbenzenes: a, c, NIST-COSMO-SAC; b, d: NIST-Modified UNIFAC.

Circles are for phenol + benzene: ○, Weissenberger *et al.* [84]; ●, Martin and George [85]; ⊕, Garner and Ellis [36]; ⧗, Gmehling [86]; ◑, Nienhaus *et al.* [87].

Triangles are for phenol + toluene: △, Weissenberger *et al.* [84]; ▲, Drickamer *et al.* [88]; ▽, Garner and Ellis [36]; ◬, Nienhaus *et al.* [87]; ▼, Klauck *et al.* [89].

Diamonds (◇) are for phenol + ethylbenzene, Anderko [90].

Squares are for phenol + isopropylbenzene: □, Byk and Stroiteleva [91]; ■, Anderko [90]; ⊞, Cepeda *et al.* [92].

This publication is available free of charge from: https://doi.org/10.6028/NIST.IR.8357

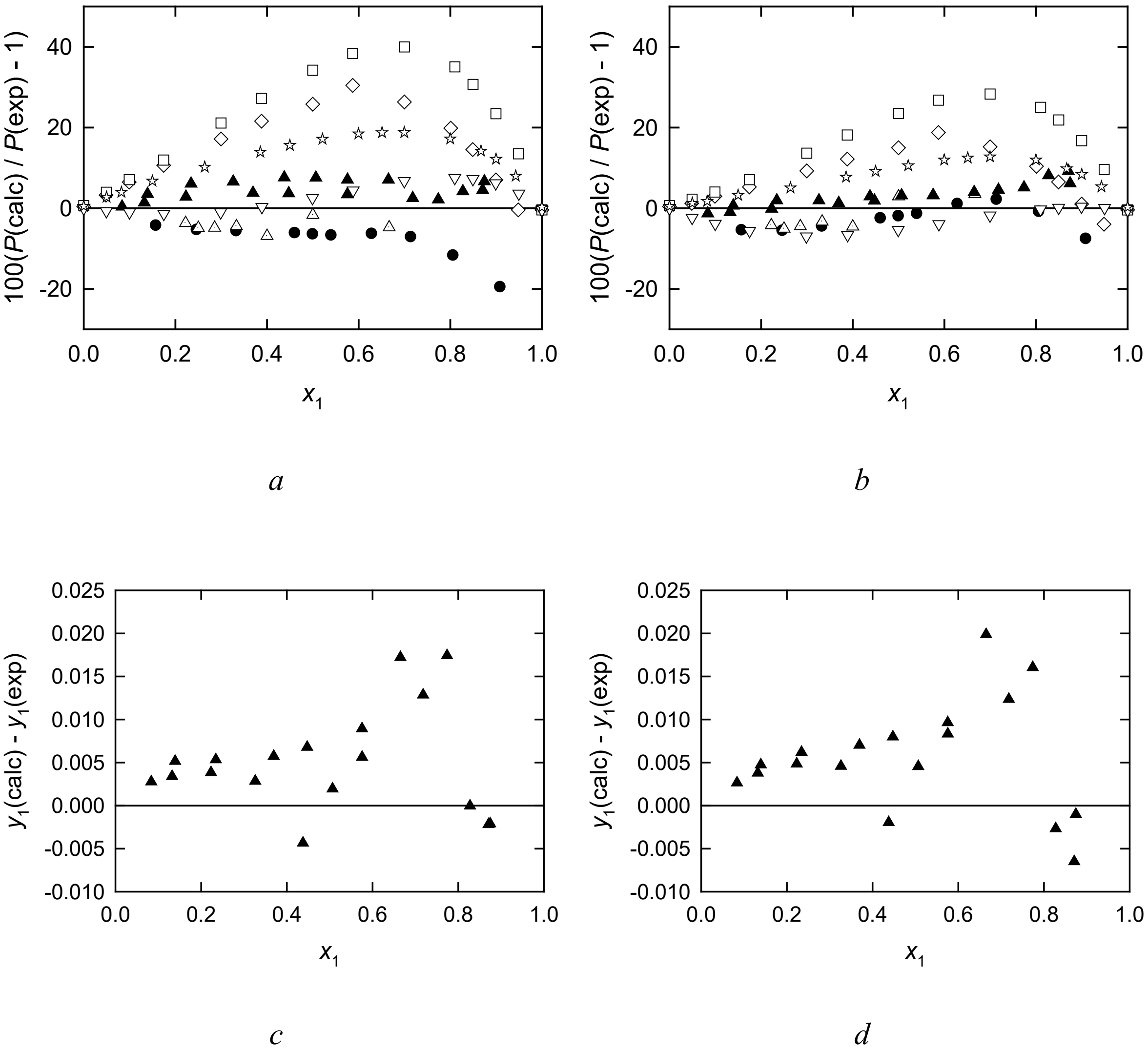

Fig. 14. Comparison of the predicted and experimental pressures *P* and first-component mole fractions y_1 in the gas phase at different first-component mole fractions in the liquid phase x_1 for the binaries of 2-methylphenol with alkylbenzenes: a, c, NIST-COSMO-SAC; b, d: NIST-Modified UNIFAC.

Circles (●) are for 2-methylphenol + benzene, Weissenberger and Piatti [93].
Triangles are for 2-methylphenol + toluene: △, Weissenberger *et al.* [94]; ▲, Klauck *et al.* [89].
Diamonds (◇) are for 2-methylphenol + 1,2-dimethylbenzene, Prasad *et al.* [95].
Squares (□) are for 2-methylphenol + 1,3-dimethylbenzene, Prasad *et al.* [95].
Triangles down (▽) are for 2-methylphenol + 1,4-dimethylbenzene, Prasad *et al.* [95].
Stars (☆) are for 2-methylphenol + ethylbenzene, Prasad *et al.* [96].

This publication is available free of charge from: https://doi.org/10.6028/NIST.IR.8357

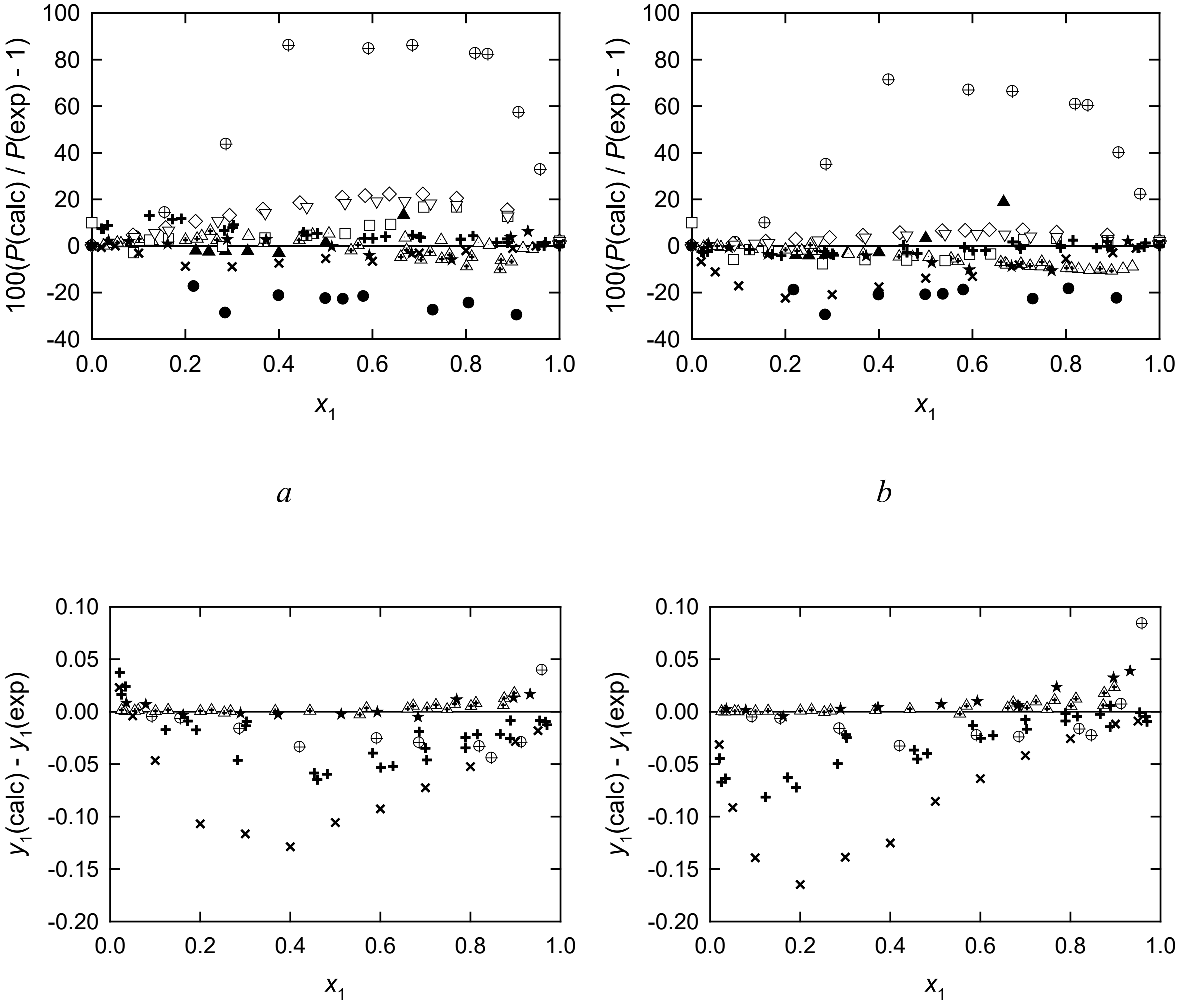

a *b*

c *d*

Fig. 15. Comparison of the predicted and experimental pressures *P* and first-component mole fractions y_1 in the gas phase at different first-component mole fractions in the liquid phase x_1 for the binaries of 3-methylphenol with alkylbenzenes and 2-methylnaphthalene: a, c, NIST-COSMO-SAC; b, d: NIST-Modified UNIFAC.

Circles are for 3-methylphenol + benzene: ●, Weissenberger and Piatti [93]; ⊕, Savitt and Othmer [97].
Triangles are for 3-methylphenol + toluene: ▲, Weissenberger *et al.* [94]; △, Sartakova *et al.* [98]; ◬, Klauck *et al.* [89].
Diamonds (◇) are for 3-methylphenol + 1,2-dimethylbenzene, Prasad *et al.* [99].
Squares (□) are for 3-methylphenol + 1,3-dimethylbenzene, Prasad *et al.* [99].
Triangles down (▽) are for 3-methylphenol + 1,4-dimethylbenzene, Prasad *et al.* [99].
Stars (★) are for 3-methylphenol + isopropylbenzene, Cepeda *et al.* [78].
3-methylphenol + 2-methylnaphthalene: ×, Othmer *et al.* [100]; +, Schmelzer *et al.* [101].

This publication is available free of charge from: https://doi.org/10.6028/NIST.IR.8357

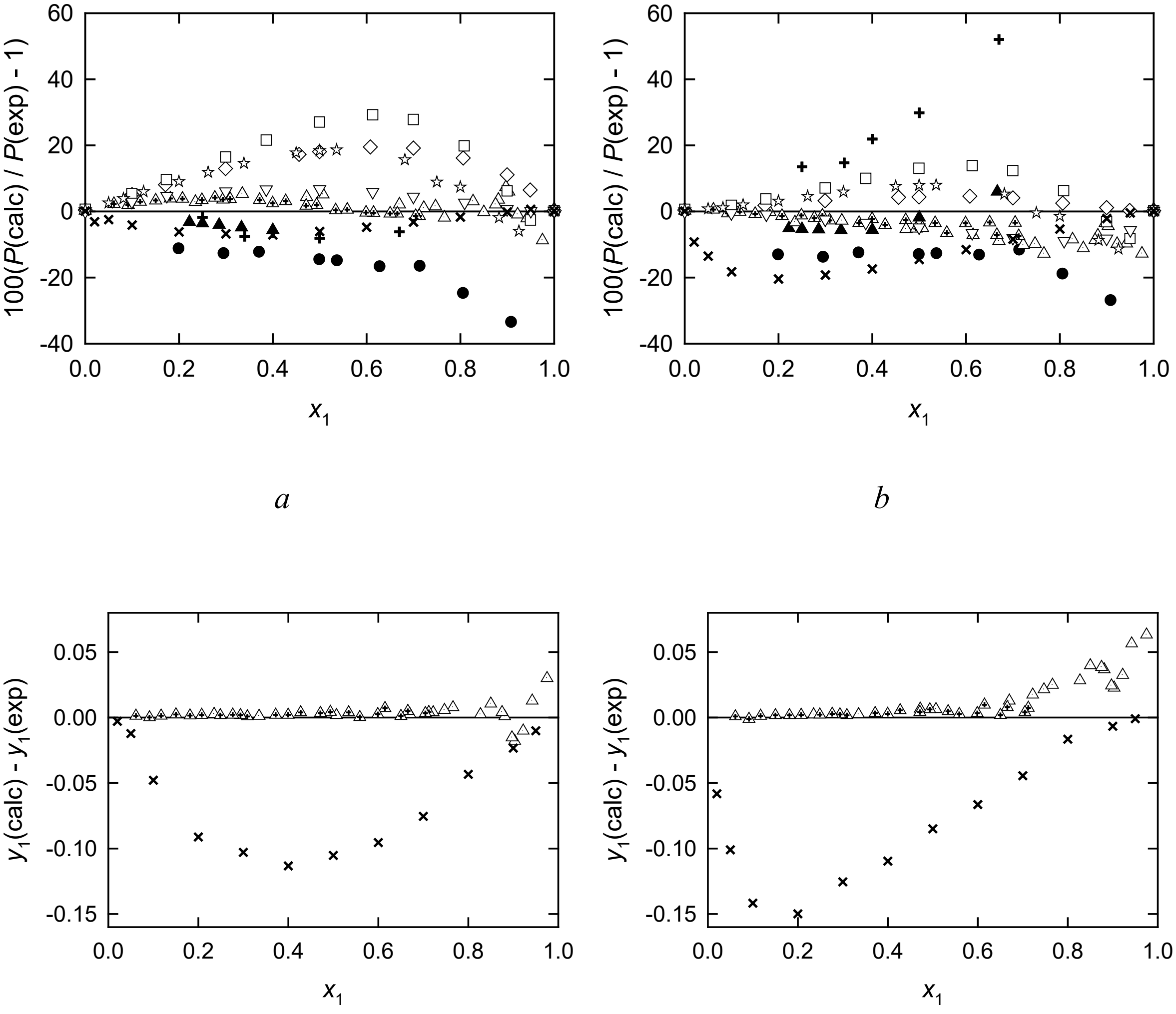

a *b*

c *d*

Fig. 16. Comparison of the predicted and experimental pressures *P* and first-component mole fractions y_1 in the gas phase at different first-component mole fractions in the liquid phase x_1 for the binaries of 4-methylphenol and 2-methoxyphenol with alkylbenzenes: a, c, NIST-COSMO-SAC; b, d: NIST-Modified UNIFAC.

Circles (●) are for 4-methylphenol + benzene, Weissenberger and Piatti [93].
Triangles are for 4-methylphenol + toluene: ▲, Weissenberger *et al.* [94]; △, Marks and Wingard [102]; ⚠, Klauck *et al.* [89].
Diamonds (◇) are for 4-methylphenol + 1,2-dimethylbenzene, Prasad *et al.* [103].
Squares (☐) are for 4-methylphenol + 1,3-dimethylbenzene, Prasad *et al.* [103].
Triangles down (▽) are for 4-methylphenol + 1,4-dimethylbenzene, Prasad *et al.* [103].
Stars (☆) are for 4-methylphenol + ethylbenzene, Prasad *et al.* [96].
Crosses (✕) are for 4-methylphenol + 2-methylnaphthalene, Othmer *et al.* [100].
Pluses (+) are for 2-methoxyphenol + benzene, Weissenberger *et al.* [104].

3.2.3. VLE with methoxybenzene

VLE phenol derivatives with methoxybenzene has been studied in two works [105, 106] (Fig. 17). Lebedeva *et al.* [105] reported VLE of phenol and 2-methylphenol with methoxybenzene at $P = 13.3$ kPa. NIST-COSMO-SAC predicts pressures of (15 to 17) kPa for most points. NIST-Modified UNIFAC has better agreement with the experimental values for (phenol + methoxybenzene) at x(phenol) = (0.3 to 0.9). Unlike the gas-phase compositions obtained with the NIST-modified UNIFAC, the ones predicted with the NIST-COSMO-SAC for (phenol + methoxybenzene) were consistent with the experimental values. The models are consistent for P and y of (2-methylphenol + methoxybenzene), but inconsistent with experimental results.

Both pressures and gas-phase compositions for (2-methoxyphenol + methoxybenzene) [106] agree with the model predictions very well. All considered systems have similar intermolecular interactions. Thus, in the former work, the experimental problems seem to occur.

3.2.4. VLE with water

In this group (Figs. 18 and 19), (phenol + water) is the most studied binary. The volatility of water is significantly higher than that of the phenols, and their mole fraction in the gas phase remains small over a wide range of liquid compositions. The differences between the predicted and experimental gas-phase mole fractions are expectedly small up to x(phenols) = 0.95.

Good agreement between the experimental and predicted pressures for (phenol + water) holds at x(phenol) < 0.4. At higher x(phenol), the deviations increase reaching ±80 % at the right-hand side of the graphs. Typically, the predicted values are higher than the experimental ones. At least, four problematic sources can be identified. The pressures reported by Campbell and Campbell for SVLE [111] are about 40 % lower than the predicted values over the considered concentration range (x_1 = (0.38 to 0.87)) and significantly deviate from most other experimental data at $x_1 < 0.6$. The gas-phase compositions from this work are reasonable. Thus, one can conclude that the problem is due to incorrect pressure measurements.

The pressures reported by Kiva *et al.* [116] originate from the same laboratory as the problematic data [105] discussed above. Their reliability is questionable as well. The scatter of the data of Shi et al. [80] is very large. The irregular deviations from the pressures predicted with NIST-COSMO-SAC vary from (1 to 86) %, which is highly unexpected. Brusset and Gaynès [112] reported VLE for (phenol + water) and (2-methylphenol + water). For these systems, large deviations from the pressures and mole fractions predicted with both models are observed at the large content of the phenols. For (phenol + water), these deviations are not supported by other experimental data at high x_1 including those of Chou et al. [121] at the same pressure. The reliability of these results is questionable.

All (phenol + water) pressures reported by Schükarew [108] are in very good agreement with the predictions except the one at $x_1 = 0.8511$. The vapor pressure of phenol at $T = 288.2$ K [113] is too low for the liquid phase and should be assigned to the crystal.

This publication is available free of charge from: https://doi.org/10.6028/NIST.IR.8357

After exclusion of the problematic data, the data scatter for the pressure over (phenol + water) becomes comparable with that for the other binaries. We believe that the large scatter for (water + furan derivatives) discussed above (Fig. 8) is partially caused by issues in the experimental data as well, although no compelling reason to exclude these data could be identified. More efforts are needed to further clarify this.

This publication is available free of charge from: https://doi.org/10.6028/NIST.IR.8357

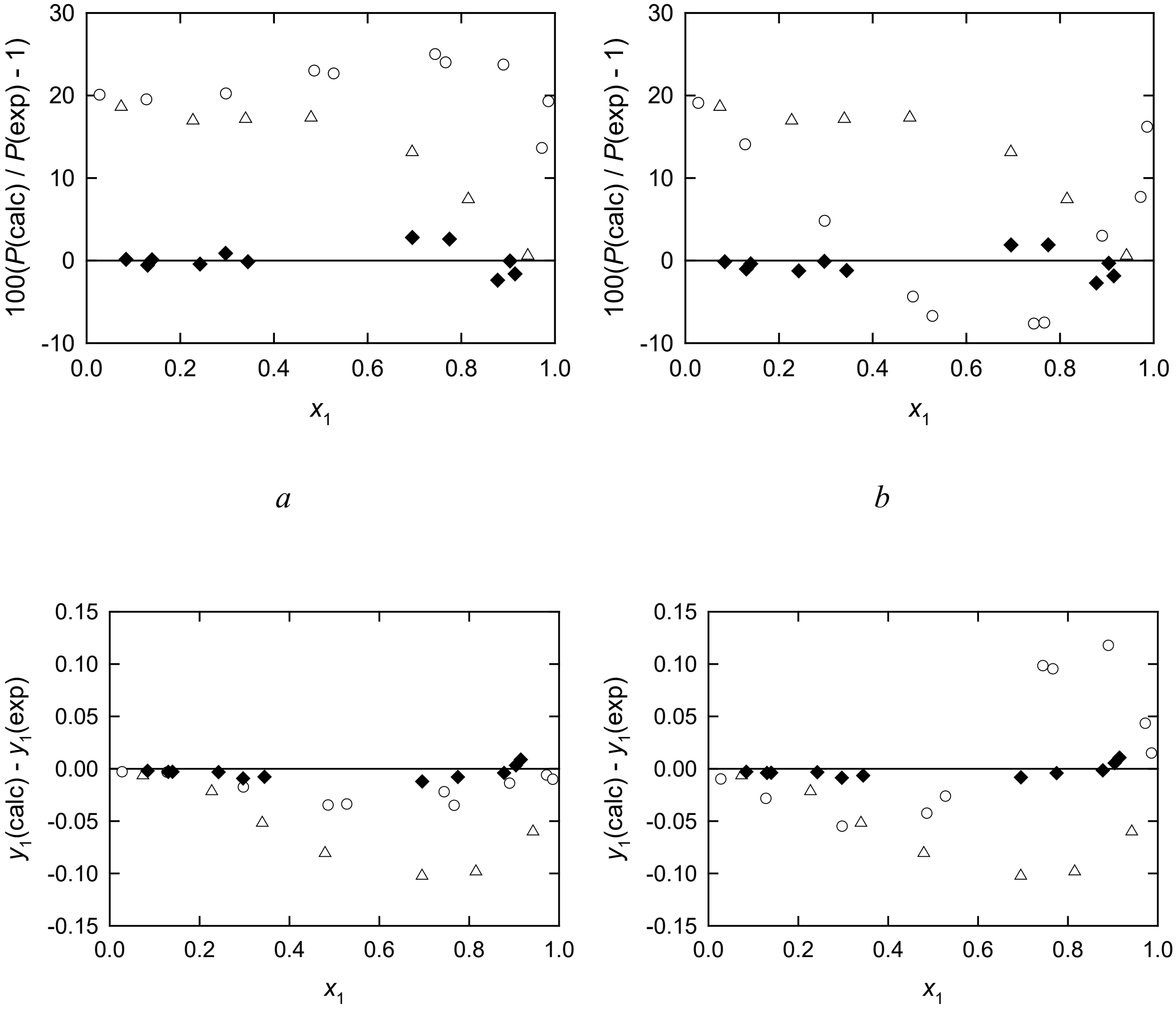

a *b*

c *d*

Fig. 17. Comparison of the predicted and experimental pressures *P* and first-component mole fractions y_1 in the gas phase at different first-component mole fractions in the liquid phase x_1 for the binaries with methoxybenzene: a, c, NIST-COSMO-SAC; b, d: NIST-Modified UNIFAC.

Circles (○) are for phenol + methoxybenzene, Lebedeva *et al.* [105].
Triangles (△) are for 2-methylphenol + methoxybenzene, Lebedeva *et al.* [105].
Diamonds (◆) are for 2-methoxyphenol + methoxybenzene, Li *et al.* [106].

This publication is available free of charge from: https://doi.org/10.6028/NIST.IR.8357

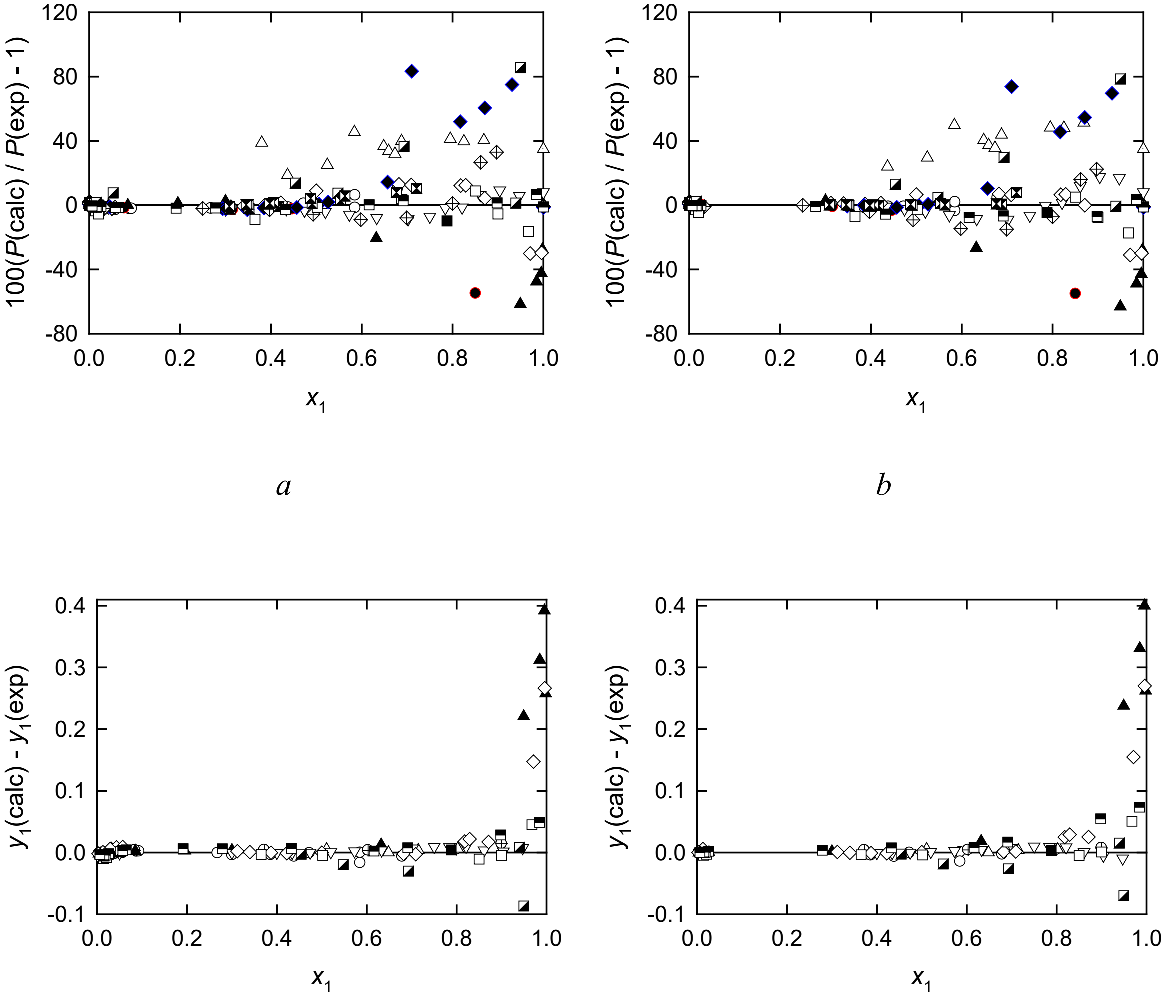

a *b*

c *d*

Fig. 18. Comparison of the predicted and experimental pressures P and first-component mole fractions y_1 in the gas phase at different first-component mole fractions in the liquid phase x_1 for (phenol + water): a, c, NIST-COSMO-SAC; b, d: NIST-Modified UNIFAC.

Circles: ○, Schreinemakers [107]; ●, Schükarew [108]; ⊕, Rhodes *et al.* [109] (pressure not available); ◑, Ferguson [110].

Triangles: △, Campbell and Campbell [111]; ▲, Brusset and Gaynès [112]; ◬, Markuzin [113]; ▽, Weller *et al.* [114].

Diamonds: ◇, Kliment *et al.* [115]; ◆, Kiva *et al.* [116]; ⟡, Kolyuchkina *et al.* [117]; ⬗, Hakuta [118].

Squares: □, Karavaeva *et al.* [119]; ■, Lyzlova and Susarev [120]; ⬒, Chou *et al.* [121]; ⊞, Tabai *et al.* [122]; ◪, Shi *et al.* [80]; ⧗, Klauck *et al.* [89].

This publication is available free of charge from: https://doi.org/10.6028/NIST.IR.8357

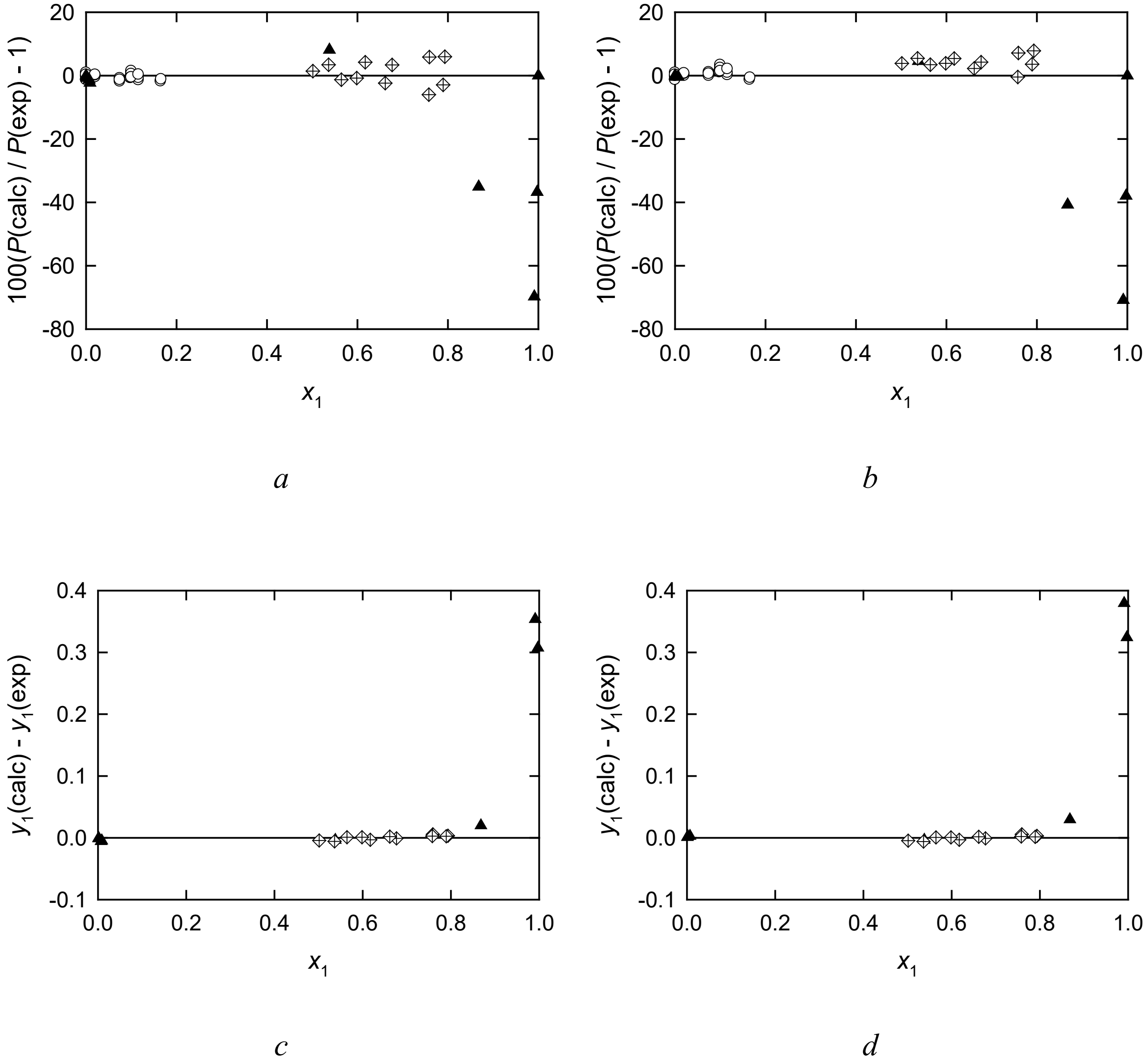

a

b

c

d

Fig. 19. Comparison of the predicted and experimental pressures P and first-component mole fractions y_1 in the gas phase at different first-component mole fractions in the liquid phase x_1 for the binaries with water: a, c, NIST-COSMO-SAC; b, d: NIST-Modified UNIFAC.

Circles (○) are for 1,3-benzenediol + water, Shakhparonov and Martynova [123].
Triangles (▲) are for 2-methylphenol + water: Brusset and Gaynès [112].
Diamonds (◇) are for 3-methylphenol + water: Klauck *et al.* [89].

This publication is available free of charge from: https://doi.org/10.6028/NIST.IR.8357

3.2.5. VLE with ketones

The results for the ketone binaries are presented in Figs. 20 and 21. The predicted pressures of (phenol + acetone) at high x(phenol) are typically lower than the experimental counterparts. The large deviations (up to 70 %) are caused by either flawed predictions or problematic experimental data. With the current information, neither of the options can be proven. For the other binaries with phenol, the agreement is significantly better.

Several data sets are found to be problematic. Comparison of the pressures of (phenol + acetone) from Ref. [124] and (phenol + butanone) from Ref. [129] with the results from both considered models and other experimental data for these mixtures (Figs. 20a and 20b) indicates that the pressures reported in these works are too low. The (phenol + acetone) pressures and gas-phase compositions at $P \approx 0.1$ MPa [127] have large deviation from the other sources reporting the results at this pressure [125,128] and the predicted data. Therefore, these results should be discarded.

The pressures predicted with the two considered models for the binaries with substituted phenols (Fig. 21) are inconsistent. The reason for this discrepancy cannot currently be determined. Another problem to be solved is an unexpectedly large deviation of the gas-phase compositions for (2-methylphenol + acetone) [125] from the predictions (Figs. 20c, 20d, 21c, 21d). Similar deviations are observed in the results on (phenol + methanol) and (2-methylphenol + methanol) from the same laboratory discussed later.

This publication is available free of charge from: https://doi.org/10.6028/NIST.IR.8357

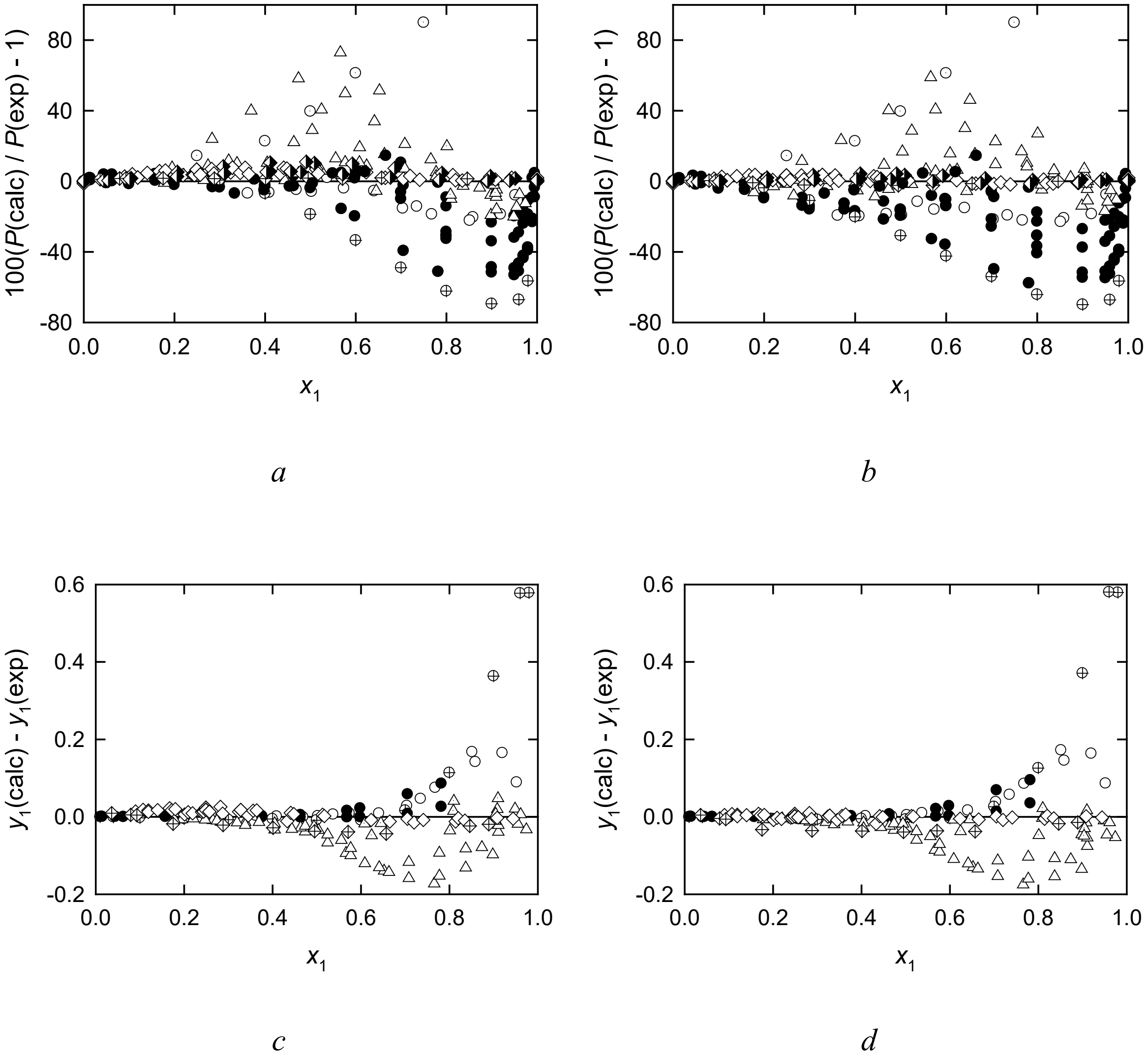

a *b*

c *d*

Fig. 20. Comparison of the predicted and experimental pressures *P* and first-component mole fractions y_1 in the gas phase at different first-component mole fractions in the liquid phase x_1 for the binaries of phenol with ketones: a, c, NIST-COSMO-SAC; b, d: NIST-Modified UNIFAC.

Circles are for phenol + acetone: ⧗, Weissenberger *et al.* [84]; ⊙, Weissenberger *et al.* [124]; ○, Chalov *et al.* [125]; ●, Gölles [126]; ⊕, Motina *et al.* [127]; ◑, Vasil'eva *et al.* [128].

Triangles are for phenol + butanone: △, Byk and Shcherbak [129]; △, Oscarson *et al.* [130].

Diamonds are for phenol + acetophenone: ◇, Fried and Pick [131]; ◈, Aarna and Kaps [132], ⬗, Giles and Wilson [133].

This publication is available free of charge from: https://doi.org/10.6028/NIST.IR.8357

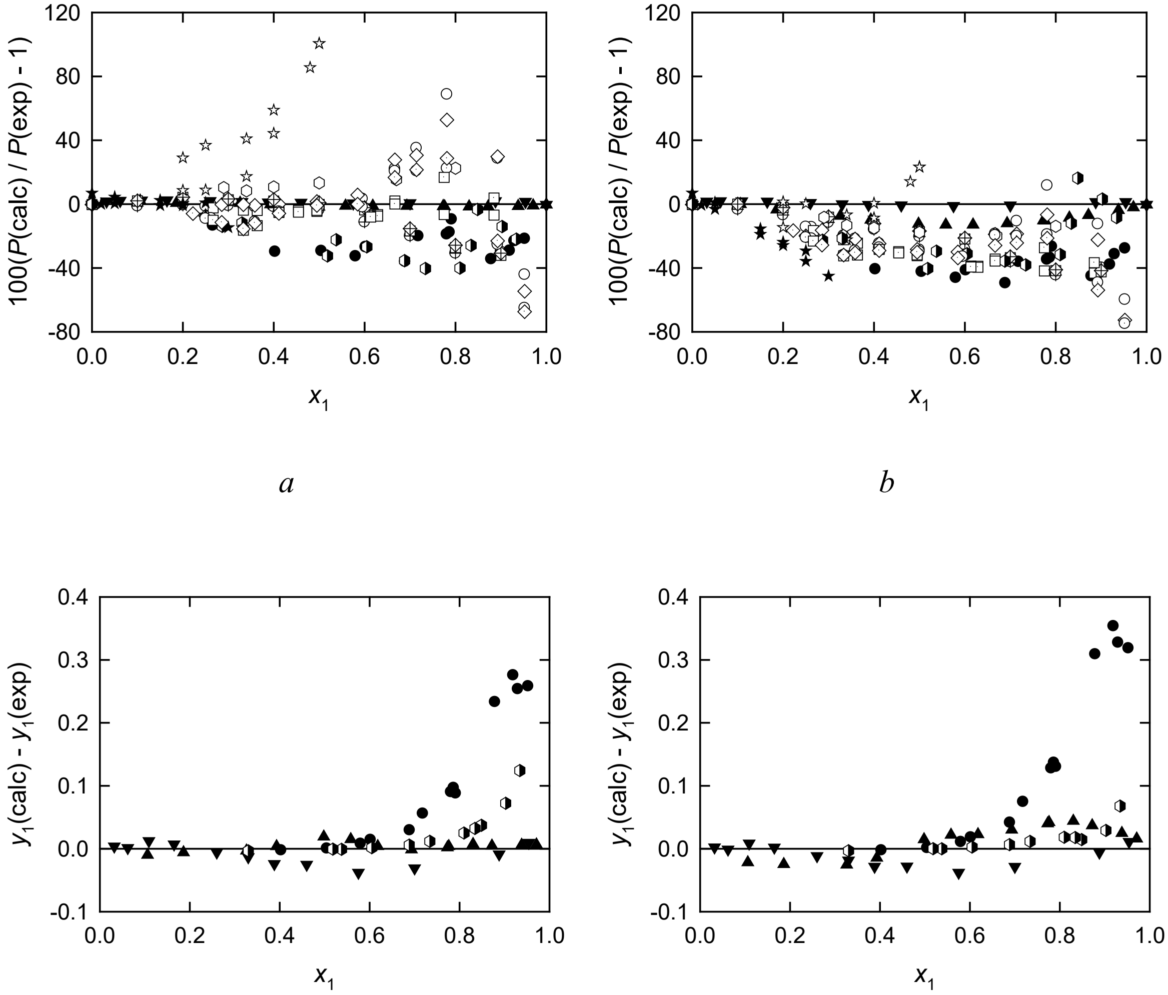

a

b

c

d

Fig. 21. Comparison of the predicted and experimental pressures *P* and first-component mole fractions y_1 in the gas phase at different first-component mole fractions in the liquid phase x_1 for the binaries of phenolic compounds with ketones: a, c, NIST-COSMO-SAC; b, d: NIST-Modified UNIFAC.

Circles are for 2-methylphenol + acetone: ○, Weissenberger and Schuster [134]; ⊙, Weissenberger and Piatti [135]; ⊕, Piatti [136]; ●, Chalov *et al.* [125].

Triangles (▲) are for 2-methylphenol + 2-octanone: filled, Aarna and Kaps [132]

Triangles down (▼) are for 2-methylphenol + acetophenone, Aarna and Kaps [132].

Squares are for 3-methylphenol + acetone: □, Weissenberger and Schuster [134]; ⊡, Weissenberger and Piatti [135]; ⊞, Piatti [136].

Diamonds are for 4-methylphenol + acetone: ◇, Weissenberger and Schuster [134]; ⟐, Weissenberger and Piatti [135]; ◈, Piatti [136].

Stars are for 1,3-benzenediol + acetone: ☆, Weissenberger *et al.* [104]; ★, Shakhparonov and Martynova [123].

Hexagons are for 2-methoxyphenol + acetone: ⬡, Weissenberger *et al.* [104]; ⬢, Chalov *et al.* [125].

This publication is available free of charge from: https://doi.org/10.6028/NIST.IR.8357

3.2.6. VLE with alcohols

For this group of compounds, the values predicted with the models considered are not always consistent. This can be explained by two factors: (i) different treatment of H-bonding, which plays an important part for these systems, and (ii) individual parameters for methanol in NIST-modified UNIFAC.

For (phenol + alcohols), a good consistency of the experimental VLE pressures with the ones predicted with the NIST-COSMO-SAC is observed (Fig. 22a). The predicted values are about 20 % low near x(phenol) = 0.85. The data scatter for the UNIFAC predictions is larger (Fig. 22b). For the VLE with 2- and 4-methylphenols, the general trend is similar to the one for phenol. The data scatter for the pressures over (3-methylphenol + alcohols) is too large to make any conclusion.

The questionable results of Prasad *et al.* introduce a significant noise to the graphs. A very large positive deviation from the NIST-COSMO-SAC predictions is observed for the pressures of (2-methylphenol + methanol) [143] (Fig. 23a). The predicted values are consistent with the other two datasets available for this binary [134, 125]. The results of Prasad *et al.* with three other alcohols demonstrate the largest negative deviation. The problematic dataset with methanol is not revealed with NIST-modified UNIFAC though, per this model, the datasets for this binary are not consistent (Fig. 23b).

Several vapor pressure datasets for (3-methylphenol + alcohol) reported by Prasad et al. [145] (four for NIST-COSMO-SAC and three for NIST-modified UNIFAC) are inconsistent with the predicted values with the deviations exceeding 150 % (Fig. 24). The results from this laboratory have the largest deviation for (4-methylphenol + methanol, ethanol, and 1-butanol) (Fig. 25a). This problem is not revealed by the NIST-modified-UNIFAC predictions because of the significant data scatter (Fig. 25b).

The data scatter and inconsistency between the predicted pressures in Fig. 26 does not allow one to determine a general trend. In the results for 1,4-benzenediol with methanol and ethanol [137], the mole fractions of the diol are below 0.005. Thus, the boiling temperatures for these results are very close to those of pure alcohols. Therefore, these data are not shown in Fig. 26 and not used for the statistical analysis.

Some predicted gas-phase compositions have a large (up to 0.45 mole fraction) deviation from the values available in the literature (particularly, [125, 138]). We believe this is partially caused by the model limitations. However, the gas-phase compositions of (phenol + methanol) at $x_1 > 0.9$ reported in these works differ by about 0.15 mole fraction. The limited available information does not allow one to find a reason of this discrepancy. New VLE measurements should be carried out for all systems considered in Refs. [125] and [138].

The statistical summary is presented in Table 3. The average standard deviations are significantly larger than for the furan derivatives that characterizes the overall data quality. Unlike the results for the furan derivatives, those for the subset without water do not change much. Removal of the questionable data significantly decreases the standard deviations. The NIST-COSMO-SAC is again more sensitive to this dataset quality improvement than NIST-modified UNIFAC.

This publication is available free of charge from: https://doi.org/10.6028/NIST.IR.8357

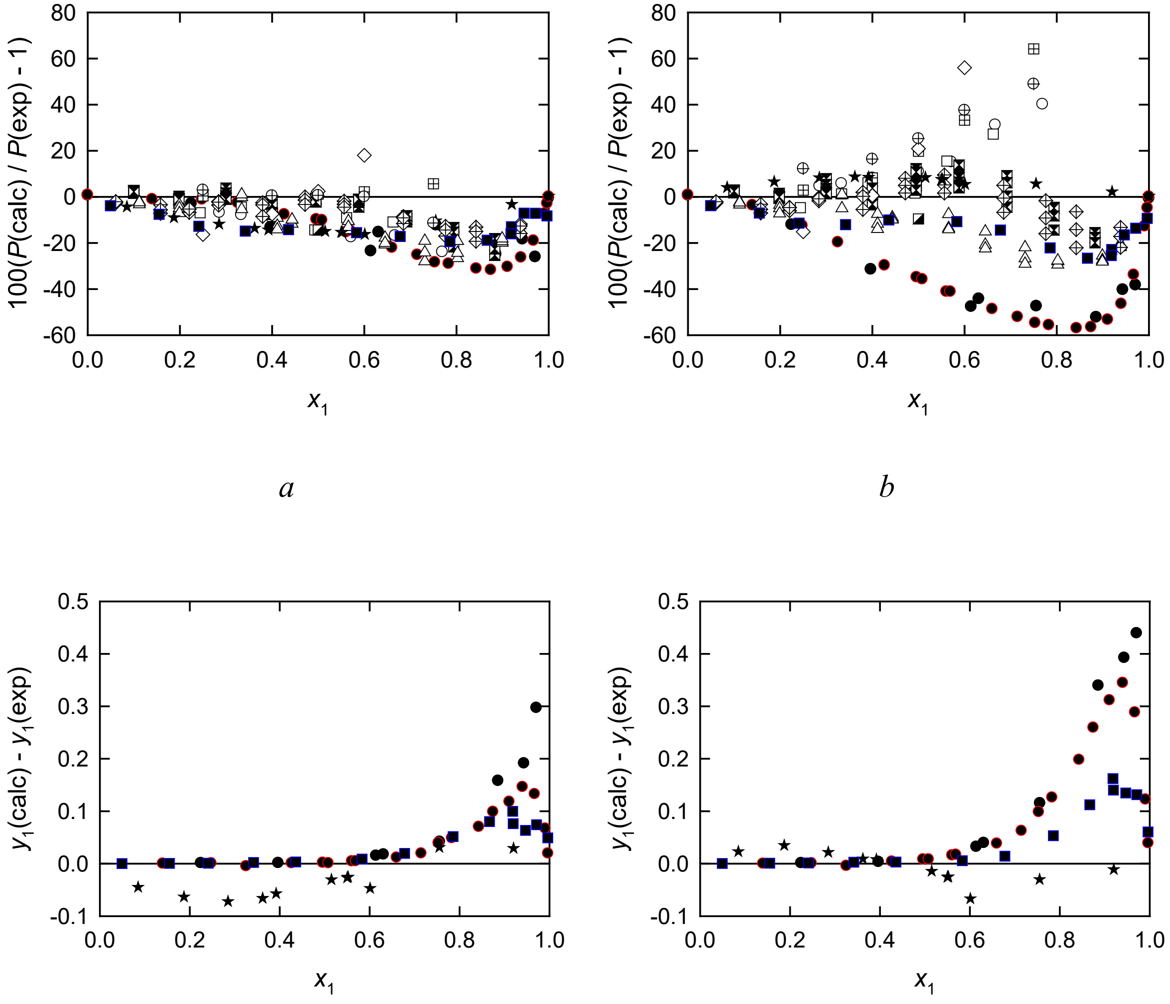

a

b

c

d

Fig. 22. Comparison of the predicted and experimental pressures *P* and first-component mole fractions y_1 in the gas phase at different first-component mole fractions in the liquid phase x_1 for the binaries of phenol with alcohols: a, c, NIST-COSMO-SAC; b, d: NIST-Modified UNIFAC.

Circles are for phenol + methanol: ○, Weissenberger *et al.* [84]; ⊕, Weissenberger *et al.* [124]; ◑, Chalov *et al.* [125]; ●, Hu *et al.* [138].

Squares are for phenol + ethanol: □, Weissenberger *et al.* [84]; ⊞, Weissenberger *et al.* [124]; ◪, Garner and Ellis [36]; ■, Chou *et al.* [121]; ⧗, Cesari *et al.* [139].

Triangles (△) are for phenol + 1-propanol, Ravikumar *et al.* [140].

Diamonds are for phenol + 2-propanol: ◇, Weissenberger *et al.* [124] (the experimental value at *x* = 0.75 has a large deviation and is not shown); ◈, Veeranna *et al.* [141].

Stars (★) are for phenol + 1,2-ethanediol, Brusset *et al.* [142].

This publication is available free of charge from: https://doi.org/10.6028/NIST.IR.8357

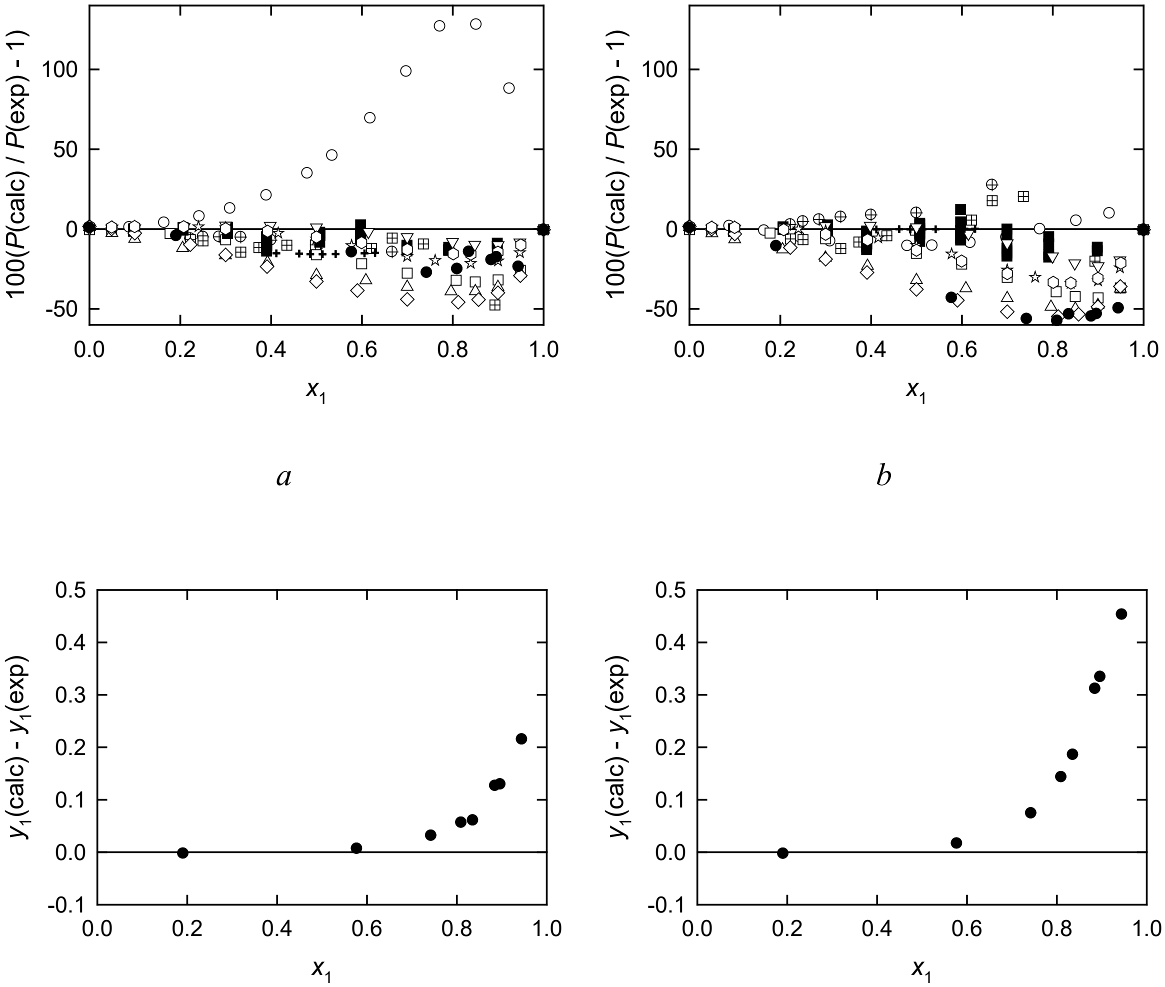

a *b*

c *d*

Fig. 23. Comparison of the predicted and experimental pressures P and first-component mole fractions y_1 in the gas phase at different first-component mole fractions in the liquid phase x_1 for the binaries of 2-methylphenol with alcohols: a, c, NIST-COSMO-SAC; b, d: NIST-Modified UNIFAC.

Circles are for 2-methylphenol + methanol: ⊕, Weissenberger and Schuster [134]; ◑, Chalov *et al.* [125]; ○, Prasad *et al.* [143].

Squares are for 2-methylphenol + ethanol: ⊞, Weissenberger and Piatti [135]; □, Prasad *et al.* [143]; ■, Cesari *et al.* [139].

Triangles (△) are for 2-methylphenol + 1-propanol, Prasad *et al.* [143].

Triangles down (▽) are for 2-methylphenol + 2-propanol, Prasad *et al.* [143].

Diamonds (◇) are for 2-methylphenol + 1-butanol, Prasad *et al.* [143].

Stars (☆) are for 2-methylphenol + 2-butanol, Prasad *et al.* [143].

Hexagons (⬡) are for 2-methylphenol + 2-methyl-1-propanol, Prasad *et al.* [143].

Pluses (+) are for 2-methylphenol + 1,2-ethanediol, Kurtyka [144].

This publication is available free of charge from: https://doi.org/10.6028/NIST.IR.8357

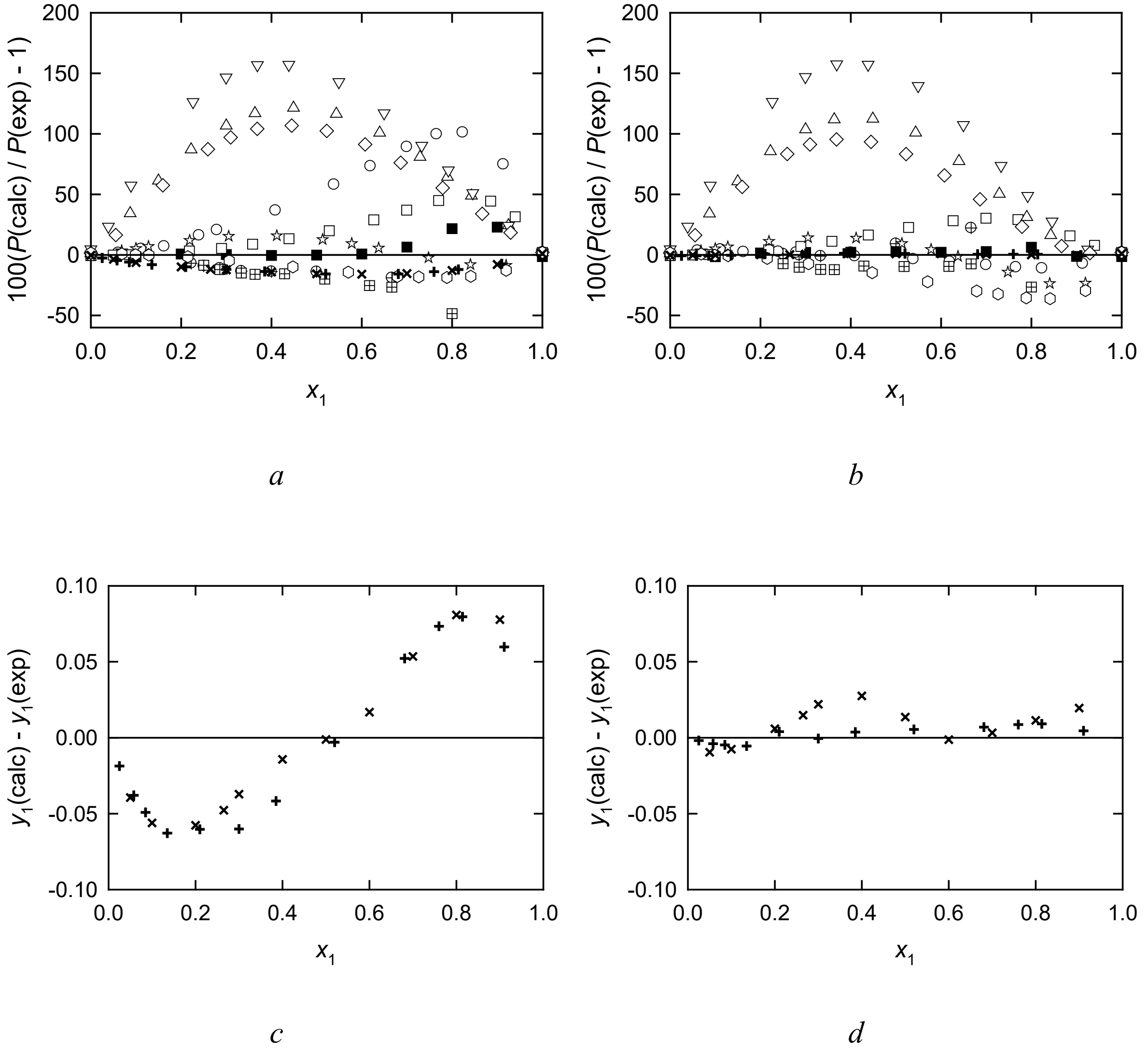

Fig. 24. Comparison of the predicted and experimental pressures *P* and first-component mole fractions y_1 in the gas phase at different first-component mole fractions in the liquid phase x_1 for the binaries of 3-methylphenol with alcohols: a, c, NIST-COSMO-SAC; b, d: NIST-Modified UNIFAC.

Circles are for 3-methylphenol + methanol: ⊕, Weissenberger *et al.* [94]; ○, Prasad *et al.* [145].
Squares are for 3-methylphenol + ethanol: ⊞, Weissenberger and Piatti [135]; ■, Piatti [146]; □, Prasad *et al.* [145].
Triangles (△) are for 3-methylphenol + 1-propanol, Prasad *et al.* [145].
Triangles down (▽) are for 3-methylphenol + 2-propanol, Prasad *et al.* [145].
Diamonds (◇) are for 3-methylphenol + 1-butanol, Prasad *et al.* [145].
Stars (☆) are for 3-methylphenol + 2-butanol, Prasad *et al.* [145].
Hexagons (⬡) are for 3-methylphenol + 2-methyl-1-propanol, Prasad *et al.* [145].
3-methylphenol + 1,2-ethanediol: ×, Othmer *et al.* [100]; +, Brusset *et al.* [142].

This publication is available free of charge from: https://doi.org/10.6028/NIST.IR.8357

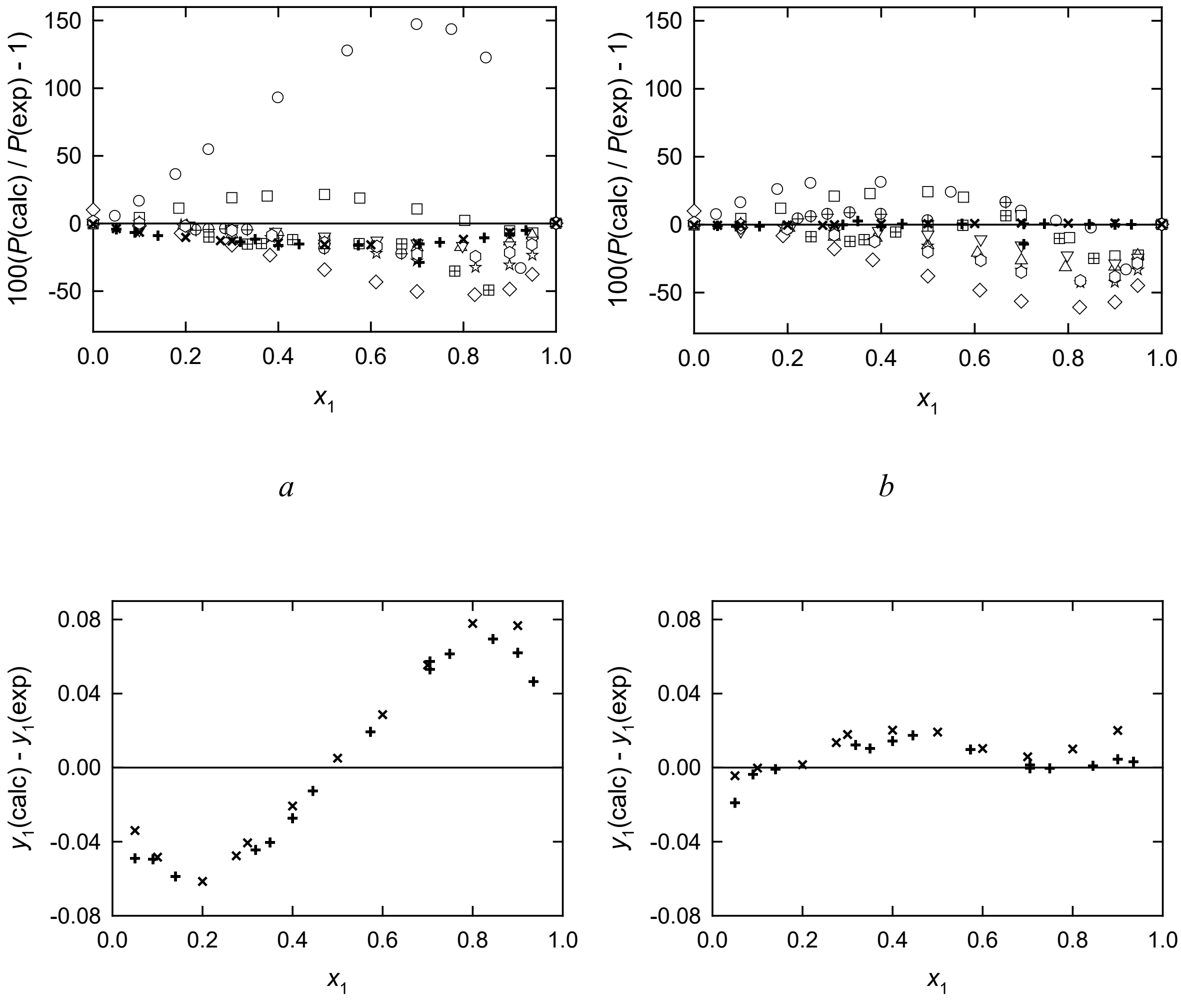

a *b*

c *d*

Fig. 25. Comparison of the predicted and experimental pressures P and first-component mole fractions y_1 in the gas phase at different first-component mole fractions in the liquid phase x_1 for the binaries of 4-methylphenol with alcohols: a, c, NIST-COSMO-SAC; b, d: NIST-Modified UNIFAC.

Circles are for 4-methylphenol + methanol: ⊕, Weissenberger *et al.* [94]; ○, Prasad *et al.* [143].
Squares are for 4-methylphenol + ethanol: ⊞, Weissenberger and Piatti [135]; □, Prasad *et al.* [143].
Triangles (△) are for 4-methylphenol + 1-propanol, Prasad *et al.* [143].
Triangles down (▽) are for 4-methylphenol + 2-propanol, Prasad *et al.* [143].
Diamonds (◇) are for 4-methylphenol + 1-butanol, Prasad *et al.* [143].
Stars (☆) are for 4-methylphenol + 2-butanol, Prasad *et al.* [143].
Hexagons (⬡) are for 4-methylphenol + 2-methyl-1-propanol, Prasad *et al.* [143].
4-methylphenol + 1,2-ethanediol: ×, Othmer *et al.* [100]; +, Brusset *et al.* [142].

This publication is available free of charge from: https://doi.org/10.6028/NIST.IR.8357

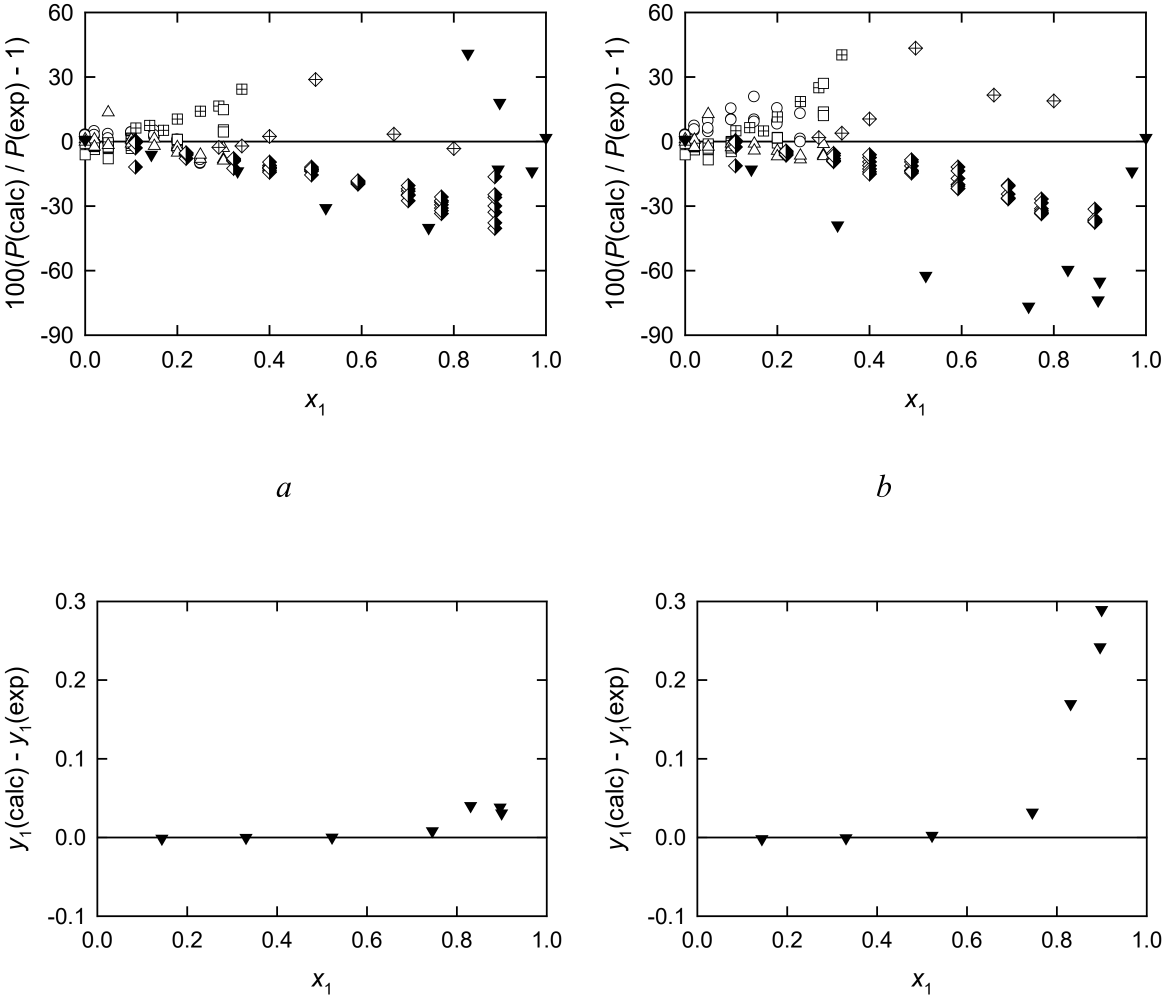

a *b*

c *d*

Fig. 26. Comparison of the predicted and experimental pressures *P* and first-component mole fractions y_1 in the gas phase at different first-component mole fractions in the liquid phase x_1 for the binaries of 1,3-benzenediol and 2-methoxyphenol with alcohols: a, c, NIST-COSMO-SAC; b, d: NIST-Modified UNIFAC.

Circles (○) are for 1,3-benzenediol + methanol, Shakhparonov and Martynova [123].

Squares are for 1,3-benzenediol + ethanol: ⊞, Weissenberger *et al.* [104]; □, Shakhparonov and Martynova [123].

Triangles (△) are for 1,3-benzenediol + 1-butanol, Shakhparonov and Martynova [123].

Triangles down (▼) are for 2-methoxyphenol + methanol, Chalov *et al.* [125].

Diamonds are for 2-methoxyphenol + ethanol: ◈, Weissenberger *et al.* [104]; ⬗, Cesari *et al.* [139].

This publication is available free of charge from: https://doi.org/10.6028/NIST.IR.8357

4. Conclusion

The experimental VLE data for the binary mixtures relevant to the catalytic fast pyrolysis of biomass have been collected. Two models based on fundamentally different approaches, NIST-COSMO-SAC and NIST-modified UNIFAC, were applied to predict equilibrium pressures and gas-phase compositions for these mixtures. If the predicted values significantly deviated from the experimental data or the experimental results were mutually inconsistent, they were analyzed using different criteria to detect problems in the theory and experimental data. Also, the mixtures were identified for which new experimental results are required to resolve the existing inconsistencies.

The main components were divided into two groups: furan derivatives and phenolic compounds. For the first group, the overall data quality is good; and more experimental data are needed to resolve inconsistencies between the experimental data, primarily, for (furan + 2-furaldehyde) and (2-furaldehyde + water). The VLE data predicted with NIST-COSMO-SAC and NIST-modified UNIFAC for phenolic compounds have a significantly worse agreement with the experimental values. Analysis of these inconsistencies in chemical series (isomers, homologs) revealed that about half of the experimental values in this group are questionable. These data are available from a single laboratory for many binaries; that is why it is especially important to be careful if the results are to be used for process simulation or model parameterization. There is a need for reliable experimental data for VLE of phenolic compounds to replace the doubtful results.

For many systems, both models behave in a similar way. Significant inconsistencies between the results of the two models occur for the binaries with alcohols, especially, methanol. The NIST-COSMO-SAC results seem to be preferable because this model has a few empirical parameters compared to the large number of group-specific ones in NIST-modified UNIFAC. However, further studies are required to improve the understanding of this problem.

Removal of the suspicious experimental data from the considered dataset decreases the relative standard deviation between the experimental pressures and NIST-COSMO-SAC predictions by about a factor of two. This effect is significantly weaker for the results from NIST-modified UNIFAC. It is probably caused by limitations of the training set and the empirical nature of the model.

Acknowledgments

This work was authored in part by the National Renewable Energy Laboratory, operated by Alliance for Sustainable Energy, LLC, for the U.S. Department of Energy (DOE) under Contract No. DE-AC36-08GO28308. Funding provided by U.S. Department of Energy Office of Energy Efficiency and Renewable Energy Bioenergy Technologies Office.

This publication is available free of charge from: https://doi.org/10.6028/NIST.IR.8357

References

[1] Collard F, Blin J (2014) A review on pyrolysis of biomass constituents: Mechanisms and composition of the products obtained from the conversion of cellulose, hemicelluloses and lignin. *Renewable and Sustainable Energy Reviews* 38:594–608. https://doi.org/10.1016/j.rser.2014.06.013

[2] Mohan D, Pittman CU, Steele PH (2006) Pyrolysis of Wood/Biomass for Bio-oil: A Critical Review. *Energy Fuels* 20:848−889. https://doi.org/10.1021/ef0502397

[3] Bridgwater AV (2012) Review of fast pyrolysis of biomass and product upgrading. *Biomass and Bioenergy* 38:68–94. https://doi.org/10.1016/j.biombioe.2011.01.048

[4] Oasmaa A, Peacocke C (2010) Properties and Fuel Use of Biomass Derived Fast Pyrolysis Liquids: A Guide (VTT, Finland), VTT Publication 731. http://www.vtt.fi/Documents/P731.pdf

[5] Venderbosch RH (2015) A Critical View on Catalytic Pyrolysis of Biomass. *ChemSusChem* 8:1306–1316. https://doi.org/10.1002/cssc.201500115

[6] Diebold JP, Scahill JW (1988) Conversion of Wood to Aromatic Gasoline with Zeolite Catalysts. *Energy Progress* 8(1):59–66.

[7] Anellotech (2018) Commercializing bio-paraxylene to make 100% bio-based PET bottles a reality. European Bioplastics Conference (Berlin, Germany). Accessed Jan 15, 2020: https://www.anellotech.com/sites/default/files/Anellotech%20Presentation%20EUBP_FINAL.pdf

[8] Ruddy DA, Schaidle JA, Ferrell III JR, Wang J, Moens L, Hensley JE (2014) Recent advances in heterogeneous catalysts for bio-oil upgrading via "ex situ catalytic fast pyrolysis": catalyst development through the study of model compounds. *Green Chem*. 16:454–490. https://doi.org/10.1039/C3GC41354C

[9] Nimlos M (2019) Performance Advantaged Bioproducts from Catalytic Fast Pyrolysis. Performance-Advantaged Bioproducts and Separations Consortium. DOE BETO Peer Review (Denver, CO). Accessed on Nov 30, 2019, at: https://www.energy.gov/sites/prod/files/2019/04/f61/Analysis%20in%20support%20of%20performance%20advantaged%20bio-products%20from%20catalytic%20fast%20pyrolysis_NL0034074.pdf

[10] Dutta A, Sahir A, Tan E, Humbird D, Snowden-Swan L, Meyer P, Ross J, Sexton D, Yap R, Lukas J (2015) Process Design and Economics for the Conversion of Lignocellulosic Biomass to Hydrocarbon Fuels – Thermochemical Research Pathways with *in situ* and *ex situ* Upgrading of Fast Pyrolysis Vapors (NREL, USA), NREL/TP-5100-62455, PNNL-23823. https://www.nrel.gov/docs/fy15osti/62455.pdf

[11] Dutta A, Schaidle J, Humbird D, Baddour F, Sahir A (2016) Conceptual Process Design and Techno-Economic Assessment of Ex Situ Catalytic Fast Pyrolysis of Biomass: A Fixed Bed Reactor Implementation Scenario for Future Feasibility. Topics in Catalysis 59:2–18. https://doi.org/10.1007/s11244-015-0500-z

[12] Griffin MB, Iisa K, Wang H, Dutta A, Orton KA, French RJ, Santosa DM, Wilson N, Christensen E, Nash C, Van Allsburg KM, Baddour FG, Ruddy DA, Tan ECD, Cai H, Mukarakate C, Schaidle JA (2018) Driving towards cost-competitive biofuels through catalytic fast pyrolysis by rethinking catalyst selection and reactor

This publication is available free of charge from: https://doi.org/10.6028/NIST.IR.8357

configuration. *Energy Environ. Sci.* 11:2904–2918. http://doi.org/10.1039/C8EE01872C

[13] Iisa K, French RJ, Orton KA, Dutta A, Schaidle JA (2017) Production of low-oxygen bio-oil via ex situ catalytic fast pyrolysis and hydrotreating. *Fuel* 207:413–422. https://doi.org/10.1016/j.fuel.2017.06.098

[14] Jasperson LV, McDougal RJ, Diky V, Paulechka E, Chirico RD, Kroenlein K, Iisa K, Dutta A (2017) Liquid−Liquid Equilibrium Measurements for Model Systems Related to Catalytic Fast Pyrolysis of Biomass. *J. Chem. Eng. Data* 62:243–252. https://doi.org/10.1021/acs.jced.6b00625

[15] Ille Y, Sánchez FA, Dahmen N, Pereda S (2019) Multiphase Equilibria Modeling of Fast Pyrolysis Bio-Oils. Group Contribution Associating Equation of State Extension to Lignin Monomers and Derivatives. *Ind. Eng. Chem. Res.* 58:7318–7331. https://doi.org/10.1021/acs.iecr.9b00227

[16] Hansen HK, Rasmussen P, Fredenslund A, Schiller M, Gmehling J (1991) Vapor–liquid equilibria by UNIFAC group contribution. 5. Revision and extension. *Ind. Eng. Chem. Res.* 30:2352–2355. https://doi.org/10.1021/ie00058a017

[17] Klamt A, Schüürmann G (1993) COSMO: A New Approach to Dielectric Screening in Solvents with Explicit Expressions for the Screening Energy and its Gradient. *J. Chem. Soc., Perkin Trans.* 2:799–805. https://doi.org/10.1039/P29930000799

[18] York DM, Karplus M (1999) A Smooth Solvation Potential Based on the Conductor-Like Screening Model. *J. Phys. Chem. A* 103:11060–11079. https://doi.org/10.1021/jp992097l

[19] Klamt A, Jonas V, Burger T, Lohrenz JCW. Refinement and Parametrization of COSMO-RS. *J. Phys. Chem. A* 102:5074–5085. https://doi.org/10.1021/jp980017s

[20] Lin ST, Sandler SI (2002) *A Priori* Phase Equilibrium Prediction from a Segment Contribution Solvation Model. *Ind. Eng. Chem. Res.* 41:899–913. https://doi.org/10.1021/ie001047w

[21] Holderbaum T, Gmehling J (1991) PSRK: A Group Contribution Equation of State Based on UNIFAC. *Fluid Phase Equilib.* 70:251–265. https://doi.org/10.1016/0378-3812(91)85038-V

[22] Gros HP, Bottini S, Brignole EA (1996) A group contribution equation of state for associating mixtures. *Fluid Phase Equilib.* 116:537–544. https://doi.org/10.1016/0378-3812(95)02928-1

[23] Paulechka E, Diky V, Kazakov A, Kroenlein K, Frenkel M (2015) Reparameterization of COSMO-SAC for Phase Equilibrium Properties Based on Critically Evaluated Data. *J. Chem. Eng. Data* 60:3554–3561. https://doi.org/10.1021/acs.jced.5b00483

[24] Kang JW, Diky V, Frenkel M (2015) New modified UNIFAC parameters using critically evaluated phase equilibrium data. *Fluid Phase Equilib.* 388:128–141. https://doi.org/10.1016/j.fluid.2014.12.042

[25] Frisch MJ, Trucks GW, Schlegel HB, Scuseria GE, Robb MA, Cheeseman JR, Scalmani G, Barone V, Mennucci B, Petersson GA, *et al.* (2013) Gaussian 09, Revision D.01 (Gaussian Inc., Wallingford, CT).

This publication is available free of charge from: https://doi.org/10.6028/NIST.IR.8357

[26] Frenkel M, Chirico RD, Diky V, Xinjian Y, Qian D, Muzny C (2005) ThermoData Engine (TDE): Software Implementation of the Dynamic Data Evaluation Concept. *J. Chem. Inf. Model.* 45:816–838. https://doi.org/10.1021/ci050067b

[27] Frenkel M, Chirico RD, Diky V, Yan X, Dong Q, Muzny C (2005) ThermoData Engine (TDE): Software Implementation of the Dynamic Data Evaluation Concept. *J. Chem. Inf. Model.* 45:816–838. https://doi.org/10.1021/ci050067b

[28] Diky V, Chirico RD, Muzny CD, Kazakov AF, Kroenlein K, Magee JW, Abdulagatov I, Frenkel M (2013) ThermoData Engine (TDE): Software Implementation of the Dynamic Data Evaluation Concept. 9. Extensible Thermodynamic Constraints for Pure Compounds and New Model Developments. *J. Chem. Inf. Model.* 53:3418–3430. https://doi.org/10.1021/ci4005699

[29] Weidlich U, Gmehling J (1987) A Modified UNIFAC Model. 1. Prediction of VLE, h^E, and γ^∞. *Ing. Eng. Chem. Res.* 26:1372–1381. https://doi.org/10.1021/ie00067a018

[30] Nala M, Auger E, Gedik I, Ferrando N, Dicko M, Paricaud P, Volle F, Passarello JP, de Hemptinne JC, Tobaly P, Stringari P, Coquelet C, Ramjugernath D, Naidoo P, Lugo R (2013) Vapour–liquid equilibrium (VLE) for the systems furan + n-hexane and furan + toluene. Measurements, data treatment and modeling using molecular models. *Fluid. Phase Equilib.* 337:234–245. https://doi.org/10.1016/j.fluid.2012.08.005

[31] Thévaneau P, Valtz A, Coquelet C (2017) Vapor Liquid Equilibrium Data for the Furan–Toluene Binary System between 313.02 and 352.99 K. *J. Chem. Eng. Data* 62:1168–1172. https://doi.org/10.1021/acs.jced.6b00424

[32] Krevor DH, Prausnitz JM (1986) Vapor–Liquid Equilibria for Model Mixtures of Coal-Derived Liquids. 1. Binary Systems with 2-Methylfuran. *J. Chem. Eng. Data* 31:349–353. https://doi.org/10.1021/je00045a027

[33] Thornton JD, Garner FH (1951) Vapour–liquid equilibria in hydrocarbon–non-hydrocarbon systems. I. The system benzene–*cyclo*hexane–furfuraldehyde. *J. Appl. Chem.* 1:S61-S68.

[34] Kenny JW (1957) Prediction of ternary liquid–liquid equilibrium from binary data (for the system furfural–iso-octane–benzene). *Chem. Eng. Sci.* 6:116–122. https://doi.org/10.1016/0009-2509(57)85004-0

[35] Stephenson RW, Van Winkle M (1962) Modification of Relative Volatilities by Addition of Solvent. *J. Chem. Eng. Data* 7:510–516. https://doi.org/10.1021/je60015a021

[36] Garner FH, Ellis SRM (1951) Applicability of vapour–liquid equilibrium relationships to extractive distillation. *Trans. Inst. Chem. Eng.* 29:45–62.

[37] Thornton JD, Garner FH. Vapour–liquid equilibria in hydrocarbon–non-hydrocarbon systems. III. The system *iso*octane–toluene–furfuraldehyde. *J. Appl. Chem.* 1:S74–S80.

[38] Garner FH, Hall RTW (1955) Vapour–liquid equilibria of C_7-hydrocarbon–furfural systems. Part I. Binary and ternary data for the system methyl*cyclo*hexane–toluene–furfural. *J. Inst. Petroleum* 41:1–18.

[39] Rivenq F (1973) Ébulliométrie des mélanges toluene–furfural, (Note de Laboratoire). *Bull. Soc. Chim. Fr.* (9):2645–2656.

This publication is available free of charge from: https://doi.org/10.6028/NIST.IR.8357

[40] Puri PS, Raju KSN (1970) Vapor–Liquid Equilibria. Systems *p*-Xylene–Furfural and Ethylbenzene–Furfural. *J. Chem. Eng. Data* 15:480–483. https://doi.org/10.1021/je60047a021

[41] Tai WP, Lee HY, Lee MJ (2014) Isothermal vapor–liquid equilibrium for binary mixtures containing furfural and its derivatives. *Fluid Phase Equilib.* 384: 134–142. https://doi.org/10.1016/j.fluid.2014.10.037

[42] Auger E, Coquelet C, Valtz A, Nala M, Naidoo P, Ramjugernath D (2016) Equilibrium data and GC-PC SAFT predictions for furanic extraction. *Fluid Phase Equilib.* 430:57–66. https://doi.org/10.1016/j.fluid.2016.09.019

[43] Chen Q, Zhang L, Zhang H, Wang X, Liu A, Chen H, Zhang L, Zhu D, Gao D (2020) Measurements and Correlation of Isobaric Vapor–Liquid Equilibrium Data for Binary Mixtures of Furan, Oxolane, and Furan-2-Carbaldehyde and Application of the Binary Model Parameters for Further Prediction of the Ternary System. *J. Chem. Eng. Data* 65:2583–2596. https://doi.org/10.1021/acs.jced.9b01210

[44] Holdren RF, Hixon RM (1946) Vapor Pressure and Vapor–Liquid Equilibria in the System Furfural–2-Methylfuran. *Ind. Eng. Chem.* 38:1061–1062. https://doi.org/10.1021/ie50442a024

[45] Negadi L, Mokbel I, Chiali-Baba-Ahmed N, Kara-Zaitri L (2014) Phase equilibrium properties of binary mixtures containing 2,5-dimethylfuran and furfuryl alcohol or methyl isobutyl ketone at several temperatures. *J. Chem. Thermodyn.* 70: 233–238. https://doi.org/10.1016/j.jct.2013.10.039

[46] Myles MG, Wingard RE (1961) Calculating Activity Coefficients. *Ind. Eng. Chem.* 53:219–222. https://doi.org/10.1021/ie50615a029

[47] Tsirlin YA, Vasil'eva VA (1971) Liquid–vapor phase equilibrium in binary mixtures of furfural with furan alcohols under reduced pressure. *Zh. Prikl. Khim.* 44: 1121–1126.

[48] Pokki JP, Lê HQ, Uusi-Kyyny P, Sixta H, Alopaeus V (2018) Isobaric Vapor–Liquid Equilibrium of Furfural + γ-Valerolactone at 30 kPa and Isothermal Liquid–Liquid Equilibrium of Carbon Dioxide + γ-Valerolactone + Water at 298 K. *J. Chem. Eng. Data* 63:4381–4391. https://doi.org/10.1021/acs.jced.8b00451

[49] Zheng H, Luo X, Yin G, Chen J, Zhao S (2018) Vapor Pressure and Isobaric Vapor–Liquid Equilibrium for Binary Systems of Furfural, 2-Acetylfuran, and 5-Methylfurfural at 3.60 and 5.18 kPa. *J. Chem. Eng. Data* 63:49–56. https://doi.org/10.1021/acs.jced.7b00574

[50] Fele L, Grilic V (2003) Separation of Furfural from Ternary Mixtures. *J. Chem. Eng. Data* 48:564–570. https://doi.org/10.1021/je020117y

[51] Ma Y, Gao J, Li M, Zhu Z, Wang Y (2018) Isobaric vapour–liquid equilibrium measurements and extractive distillation process for the azeotrope of (*N,N*-dimethylisopropylamine + acetone). *J. Chem. Thermodyn.* 122:154–161. https://doi.org/10.1016/j.jct.2018.03.019

[52] Hauschild T, Wu HS, Sandler SI (1987) Vapor–liquid equilibrium of the mixtures 2-furaldehyde/1-butanol and 2-furaldehyde/4-methyl-2-pentanone. *J. Chem. Eng. Data* 32:226–229. https://doi.org/10.1021/je00048a028

[53] Zaitseva A, Laavi H, Pokki JP, Uusi-Kyyny P, Alopaeus V (2014) Isothermal vapor–liquid equilibrium and excess molar enthalpies of the binary mixtures

This publication is available free of charge from: https://doi.org/10.6028/NIST.IR.8357

furfural + methyl isobutyl ketone, +2-butanol and +2-methyl-2-butanol. *Fluid Phase Equilib.* 372:85–99. https://doi.org/10.1016/j.fluid.2014.03.033

[54] Smith AS, Labonte JF (1952) Dehydration of Aqueous Methyl Ethyl Ketone with 2-Methyl Furan. *Ind. Eng. Chem.* 44:2740–2743. https://doi.org/10.1021/ie50515a064

[55] Dudutkina IV, Lutugina NV (1981) Study of phase equilibria in the binaries containing furfuryl alcohol. *Sovremennye Problemy Fizicheskoy Khimii Rastvorov*, Part 2, pp 40–46. Deposited in ONIITEKhIM (Cherkassy, USSR), #916 KhP-D81.

[56] Hickman JB, Hall JL (1950) Liquid–Vapor Equilibria, Refractive Indices and Freezing Points in the System: 2-Methylfurane–Methanol. *Proc. W. Va. Acad. Sci.* 22:72–79.

[57] Mejía A, Segura H, Cartes M (2013) Isobaric Vapor Liquid Equilibrium and Isothermal Interfacial Tensions for the System Ethanol + 2,5-Dimethylfuran. 58: 3226–3232. https://doi.org/10.1021/je400683g

[58] Ni X, Wang Z (1987) Studies on VLE of Carbinol–Furfual–Water–Acetic Acid. Huaxue Gongcheng. (3):50–58.

[59] Staroske J, Figurski G (1992) Das Dampf–Flüssigkeits–Gleichgewicht des ternären Systems Furfural–Ethylacetat–Methanol und dessen binäre Randsysteme bei 298,15 K. *Chem. Tech.* 44:64–66.

[60] Kharin SE, Perelygin VM, Polyanskii KK (1970) Liquid–vapor phase equilibrium in the water–furfural and ethanol–furfural systems. *Gidroliznaya I Lesokhimicheskaya Promyshlennost'* 23:15–16.

[61] Havasi D, Pátzay G, Kolarovszki Z, Mika LT (2016) Isobaric Vapor–Liquid Equilibria for Binary Mixtures of γ-Valerolactone + Methanol, Ethanol, and 2-Propanol. *J. Chem. Eng. Data* 61:3326–3333. https://doi.org/10.1021/acs.jced.6b00384

[62] Rigamonti R, Spaccamela Marchetti E (1955) Estrazione del furfurolo dale soluzioni acquose diluite – Nota II. *Chim. Ind.* 37:1039–1044.

[63] Mains GH (1922) The System Furfural–Water – I. *Chem. Metal. Eng.* 26:779–784.

[64] Pearce EJ, Gerster JA (1950) Furfural–Water System – Experimental and Theoretical Vapor–Liquid Relationships. *Ind. Eng. Chem.* 42:1418–1424. https://doi.org/10.1021/ie50487a043

[65] Tsirlin YA. (1962) Liquid–vapour equilibrium in the furfural–water system at reduced pressures. *Russ. J. Phys. Chem.* 36:903–905.

[66] Staroske J, Schuberth H (1988) Das Phasengleichgewichtsverhalten des ternären Systems Furfural/Ethylacetat/Wasser (1/2/3) bei 25 °C. *Z. Phys. Chem.* 269O:572–575. https://doi.org/10.1515/zpch-1988-26961

[67] Sunder MS, Prasad DHL (2003) Phase Equilibria of Water + Furfural and Dichloromethane + *n*-Hexane. *J. Chem. Eng. Data* 48:221–223. https://doi.org/10.1021/je020053r

[68] Boldyrev AV, Komarov VM, Krichevtsov BK (1972) Liquid–vapor equilibrium in the system water–furfuryl alcohol. *Zh. Prikl. Khim.* 46:2338–2339.

[69] Dudkina IV, Lutugina NV, Syrovarova TK (1982) Liquid–vapor equilibrium in the water–ethanol–acetone–methyl ethyl ketone–furfural system and its binary and ternary subsystems. *Vestn. Leningr. Univ., Ser. 4: Fiz. Khim.* (10):101–104.

This publication is available free of charge from: https://doi.org/10.6028/NIST.IR.8357

[70] Havasi D, Mizsey P, Mika LT (2016) Vapor–Liquid Equilibrium Study of the Gamma-Valerolactone–Water Binary System. *J. Chem. Eng. Data* 61:1502–1508. https://doi.org/10.1021/acs.jced.5b00849

[71] Zaitseva A, Pokki JP, Le HQ, Alopaeus V, Sixta H (2016) Vapor–Liquid Equilibria, Excess Enthalpy, and Density of Aqueous γ-Valerolactone Solutions. *J. Chem. Eng. Data* 61:881–890. https://doi.org/10.1021/acs.jced.5b00724

[72] Fox JJ, Barker MF (1917) Determination of phenol in commercial cresylic acid. *J. Soc. Chem. Ind. (London)* 36:842–845.

[73] Schneider KW, Oberkobusch R. (1951) Die Analyse von Phenolgemischen unter Anwendung der Rektifikation und Chromatographie. *Brennst.-Chem.* 32:110–117.

[74] Vostrikova VN, Komarova TV, Reshetov SA (1981) Study of liquid–vapor equilibrium in phenol–*o*-cresol and styrene–benzaldehyde binary systems at reduced pressures. *Zh. Prikl. Khim.* 54:1178–1179.

[75] Clausse D, Lambert JP, Guigon P, Boudehen-Boiveaut A (1988) Determination d'equilibres liquid–vapeur et liquid–liquide pour l'elaboration de procedes industriels. *Calorim. Anal. Therm.* 19:C21.1-C21.9.

[76] Selvam SP, Dutt NVK, Balkishan Rao I, Subba Rao YV (1992) Isobaric VLE data for the binary systems phenol + O-cresol, phenol +p-cresol, O-cresol +P-cresol and P-cresol + 2,4-xylenol. *Fluid Phase Equilib.* 78:261–267. https://doi.org/10.1016/0378-3812(92)87040-T

[77] Vostrikova VN, Komarova TV, Reshetov SA, Vinogradova VV (1978) Liquid–vapor equilibrium in the binary systems found in products from the oxidative methylation of toluene. *Khimicheskaya Promyshlennost'* (5):345–346.

[78] Cepeda E, Gonzalez C, Resa JM, Ortiz de Salido C (1989) Isobaric vapor–liquid equilibrium for the cumene–*m*-cresol and phenol–*m*-cresol systems at 13.33 kPa. *J. Chem. Eng. Data* 34:429–431. https://doi.org/10.1021/je00058a017

[79] Hwang SM, Lee MJ, Lin H (2000) Isothermal vapor–liquid equilibria for mixtures of 4-methoxyphenol, catechol, and *p*-cresol. *Fluid Phase Equilib.* 172:183–196. https://doi.org/10.1016/S0378-3812(00)00370-8

[80] Shi X, Qi M, Zhang Q, Zhou W, Lu M (2000) Measurement and Prediction of VLE of Catechol System. *J. East China Univ. Sci. Technol.* 26:236–239.

[81] Wang J, Ou J, Sun X, Huang C, Sun J, Shao H, Leng Y (2018) Measurement and correlation of isobaric vapour–liquid equilibrium for systems of *o*-cresol, *m*-cresol and 2,6-dimethylphenol at 20.0 kPa. *Fluid Phase Equilib.* 459:44–50. https://doi.org/10.1016/j.fluid.2017.12.011

[82] Vostrikova VN, Komarova TV, Sobolev OB (1980) Vapor–liquid equilibrium under vacuum in binary systems containing styrene, benzaldehyde, and *p*- and *o*-cresols. *Zh. Prikl. Khim.* 53:2118–2119.

[83] Ye R, Xia MS, Yu D, Liu H, Hu Y (1998) Isobaric Vapor–Liquid Equilibria for 2-Methylphenol–2,6-Dimethylphenol–2,4,6-Trimethylphenol Ternary System. *Chin. J. Chem. Eng.* 6:183–188.

[84] Weissenberger G, Schuster F, Schuler K (1924) Über die Molekülverbindungen der Phenole. IV. Das Verhalten der binären Systeme mit Phenol und Phenoläthern. *Monatsh. Chem.* 45:425–435. https://doi.org/10.1007/BF01521924

This publication is available free of charge from: https://doi.org/10.6028/NIST.IR.8357

[85] Martin AR, George CM. 330. Partial vapour pressures and refractivities of mixtures of benzene with nitrobenzene, phenol, benzyl alcohol, or *p*-dichlorobenzene. *J. Chem. Soc.* 1413–1416. https://doi.org/10.1039/JR9330001413

[86] Gmehling J (1982) Phase Equilibria in Binary Systems Formed by Phenol with Benzene, *n*-Octane, and *n*-Decane. *J. Chem. Eng. Data* 27:371–373. https://doi.org/10.1021/je00030a002

[87] Nienhaus B, Limbeck U, Bölts R, de Haan AB, Niemann SH, Gmehling J (1998) Vapor−Liquid Equilibria at 413.65 K and Excess Enthalpies at 323.15, 363.15, and 413.15 K for Mixtures of Benzene, Toluene, Phenol, and Benzaldehyde. *J. Chem. Eng. Data* 43:941–948. https://doi.org/10.1021/je980116z

[88] Drickamer HG, Brown GG, White RR (1945) Vapor–Liquid Equilibria in Phenol–Hydrocarbon Systems. *Trans. Am. Inst. Chem. Eng.* 41:555–605.

[89] Klauck M, Grenner A, Taubert K, Martin A, Meinhardt R, Schmelzer J (2008) Vapor−Liquid Equilibria in Binary Systems of Phenol or Cresols + Water, + Toluene, and + Octane and Liquid−Liquid Equilibria in Binary Systems of Cresols + Water. *Ind. Eng. Chem. Res.* 47:5119–5126. https://doi.org/10.1021/ie071214t

[90] Anderko A (1989) (Vapour+liquid) equilibria of (phenol + butylbenzene or propylbenzene or isopropylbenzene or 1,2,4-trimethylbenzene or ethylbenzene) at 393.15 and 403.15 K. *J. Chem. Thermodyn.* 21:731–738. https://doi.org/10.1016/0021-9614(89)90056-6

[91] Byk SS, Stroiteleva RG (1956) Phase equilibria in the phenol + isopropylbenzene system in the presence of α-methylstyrene. *Zh. Fiz. Khim.* 30: 2451–2455.

[92] Cepeda E, Gonzalez C, Resa JM (1989) Isobaric Vapor–Liquid Equilibrium for the Cumene–Phenol System. *J. Chem. Eng. Data* 34:270–273. https://doi.org/10.1021/je00057a004

[93] Weissenberger G, Piatti L (1924) Über die Molekülverbindungen der Phenole. II. Das Verhalten der Kresole gegen aromatische Kohlenwasserstoffe. *Monatsh. Chem.* 45:281–285. https://doi.org/10.1007/BF01524670

[94] Weissenberger G, Schuster F, Wojnoff K (1925) Über die Molekülverbindungen der Phenole. VII. Das Verhalten der hydrierten Kresole und verwandter Verbindungen. *Monatsch. Chem.* 46:1–8. https://doi.org/10.1007/BF01525485

[95] Prasad TEV, Harish G, Krupavaram N, Prasad S, Jaiswal A, Prasad DHL (2005) Bubble points of some binary mixtures formed by *o*-cresol at 95.75 kPa. *Fluid Phase Equilib.* 238:45–51. https://doi.org/10.1016/j.fluid.2005.09.012

[96] Prasad TEV, Vasavi M, Jyotsna M, Jhansi V, Smitha G, Prasad DHL (2008) Bubble point measurements of binary mixtures formed by ethyl benzene with selected compounds at 95.35 kPa. *J. Chem. Thermodyn.* 40:1418–1421. https://doi.org/10.1016/j.jct.2008.05.002

[97] Savitt SA, Othmer DF (1952) Separation of *m*- and *p*-Cresols from Their Mixtures. *Ind. Eng. Chem.* 44:2428–2431. https://doi.org/10.1021/ie50514a041

[98] Sartakova OY, Krut'ko OM, Khristenko MS, Kormina LA (1996) Design of flow diagrams for the separation of toluene–diglyme mixtures with the use of additional components. *Zh. Prikl. Khim.* 69:1077–1080.

[99] Prasad TEV, Reddy NM, Kiran NA, Prasad DHL (2006) Activity coefficients of binary mixtures of *m*-cresol + selected compounds at 95.5 kPa. *Phys. Chem. Liq.* 44:227–231. https://doi.org/10.1080/00319100500329077

This publication is available free of charge from: https://doi.org/10.6028/NIST.IR.8357

[100] Othmer DF, Savitt SA, Krasner A, Goldberg AM, Markowitz D (1949) Composition of Vapors from Boiling Binary Solutions. Systems with *m*- or *p*-Cresol as One Component. *Ind. Eng. Chem.* 41:572–574. https://doi.org/10.1021/ie50471a028

[101] Schmelzer J, Niederbroeker H, Partzsch S, Voeckler R, Meinhardt R (1996) Isothermal vapor–liquid equilibria in binary mixtures containing hydrocarbons (nonane, decane, dodecane, butylbenzene, or 2-methylnaphthalene) and phenol or cresols (2-methylphenol or 3-methylphenol) at 373 and 453 K. *ELDATA: Int. Electron. J. Phys.-Chem. Data* 2:153–162.

[102] Marks DE, Wingard RE (1960) Vapor-Liquid Equilibrium in the Toluene–*p*-Cresol System. *J. Chem. Eng. Data* 5:416–419. https://doi.org/10.1021/je60008a004

[103] Prasad TEV, Venkanna N, Kumar YN, Ashok K, Sirisha NM, Prasad DHL. Activity coefficients and excess Gibbs' free energy of some binary mixtures formed by *p*-cresol at 95.23 kPa. *J. Chem. Thermodyn.* 39:1022–1026. https://doi.org/10.1016/j.jct.2006.12.017

[104] Weissenberger G, Hencke R, Bregmann L (1925) Zur Kenntnis organischer Molekülverbindungen. XVI. Zweiwertige Phenole und ihre Äther. *Monatsh. Chem.* 46:471–482. https://doi.org/10.1007/BF01525702

[105] Lebedeva AA, Kiva VN, Pariychuk LV (1970) Vapor–liquid equilibrium in mixtures of anisole, phenol, and *o*-cresol. *Trudy, Nauchno-Issledovatel'skii Institut Neftekhimicheskikh Proizvodstv* 2:92–95.

[106] Li H, Xia S, Ma P, Yan F, Yang Z, Li Y (2014) Isobaric (vapour + liquid) equilibria for three binary systems (toluene + anisole, *n*-butylbenzene + anisole, and guaiacol + anisole) at 101.33 kPa. *Fluid Phase Equilib.* 369:109–114. https://doi.org/10.1016/j.fluid.2014.02.025

[107] Schreinemakers FAH (1900) Dampfdrucke binärer und ternärer Gemische. *Z. Phys. Chem.* 35U:459–479. https://doi.org/10.1515/zpch-1900-3530

[108] Schükarew A (1910) Über die Eigenschaften der Lösungen bei ihrer kritischen Lösungstemperatur. *Z. Phys. Chem.* 71U:90–108. https://doi.org/10.1515/zpch-1910-7107

[109] Rhodes FH, Wells JH, Murray GW (1925) Vapor Composition Relationships in the Systems Phenol–Water and Phenol–Cresol. *Ind. Eng. Chem.* 17:1199–1201. https://doi.org/10.1021/ie50191a044

[110] Ferguson JB (1927) The System Water–Phenol. *J. Phys. Chem.* 31:757–763. https://doi.org/10.1021/j150275a013

[111] Campbell AN, Campbell AJR (1937) Concentrations, Total and Partial Vapor Pressures, Surface Tensions and Viscosities, in the Systems Phenol–Water and Phenol–Water–4% Succinic Acid. *J. Am. Chem. Soc.* 59:2481–2488. https://doi.org/10.1021/ja01291a001

[112] Brusset H, Gaynès J (1953) Courbes d'ébullition et de rosée des systems binaires eau–phénol et eau–orthocrésol. *C. R. Hebd. Seances Acad. Sci.* 236:1563–1565.

[113] Markuzin NP (1961) Equilibrium between solution and vapor in the system triethylamine–phenol and phenol–water at 15°. *Zh. Prikl. Khim.* 34:1175–1176.

[114] Weller R, Schuberth H, Leibnitz E (1963) Die Phasengleichgewichte dampfförmig/flüssig des Systems Phenol/*n*-Butylacetat/Wasser bei 44,4°C. *J. Prakt. Chem.* 21:234–249.

[115] Kliment V, Fried V, Pick J (1964) Gleichgewicht Flüssigkeit-Dampf XXXIII. Systeme Butylacetat–Phenol und Wasser–Phenol. *Collect. Czech. Chem. Commun.* 29:2008–2015. https://doi.org/10.1135/cccc19642008

[116] Kiva VN, Lebedeva AA, Kirichenko GA, Mozgovaya VP (1970) Study of azeotropy in some ternary mixtures of the decomposition products of cumene hydroperoxide. Document # 2270-70 deposited in VINITI.

[117] Kolyuchkina GY, Timofeev VS, Serafomov LA (1971) Study of phase equilibrium in the heptane–phenol–water system. *Uch. Zap., Mosk. Inst. Tonkoi Khim. Tekhnol.* 1(3):78–87.

[118] Hakuta T (1975) Vapor–liquid equilibria of pollutants in sea water. II. Vapor–liquid equilibria of phenolic substance–water systems. *Nippon Kaisui Gakkaishi* 28: 379–385.

[119] Karavaeva AP, Koshel' GN, Galiaskarova LM (1975) Mutual solubility and liquid–vapor equilibrium in the cyclohexanone–phenol–water ternary. *Osnovn. Org. Sint. Neftekhim.* 3:98–104.

[120] Lyzlova RV, Susarev MP (1982) Phase equilibria in the water–hydrogen chloride–phenol ternary. *Zh. Prikl. Khim.* 55:261–265.

[121] Chou CH, Perng JL, Lee MD, Chen YP (1987) Vapor–liquid equilibrium measurements of the ternary system of ethanol, water and phenol at 760mmHg. *J. Chin. Inst. Chem. Eng.* 18:393–399.

[122] Tabai S, Rogalski M, Solimando R, Malanowski SK (1997) Activity Coefficients of Chlorophenols in Water at Infinite Dilution. *J. Chem. Eng. Data* 42: 1147–1150. https://doi.org/10.1021/je960336h

[123] Shakhparonov MI, Martynova ME (1953) On the theory of the thermodynamic properties of solutions. VII. Vapor pressure of resorcinol solutions in various solvents. *Zh. Fiz. Khim.* 27:197–205.

[124] Weissenberger G, Hencke R, Sperling E (1925) Zur Kenntnis organischer Molekülverbindungen. XVII. Das Verhalten des Dekahydronaphthalins. *Monatsh. Chem.* 46:483–497. https://doi.org/10.1007/BF01526344

[125] Chalov NV, Goryachikh EF, Vodolazova LK (1955) Study of the liquid–vapor compositions in binary solutions of phenol. *Gidroliznaya I Lesokhimicheskaya Promyshlennost'* 8:11–12.

[126] Gölles F (1963) Zur Ermittlung und rechnerischen Überprüfung thermodynamischer Daten aus experimentell gefundenen Werten, 4. Mitt.: Zur Bestimmung der Partialdrucke im System Phenol(2)–Aceton(3). *Monatsh. Chem.* 94:1108–1117. https://doi.org/10.1007/BF00905699

[127] Motina GL, Tentser NZ, Aerov ME (1968) Liquid–vapor equilibrium in the system phenol–acetone and phenol–acetone–water. *Zh. Prikl. Khim.* 41:1048–1055.

[128] Vasil'eva II, Gryaznov AK, Zakoshanskiy VM, Naumova AA, Polyakov AA (1991) Study of the liquid–vapor equilibrium in the acetone–phenol system. *Zh. Prikl. Khim.* 64:444–448.

[129] Byk SS, Shcherbak LI (1956) Liquid–vapor equilibrium in the phenol–methyl ethyl ketone system. *Zh. Fiz. Khim.* 30:56–60.

[130] Oscarson JL, Lundell SO, Cunningham JR (1987) Phase equilibria for ten binary systems. *AIChE Symp. Ser.* 83:1–17.

This publication is available free of charge from: https://doi.org/10.6028/NIST.IR.8357

This publication is available free of charge from: https://doi.org/10.6028/NIST.IR.8357

[131] Fried V, Pick J (1961) Liquid–vapor equilibria. XXV. System phenol–acetophenone at reduced pressures. *Collect. Czech. Chem. Commun.* 26:954–960. https://doi.org/10.1135/cccc19610954

[132] Aarna A, Kaps T (1974) Vapor–liquid isobaric equilibrium in phenol + oxygen-compound binary mixtures. *Eesti NSV Tead. Akad. Toim., Keem., Geol.* 23:16–21.

[133] Giles NF, Wilson GM (2006) Vapor−Liquid Equilibria on Seven Binary Systems: Ethylene Oxide + 2-Methylpropane; Acetophenone + Phenol; *cis*-1,3-Dichloropropene + 1,2-Dichloropropane; 1,5-Hexadiene + Allyl Chloride; Isopropyl Acetate + Acetonitrile; Vinyl Chloride + Methyl Chloride; and 1,4-Butanediol + γ-Butyrolactone. *J. Chem. Eng. Data* 51:1954–1962. https://doi.org/10.1021/je050317k

[134] Weissenberger G, Schuster F (1924) Über die Molekülverbindungen der Phenole. V. Zur Kenntnis der Dampfdruckkurven. *Monatsh. Chem.* 45:437–448. https://doi.org/10.1007/BF01524551

[135] Weissenberger G, Piatti L (1925) Über die Molekülverbindugen der Phenole. I. Das Verhalten Kresole gegen Alkohol, Äther und Aceton. *Monatsh. Chem.* 45:187–206. https://doi.org/10.1007/BF01524660

[136] Piatti L (1936) Zur Kenntnis binärer Gemische IV. *Angew. Chem.* 49:77–78. https://doi.org/10.1002/ange.19360490304

[137] Kodama D, Tanaka H, Kato M (2002) Vapor−Liquid Equilibrium of 1,4-Dihydroxybenzene in Methanol or Ethanol. *J. Chem. Eng. Data* 47:91–92. https://doi.org/10.1021/je010158e

[138] Hu WM, Shen LM, Zhao LJ (2004) Measurement of vapor–liquid equilibrium for binary mixtures of phenol–dimethyl carbonate and phenol–methanol at 101.3 kPa. *Fluid Phase Equilib.* 219:265–268. https://doi.org/10.1016/j.fluid.2004.01.023

[139] Cesari L, Namysl S, Canabady-Rochelle L, Mutelet F (2017) Phase equilibria of phenolic compounds in water or ethanol. *Fluid Phase Equilib.* 453:58–66. https://doi.org/10.1016/j.fluid.2017.09.008

[140] Ravikumar YVL, Ramakrishna M, Veeranna D (1991) Bubble Temperature Data for Phenol–*n*-Propanol System. *Phys. Chem. Liq.* 23:109–114. https://doi.org/10.1080/00319109108030640

[141] Veeranna D, Ravi Kumar YVL, Ramakrishna M (1989) Bubble Temperature Data for Phenol–Alcohol Systems 1. Phenol–*i*-Propanol System. *Phys. Chem. Liq.* 19:17–22. https://doi.org/10.1080/00319108908028404

[142] Brusset H, Kaiser L, Hocquel J (1968) Étude de quelques systems binaires du glycol. *Chim. Ind. Genie Chim.* 99:207–219.

[143] Prasad TEV, Jaiswal A, Prasad S, Harish G, Krupavaram N, Sirisha NM, Ashok K, Kumar YN, Venkanna N, Prasad DHL (2006) Activity coefficients of the binary mixtures of *o*-cresol or *p*-cresol with C_1–C_4 aliphatic alcohols near ambient pressure. *Fluid Phase Equilib.* 244:86–98. https://doi.org/10.1016/j.fluid.2006.03.018

[144] Kurtyka Z (1956) The Positive-Negative Azeotrope: Glycol–*o*-Cresol–2,4,6-Collidine. XXIII. *Bull. Acad. Pol. Sci., Cl. III* 4:49–53.

[145] Prasad TEV, Kiran NA, Reddy NM, Prasad DHL (2006) (Vapor + liquid) equilibria of the binary mixtures of *m*-cresol with C_1–C_4 aliphatic alcohols at 95.5 kPa. *J. Chem. Thermodyn.* 38:1696–1700. https://doi.org/10.1016/j.jct.2006.03.006

[146] Piatti L (1931) Zur Kenntnis binärer Gemische. *Z. Phys. Chem.* 152A:36–46. https://doi.org/10.1515/zpch-1931-15204

This publication is available free of charge from: https://doi.org/10.6028/NIST.IR.8357